PERIMENOPAUSAL TRANSITION INCREASES BLOOD BRAIN PERMEABILITY: IMPLICATIONS FOR NEURODEGENERATIVE DISEASES

by

Maunil Kandarp Desai

A Dissertation Presented to the
FACULTY OF THE USC GRADUATE SCHOOL
UNIVERSITY OF SOUTHERN CALIFORNIA
In Partial Fulfillment of the
Requirements for the Degree
DOCTOR OF PHILOSOPHY
(CLINICAL AND EXPERIMENTAL THERAPEUTICS)

May 2019

Dedication

ॐ

सर्वे भवन्तु सुखिनः।

सर्वे सन्तु निरामयाः।

सर्वे भद्राणि पश्यन्तु।

मा कश्चित् दुःख भाग्भवेत्॥

ॐ शान्तिः शान्तिः शान्तिः ॥

May all be happy

May all be free from illness

May all see what is spiritually uplifting

May no one suffer

May peace reign supreme

To all women and men; researchers, scientists, healthcare providers, patients and participants; to each and every one who has contributed to moving the needle to understand, prevent, detect, diagnose and cure every disease we know.

Acknowledgements

To my parents, for all the sacrifices they made to give me the opportunities that I have; for the unconditional love and support that they always and unquestioningly bestowed upon me and for the blessings they shower upon me.

To the Bhavsar family, for taking me under their wings, treating me as a family member and making me feel at home away from home.

To my wife and my in-laws who were ever so supportive in my quest for knowledge and whose contributions are too numerous to list.

To my advisor, Dr. Roberta Diaz Brinton, thank you for your mentorship; for encouraging me to grow as a researcher and for providing me opportunities to learn and gain experience, both in pre-clinical and translational science projects as well as the Allopregnanolone clinical trial. I very much value and appreciate your faith, support and guidance.

To my committee chair, Dr. Stan Louie who has always been supportive, understanding and cared about students with the deepest affection, and Dr. Enrique Cadenas for honoring me by being on my committee and being an amazingly helpful, kind and wonderful role model. Special thanks to Dr. Curtis

Okamoto, Dr. Ronald Irwin, Dr. Annie Wong-Beringer, Wade Thompson-Harper and Rosie Soltero.

To the members of the Brinton Lab, and Dr. Yibu Chen and Meng Li from the Bioinformatics Center, thank you so much for all the help and assistance you all have provided through the years. I appreciate everything each one of you taught me and consider myself fortunate to have you as colleagues and friends.

Last but not the least, to the participants of the Allopregnanolone clinical trial, who were some of the most amazing women and men I have had to opportunity to converse with and whose selfless and anonymous contribution to science is immortalized.

Table of Contents

List of Figures

List of Tables

Abstract

Introduction. The onset of reproductive senescence occurs at the perimenopause, which is characterized by major physiological changes in the endocrinological and reproductive systems which can be associated with altered energy metabolism, cognition, bone-mineral density, cardiovascular function and immune system responses. Our rat model of the perimenopause to menopause to post menopause transitions captures both chronological and endocrinological conversions. In the current study, differential regulation of genes in the hippocampi of the endocrine characterized female rats by sequencing hippocampal total RNA was investigated, based on which it was hypothesized that perimenopausal transition increases blood brain permeability with grave implications for neurodegenerative diseases in women. However, based on rodent model, a novel neuroregenerative therapeutic, Allopregnanolone, may help ameliorate the increase in permeability and improve cognitive function.

Methods. Paired end sequencing of hippocampal total RNA from 36 Sprague Dawley (SD) female rat hippocampi, belonging to six different groups was conducted. A list of differentially expressed genes (DEG) for each comparison was obtained using TopHat and Cufflinks employed in the Partek Flow environment (http://www.partek.com/). Differentially expressed genes were analyzed using Ingenuity Pathway Analysis and PANTHER to identify gene pathways altered during the perimenopause. Blood brain barrier (BBB) permeability was measured in different groups of female SD rats using sodium fluorescein. Both male and female mice were treated with Allopregnanolone intramuscularly. Behavior was assessed using Novel Object Recognition. Plasma and

cortex from mice were queried for 185 metabolites using ultra-performance-LCMS. Mice hippocampi were used for RNA-Seq.

Results. RNA-Seq detected a decrease in platelet-derived growth factor (PDGF) activity, associated with decreased brain estrogen, indicating potential for increased blood brain barrier permeability during the perimenopausal hippocampus. Analyses of significantly differentially expressed genes (DEG) using PANTHER (http://pantherdb.org/index.jsp) revealed enrichment of leukocytes, B and T lymphocyte genes. Curated literature based bioinformatic analysis indicated activation of pathways related to lymphocytic proliferation and differentiation during the transition from regular to irregular cycling, and inactivation of pathways responsible for T cell apoptosis. Interestingly, interleukin-27, a pan-T lymphocyte regulator was down-regulated in the hippocampal transcriptome during the perimenopausal transition, hinting at potential T lymphocyte dysregulation associated with the perimenopausal transition. Increased permeability of BBB during the perimenopausal transition was confirmed using sodium fluorescein. A separate experiment suggested that Allopregnanolone improved cognitive function in human ApoE ε4 allele containing Targeted Replacement mice, potentially upregulated PDGF signaling pathway in the hippocampal transcriptome which suggests protection of blood brain barrier integrity, increased lipid metabolism to generate acetyl-CoA to feed into the TCA cycle and promoted ATP generation in the mitochondria. Further, Allo treatment increased indicators of protein metabolism and potentiated mitochondria in human neural stem cells.

Conclusions. These RNA-Seq and bioinformatic analyses suggested a functional disruption of the blood brain barrier during the perimenopausal transition state that was confirmed. Both chronological and endocrinological aging in female rats resulted in divergence into sub-populations based on blood brain barrier permeability corroborating

evidence of inter-individual variation in neurodegenerative diseases. Allopregnanolone not only ameliorated cognitive function but based on analysis of hippocampal transcriptome suggested amelioration of blood brain barrier permeability, which must be functionally confirmed, and its mechanism elicited in future studies.

1 Background

1.1 Women and Alzheimer's Disease

Alzheimer's disease (AD) is a major cause of morbidity and mortality in the United States. (Association, 2018). Women bear and unequal burden of AD by being more likely to be AD patients as well as caregivers (Beydoun et al., 2013). At age 65, a woman's risk of being diagnosed with AD is almost double that of a man of the same age (Association, 2014).

Recent publications have explored the extent of contribution of sex biology to vulnerability to AD. Even when healthy, adult men suffer from faster reduction in brain volume compared to women (Pfefferbaum et al., 2013), but this is reversed in AD where brain volume declines faster in women than men (Skup et al., 2011). More clarity is needed regarding the contribution of X and Y chromosomes in AD (Snyder et al., 2016).

ApoE ε4 gene, known to increase risk of AD in general, (Corder et al., 1993; Liu et al., 2013), elevates women's risk of developing AD more than men (Farrer et al., 1997b) and causes higher dysregulation of brain functions in women (Altmann et al., 2014; Damoiseaux et al., 2012; Fleisher et al., 2008; Sampedro et al., 2015).

Even though research conducted *in vitro* and in animal models suggested neuroprotective effects of sex steroids (estrogens and progestins) in women, such evidence has been lacking in the clinic and trials in large number of women have not shown benefit of hormonal supplements (Carcaillon et al., 2014; Dubal et al., 2012; Espeland et al., 2004; Gleason et al., 2015; Henderson et al., 2016; Laughlin et al., 2010) and need further investigation. In the future, studies could focus on the mechanisms by which hormones affect the ability of the brain to respond to injury and ameliorate effects of noxious stimuli

in men and women in mid- and late-life thereby clarifying the protective role of sex hormones in AD.

1.2 Women and Immune System

Postmenopausal females are at greater risk for not only AD (Christensen and Pike, 2015) but also autoimmune diseases (Fairweather et al., 2008). Incidence of autoimmune diseases such as Rheumatoid Arthritis and Multiple Sclerosis rise in women through perimenopausal age, peak around menopause and decrease thereafter (Grytten et al., 2015; Peppercorn, 2014). Additionally, evolutionary biologists have hypothesized that earlier age at menopause would shift the onset of RA to the left i.e. the disease incidence would peak earlier in younger age groups (Straub and Schradin, 2016).

Differences in the immune system have been known to exist among males and females across their lifespan, across different mammalian species and in both innate and adaptive immune system (Griesbeck et al., 2015; Klein and Flanagan, 2016; Pisitkun et al., 2006) with an important role for sex steroids (Griesbeck et al., 2015) which suggests that sex steroids, such as androgens and estrogens may be directly responsible for differences in innate immune responses (Hannah et al., 2008).

Males and females differ in the production of cytokines and chemokines (Aomatsu et al., 2013; Rettew et al., 2008; Torcia et al., 2012) and females across different ethnicities have higher counts of helper T cells compared to males (Abdullah et al., 2012; Lee et al., 1996; Lisse et al., 1997; Uppal et al., 2003), and sexes also show differences in the way these helper T cells set up an immune response (Giron-Gonzalez et al., 2000; Hewagama et al., 2009; Roberts et al., 2001; Sankaran-Walters et al., 2013; Zhang et al., 2012). Studies in mice exploring sex-based differences in regulatory T cells describe contrasting results with

respect to organ-specific regulatory T cell counts in multiple diseases; on the other hand, human studies show more regulatory T cells in men versus women (Afshan et al., 2012). Studies have shown that not only B cells are higher in females among older (Teixeira et al., 2011) and younger adults (Abdullah et al., 2012), but PBMCs from both sexes when stimulated lead to a significantly differential alteration in Natural Killer cell count (Abdullah et al., 2012). Another study found sex-based differences in expression of genes in B cells, and authors of the study suspected gonadal hormonal influence (Fan et al., 2014).

1.3 Cognition and Perimenopause

Perimenopause is the period that precedes menopause when women begin to experience menstrual cycle changes (McKinlay et al., 1992; Nelson, 2008) and is associated with hormonal fluctuations (Brinton et al., 2015; Burger et al., 1998). Perimenopausal women not only undergo changes in the reproductive system but neurological alterations are also observed (Genazzani et al., 2005; Greendale et al., 2010; Maki et al., 2008).

Decline in levels of estrogen around menopausal transition are associated with declines in cognitive function as well as receptor expression alterations (Arimoto et al., 2013; Paris et al., 2011; Sherwin, 1994, 2003; Woods et al., 2000). It has also been shown that this cognitive decline due to change in the hormonal environment is age independent (Berent-Spillson et al., 2012) but dependent on endocrine status (Weber et al., 2014). A clinical review published in 2016 concluded that while cognitive decline is attributable to menopause, HRT is not recommended as treatment (Maki and Henderson, 2016).

A large number of women will be undergoing menopausal transition in the next decade, with estimates of up to 1.1 billion women (Shifren et al., 2014) and these women will be vulnerable to neurodegenerative diseases such as AD. Therefore, it is important to

understand perimenopause-induced changes in the brain using a translationally valid model, such as in rodents (Diaz Brinton, 2012; Finch, 2014).

1.4 Estrogen, Blood Brain Barrier and AD

Brain has always been believed to be an immune-privileged site protected by the BBB from circulating immune cells, until recently when lymphatic vessels were discovered in the walls of dural sinuses (Louveau et al., 2015). The BBB consists of a physical barrier of endothelial cells, astrocytes, and pericytes, all of which regulate transport of substances from general circulation to the brain. Transcellular passage of proteins requires ligand-specific receptors and transporters, while paracellular passage of cells is strictly limited by junctional proteins located in the clefts between endothelial cells (Raub et al., 1992; Wolburg and Lippoldt, 2002).

1.4.1 SEX STEROIDS AND BBB

Sex-steroid dependent changes in BBB have been observed (Bake and Sohrabji, 2004) which may be due to control of gap junction protein, connexin 43, being under the control of steroid hormones (Gulinello and Etgen, 2005). 17β-estradiol (or E2) affects tight junction (TJ) protein, such as occludin, and endothelial cells of blood vessels (Ye et al., 2003) along with another TJ protein called zonula occludens-1 (ZO-1) (Khan-Dawood et al., 1996). Recently, a study proved the protective role of estrogen in specifically guarding the BBB against lymphocytic invasion in a proinflammatory environment (Maggioli et al., 2016), which would explain previous published observation that repeated estradiol treatment prevents BBB disruption due to antigenic stimulation (Tomás-Camardiel et al., 2005).

Mechanistically estrogens play a major role in maintaining healthy BBB (Fig. 1.1), via upregulation of PDGF, VWF and TGFBR1, and downregulation of SLC38a3, Aqp4, SLC13a3 and VCAM1 (Humphreys et al., 2014).

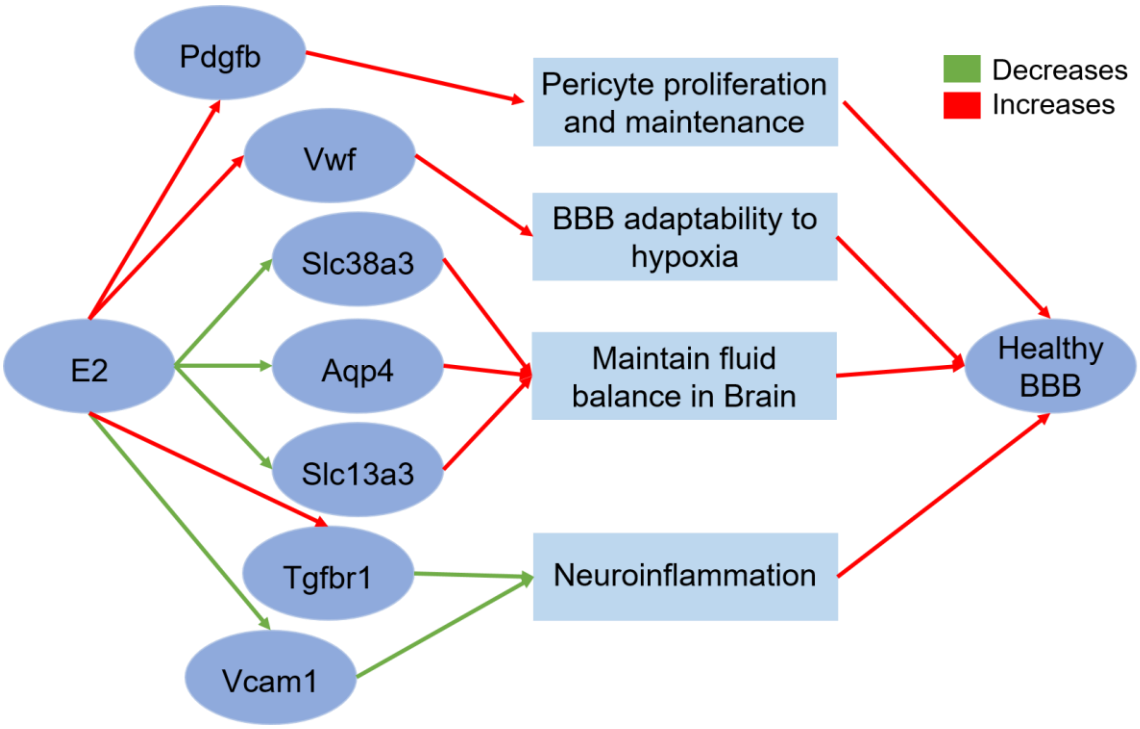

Figure 1.1 **Role of estrogen in maintaining a healthy blood brain barrier**.
Estradiol (E2) upregulates Pdgf, Vwf, Tgfbr1 and downregulates Slc38a3, Aqp4, Slc13a3, and Vcam1 to promote pericyte proliferation and maintenance, enhance BBB adaptability to hypoxia, maintain fluid balance in brain and prevent or reduce neuroinflammation.
Pdgf=Platelet Derived Growth Factor, Vwf=von Willebrand Factor, Tgfbr1=Transforming growth factor beta 1, Aqp4=Aquaporin-4, VCAM1=vascular adhesion molecule 1, SLC38a3 SLC13a3 are both solute carrier proteins.

Evidence exists that implies that female gender is at a higher risk for increased BBB permeability, based on findings from an acute sepsis model (Minami et al., 2002), and extravasation of Evan's blue dye in a hypoosmolality model (Oztaş et al., 2000). One study also found that in CSF expression of IgG increases significantly with increase in age (Pakulski et al., 2000).

Although the family of estrogens are grouped together, they have specific effect on the BBB. Artificial estrogen such as ethinyl estradiol was found to elevate BBB permeability to albumin (Gammal and Zuk, 1980), water (Reid et al., 1983), inulin and sucrose (Ziylan et al., 1990), whereas endogenously produced estrogen, 17β-estradiol, was found to be protective in cases of neural injury models, such as injury caused by ischemia (Chi et al., 2005; Chi et al., 2002), VEGF- (Chi et al., 2004) or 3-nitropropionic acid (Nishino et al., 1998) in which estradiol treatment resulted in a less leaky BBB. Literature also suggests that estrogenic neuroprotection is likely mediated via both ERα and ERβ (Naderi et al., 2015). Thus, the effect of estrogens on the BBB integrity may be compound specific and dependent on the type of cells that it may affect.

1.4.2 AD AND BBB

In AD, it is found that capillary density (Fischer et al., 1990) and capacity (Bell and Ball, 1986) both change. Also, nerve plexuses adjacent to blood vessels are lost (Scheibel and Duong, 1988) with an increase in nitric oxide synthase activity (Dorheim et al., 1994) and lipid peroxidation (Andorn et al., 1998). Post-mortem studies have found blood-borne proteins from the periphery (pro-thrombin, albumin, immunoglobulins, fibrinogen, and thrombin) accumulated in the brain of AD patients implying BBB disruption (Fiala et al., 2002; Hultman et al., 2013; Ryu and McLarnon, 2009; Salloway et al., 2002; Zipser et al., 2007). D'Andrea has suggested that AD exhibits signs of being an autoimmune disease where neurons may be targeted after the BBB is disrupted (D'Andrea, 2005) based on findings that show increase in IgG-positive neurons in the hippocampus and entorhinal regions of AD brains which was 8 times when compared to brains of non-AD individuals in similar age range (D'Andrea, 2003). Aβ overproduction in AD due to APP gene mutation results in amyloid accumulation in the brain and cerebrovasculature, concurrently with

BBB disruption (Iadecola, 2004; Jellinger, 2002; Zlokovic, 2005). A pilot study found that amyloid deposition in cerebral vessels correlates with recognized criteria for AD diagnosis (Attems and Jellinger, 2004). In the triple transgenic AD mouse model, both the amyloid deposition and memory deficits are preceded by a disruption of the BBB (Ujiie et al., 2003). It is evident that estrogen is an important regulator of BBB integrity, thus the decline in sex steroids, specifically estradiol, in the perimenopausal rats, is likely to negatively affect BBB integrity. A compromised BBB would increase women's risk of cognitive decline as seen in AD as well as susceptibility to autoimmune diseases.

1.5 The Rodent Perimenopausal Model

While both men and women undergo puberty, menopause is unique to women. Menopausal transition takes years to complete. It begins with subtle changes in experience which can last for up to 5 years, then proceeds to irregular periods and this may last for 3 years before the Last Menstrual Period (LMP) and cessation of menses, ushering in menopause (Nelson, 2008). The years of transition before menopause are termed as the perimenopausal period. Even though symptoms of menopause do not begin till mid to late forties, estrogen levels, after peaking between late twenties and early thirties, begin to decline years before the last menstrual period (Sherman et al., 1976).

1.5.1 DIFFERENT RODENT MODELS OF MENOPAUSE

Studies of reproductive aging in humans are complex (Henderson and Brinton, 2010; Soares and Maki, 2010; Soules et al., 2001). This complexity can be better understood using animal models that offer a glimpse into the biology of human reproductive senescence. Animal models make it easier to explore and understand the multiple parallel events that occur in organs and organ systems, as well as changes in cellular, molecular,

and genomic processes during perimenopausal transition (Bellino, 2000; Bellino and Wise, 2003; Van Kempen et al., 2011; Walker and Gore, 2011; Walker and Herndon, 2008). Accordingly, the translational validity of animal models is of extreme importance in order to understand etiopathogenesis of diseases suspected to begin during this period, identify and develop new drugs, and predict results of therapeutic interventions (Brown, 2012; Jucker, 2010; Nakao et al., 2009; Shineman et al., 2011). Comprehending the validity of translational animal models of human menopause would allow the scientific community to better integrate *in vitro* data, *in vivo* observations in animal models, evidence and observations from population-based epidemiological studies, as well as results of intervention trials (Diaz Brinton, 2012). Three of the most commonly used animal models to study human reproductive senescence in women are (1) natural reproductive senescence or ovary-intact model, (2) ovariectomy or surgical menopause model and (3) using ovotoxins to induce accelerated ovarian failure (Koebele and Bimonte-Nelson, 2016).

Female rodents undergo estrus cycles, akin to humans' menstrual cycle and these estrus cycles become irregular in mid-to-old aged rodents before ceasing to operate and these changes in estrus cyclicity are associated with neuroendocrine changes (Downs and Wise, 2009; Kermath and Gore, 2012; Wise et al., 2002). Hence, the natural reproductive senescence model can be used to understand age-related alterations in the brain at cellular and molecular levels that are part of normal reproductive aging which in turn would help us develop better therapies to address symptoms associated with aging and menopause (Koebele and Bimonte-Nelson, 2016), despite some drawbacks of the ovary-intact model such as differences in hormonal levels and ovarian follicle reserve compared to humans and inter-animal variability (Burger, 2006; Lu et al., 1979; Timiras et al., 1995).

The ovariectomy (OVX) model of surgical menopause entails bilateral excision of the ovaries (Olson and Bruce, 1986). The OVX model helps explore and understand the effects of lack of sex hormones on various organs and organ systems as well as delineate the effect of externally administered steroids on brain and periphery (Koebele and Bimonte-Nelson, 2016). As far as translational research is concerned, OVX model is quite different from how most women undergo perimenopausal transition. Also, the age at which ovaries are excised in rodents has bearing on the results (Chakraborty and Gore, 2004; Diz-Chaves et al., 2012; Foster et al., 2003). The hormonal profile in the OVX model is different from the one found in human females (Mayer et al., 2004; Mayer et al., 2002). While the surgical model of menopause has its own merits in assessing the effects of specific hormones and drugs on brain and body systems in the absence of steroid hormones produced endogenously, it is also equally important to understand the processes of natural reproductive senescence as well as the manner in which exogenous hormones interact with the organ systems in presence of intact ovaries.

The ovotoxic model of human menopause in rodents is dependent on using a chemical called 4-vinylcyclohexene diepoxide, or VCD, a metabolite of 4-vinylcyclohexene (Hoyer et al., 2001; National Toxicology, 1989). Researchers have used this chemical to develop a rodent model of menopause since the chemical reduced the pool of ovarian follicles that are not growing but leaves growing follicles unaffected, (Borman et al., 1999; Flaws et al., 1994; Hirshfield, 1991; Hoyer et al., 2001; Hu et al., 2001a; Hu et al., 2001b; Kao et al., 1999; Mayer et al., 2004; Mayer et al., 2005; Mayer et al., 2002; Springer et al., 1996a; Springer et al., 1996b; Springer et al., 1996c) which is the result of the chemical upregulating pro-apoptotic proteins in affected follicles (Hu et al., 2001a; Hu et al., 2001b; Springer et al., 1996a; Springer et al., 1996b; Springer et al., 1996c; Van Kempen et al.,

2011). Follicular depletion caused by VCD in female rodents results in hormone profiles similar to ovary-intact menopausal women (Acosta et al., 2009; Acosta et al., 2010; Mayer et al., 2004; Mayer et al., 2002; Timiras et al., 1995).

Toxic and carcinogenic effects of this compound as well its potential for accumulation in the brain due to its lipophilic nature are major drawbacks of this model (Diaz Brinton, 2012; Van Kempen et al., 2011).

While each animal model has its own strengths and weaknesses with regards to human menopause, natural reproductive senescence in rodents closely mimics many features of human menopausal transition (Morrison and Baxter, 2012; Walker and Herndon, 2008). This perimenopausal rodent model may help better understand the biological processes occurring in humans and subsequently assist in developing effective therapies (Bethea et al., 2000; Choi et al., 2003; Kaplan et al., 2010). While the perimenopausal transition in the rodents takes place over a much shorter time period, it shows many features found in the human natural reproductive senescence such as decline in ovarian follicles, lengthening of estrus cycles that results in irregular cycling due to steroid hormone fluctuations, and irregular fertility (Finch et al., 1984; Van Kempen et al., 2011). Cycle length irregularity is a good proxy for irregular fertility and advancing reproductive senescence, which begins at approximately 8 months of age (Finch et al., 1984).

1.5.2 THE NATURAL REPRODUCTIVE SENESCENCE OR OVARY-INTACT MODEL IN PRACTICE

Previously, Brinton lab has conducted studies using the ovary-intact or natural reproductive senescence model of human menopause in female Sprague-Dawley (SD) rats (Yin et al., 2015). Young female SD rats have 4-5-day estrus cycle, and these rats are called regular cyclers (Finch, 2014). 5-8 day long irregular cycles observed at the

beginning of reproductive senescence are found in a small percentage of rats around 6 months of age, but the rest of female rats at that age were found to be regular cyclers (Yin et al., 2015). The percentage of irregular cyclers increase in number until 9-10 months of age when irregularly cycling rats constitute the majority of female rats in the group at that

Comparison	Transition focus
Regular cyclers 9m vs. Regular cyclers 6m	Chronological aging pre-transition
Irregular cyclers 9m vs. Regular cyclers 9m	Endocrinological transition
Acyclic 9m vs. Irregular cyclers 9m	Endocrinological transition
Acyclic 16m vs. Acyclic 9m	Chronological aging post-transition

Table 1.1 **Comparisons of the different chronological and endocrinological groups of female rats**.
The first comparison aims to detect the effect of chronological aging before endocrinological transition (pre-transition). The second and the third comparisons aim to detect the effect of endocrinological transition to menopause while controlling the age variable, and the last comparison aims to detect the effect of chronological aging post-transition.

age (Yin et al., 2015). At the same time, some female rats no longer undergo estrus cycling and transition to constant estrus phase of reproductive senescence that continues up to at least 16 months of age (maximum period under study). Hence, we have five groups of female rats, 6 month old female rats that cycle regularly (Regular cyclers 6m), 9-10 month old female rats that cycle regularly (Regular cyclers 9-10m), 9-10 month old female rats that cycle irregularly (Irregular cyclers 9-10m), 9-10 month old female rats that no longer cycle (Acyclic 9-10m) and 16 month old female rats that no longer cycle (Acyclic 16m). Table 1.1 summarizes the different aspects of menopausal transition that can be studied using the rat model described, while keeping either the age or the endocrinological status as a constant. Regular cyclers 6m and Regular cyclers 9-10m groups of female rats differ in age but have similar estrus cycles (regular 4-5-day cycles) and therefore allow the

detection of effects of aging in female rats before the occurrence of menopausal transition. The three groups of 9-10-month-old animals (Regular cyclers 9-10m, Irregular cyclers 9-10m, Acyclic 9-10m) allow the comparison of the perimenopausal transition stages while keeping age constant. The last group of animals (Acyclic 16m) helps detect age related changes in acyclic animals when compared to Acyclic 9-10m group.

1.6 Conclusion/Hypothesis

Thus, it can be concluded that women are more susceptible to cognitive decline and AD, immune dysregulation and even autoimmune diseases later in life to which perimenopausal transition maybe a contributing factor, and sex-specific steroids, mainly estrogen, play a major role in maintaining both cognition and healthy immune system. A systems biology approach to understanding the hippocampal transcriptomic changes during the perimenopausal transition in female SD rats could elucidate the pathways in the hippocampus that influence physiologic alterations preceding actual pathologies. A breached blood brain barrier could make women increasingly more susceptible to noxious substances from the peripheral circulation and I hypothesize that this breach happens during the perimenopausal transition. A compromised BBB by itself may not result in outward manifestation of pathogenesis specific to a particular disease. However, interaction between a compromised BBB and other injurious stimuli such as aggregates of Aβ or α-synuclein, low-grade chronic inflammation seen in aging or environmental factors in the presence of genetic susceptibility could further accelerate the erosion of BBB integrity potentially subjecting females to increased vulnerability to AD or autoimmune disease states. The breached BBB could potentially be ameliorated by a neurosteroid such as Allopregnanolone which in pre-clinical studies has resulted in improvement of cognitive function.

2 Transcriptomic Analysis

2.1 Abstract

In this study I applied a systems biology approach to the hippocampal transcriptome during the perimenopausal transition in order to determine the underlying mechanisms that make women susceptible to AD and other degenerative disease during and after the menopausal transition. Hippocampal transcriptome from six different groups of female rats was queried using high-throughput RNA sequencing and the data was analyzed using two different bioinformatic tools. Findings suggested immune dysregulation, compromised blood brain barrier and downregulation of metabolic and bioenergetic pathways in the hippocampus during the perimenopausal transition and these findings need to be examined in greater detail to understand cell-type specific and pathway dependent alterations in the hippocampus during perimenopause.

2.2 Introduction

Aging hippocampus (Colangelo et al., 2002; Terao et al., 2002), and other parts of the brain (Lee et al., 2000) exhibit differential expression of genes that are known to have immune system functions. These changes were known to be sexually dimorphic with proportionally greater activation of immune system in the female brain (Berchtold et al., 2008). Also genes that were highly expressed with age appeared to be involved in activation of T cells and microglia and also included proinflammatory cytokines and chemokines (Wyss-Coray, 2006). In adult human brain it was found that among the genes that are most differentially expressed between the two sexes, the most significant genes seem to have immune functions (Trabzuni et al., 2013). This would explain why immune-

related diseases have a gender dependent bias (Fung et al., 2012; McCombe et al., 2009) such as the bias seen in multiple sclerosis and AD (Amor et al., 2010). Innate immune system found in the aging hippocampus of female rats was detected to be responsive to the hormonal environment (Sárvári et al., 2012; Sárvári et al., 2014). As aging proceeds immune system becomes senescent along with development of age-related long-term low-grade inflammation which in turn could repeatedly prime microglia, which likely lose their neuroprotective function and further activate innate and adaptive immune pathways in the brain (Deleidi et al., 2015). This profile of high-risk of abnormal immune response associated with aging results in atypical inflammatory cascades which in turn could increase susceptibility to diseases.

Based on these observations in literature as well as the results of the customized gene array data obtained and published earlier (Yin et al., 2015) by Brinton lab, led to a more bioinformatics intensive approach using transcriptomic analysis for an in-depth understanding of the systems biology of the aging female hippocampus during the perimenopausal transition in female SD rats.

2.3 Materials & Methods

2.3.1 ANIMALS

The process by which animals were classified into groups for this experiment is outlined in detail in the published work by Dr. Fei Yin from Brinton lab (Yin et al., 2015). Briefly, 5 and 8-month-old female Sprague-Dawley (SD) were cycled and their estrus cycle status was documented every day in the morning using vaginal cytology of smears obtained via lavage with PBS. Based on age and regularity of estrus cycling animals were classified into Regular and Irregular groups at 6 and 9-10-months of age. Those female rats that did not cycle and exhibited a constant estrus stage every day for at least nine consecutive

days were labeled as Acyclic, which were divided into two groups based on age: 9-10-months old and 16 months old. Rats that did not meet the predetermined criteria for classification into groups were not included in the study. An OVX group of female rats was added which consisted of regularly cycling female rats at 9-10 months of age that were ovariectomized at 9-10-months of age and euthanized at 10-10.5-months. Thus, I had six groups in the study based on age and endocrine status: Regular cyclers 6m, Regular cyclers 9-10 months, Irregular cyclers 9-10 months, Acyclic 9-10 months, Regular OVX 10-10.5 months and Acyclic 16 months.

After anesthesia, we rapidly dissected the brains on ice, dissected out cerebellum and brain stem and separated the two hemispheres, which were peeled laterally to obtain the hippocampus from each brain. All dissected tissues were frozen in −80 °C for planned experiments. PureLink RNA Mini Kit (Invitrogen) was used to isolate RNA from rat hippocampal tissues. Some of the data obtained from these rats were published in Yin et al., 2015.

2.3.2 SEQUENCING OF HIPPOCAMPAL RNA

The RNA extracted from the hippocampus of female rats was sent to Active Motif (Active Motif Inc., Carlsbad) for sequencing and raw reads in the form of FASTQ files were obtained. Before sequencing Active Motif analyzed RNA quantity and quality using Qubit RNA IQ Assay (Thermo Fisher, MA) and all samples exhibited high RNA quality. RNA from 36 female rats that belonged to the six groups mentioned earlier were sequenced, with six rats per group. Paired end sequencing of hippocampal RNA was carried out with read length of 50 base pairs and a read depth of about 50 million reads per sample using Illumina HiSeq 2500.

2.3.2.1 The RNA-Seq process

The comprehensive set of transcripts in a cell i.e. the transcriptome, sheds light on the processes occurring in the cell and can help understand the physiology and pathology of various cellular function and disease states. (Wang et al., 2009). Transcriptomic studies via microarrays and Sanger sequencing both have drawbacks. (Boguski et al., 1994; Gerhard et al., 2004; Kodzius et al., 2006; Okoniewski and Miller, 2006; Royce et al., 2007; Wang et al., 2009). RNA-Seq can detect previously unknown transcripts (Vera et al., 2008), provide data on Single Nucleotide Polymorphisms (SNPs) (Cloonan et al., 2008; Morin et al., 2008), shows very low background signal (Wang et al., 2009) and possesses high level of accuracy and reproducibility (Cloonan et al., 2008; Mortazavi et al., 2008; Nagalakshmi et al., 2008) and 1% error rate (Dohm et al., 2008). Isolated total RNA is first selected or enriched for mRNA or other RNAs such as long non-coding RNA, and then converted to cDNA, which is then sequenced through repeated rounds of pre-determined steps such as incorporation of nucleotide base, washing, imaging and severance, and fluorescent imaging is used for detection of the incorporated nucleotide (Bentley et al., 2008; Guo et al., 2008; Wang et al., 2009). The Illumina HiSeq 2500 was used to sequence RNA for this study.

2.3.3 ANALYSIS OF SEQUENCED HIPPOCAMPAL RNA

I first trimmed raw reads (files with extension .fastq) from both ends using a Phred score threshold of 20 and read length of 25 in Partek Flow version 5.0. The Partek Flow software suite is available through the USC Norris Medical Library Bioinformatics Services (http://norris.usc.libguides.com/nml-bioinfo). I mapped the reads using TopHat2 to the Rn6 rat reference genome (Ensemble 80) and quantified to transcriptome using Cufflinks. Only annotated transcripts were quantified, and I used bias correction and multi-read

correction along with upper quartile normalization to generate deferentially expressed genes (DEG) list for each comparison group. The development of this bioinformatics pipeline is discussed in detail in the results section. The DEG lists for each comparison group was then uploaded into Ingenuity Pathway Analysis (IPA) software and Protein ANalysis THrough Evolutionary Relationships (PANTHER) to explore differential regulation of critical pathways during the perimenopausal transition in the hippocampus.

2.3.4 STATISTICAL CONSIDERATIONS

Differential gene expression data obtained through gene arrays and RNA-Seq methods necessitate a rethink of statistical considerations. A simple statistical cut-off of $p<0.05$ for significantly differentially expressed genes does not suffice due to the errors introduced by multiple comparisons which essentially includes thousands or even tens of thousands of genes. For this purpose, I used a cut-off of FDR <0.05 for individual genes of statistical significance. FDR (also termed 'q') is defined as the expected proportion of type I errors or false positives (Colquhoun, 2014). At the same time, I used FDR<0.2 while carrying out analyses of biological pathways. (FDR=False Discovery Rate=q)

2.3.5 CHOICE OF SOFTWARE FOR PATHWAY & NETWORK ANALYSIS

At the end of many experiments that result in large amount of data of protein expression, gene expression or metabolic data, the next question is how to obtain meaningful and biologically relevant analyses from these datasets. The abundance of transcriptomic data that resulted from the RNA-Seq required a way to analyze and interpret it. Annotation enrichment, also called pathway analysis (Curtis et al., 2005), allows us to understand the biological underpinnings of differences in gene expression related to experimental conditions. Researchers have mapped genes and proteins to their associated expression,

structure and functions and have divided each of these parameters into three domains: cellular component, molecular function and biological process and then provided a name (term) and a unique numeric identifier for each such term called Gene Ontology (GO) term (Ashburner et al., 2000). The presence of these GO terms in the experimental data with higher than background frequency is called “enrichment” (Huang et al., 2008a). It is important to note that GO is not complete and it’s a work currently in progress (Baumgartner Jr et al., 2007; Lewis, 2017). Therefore, its annotations could be biased towards well-studied genes and well-studied diseases (Alterovitz et al., 2006; Young et al., 2010).

Functional tools for enrichment such as Database for Annotation, Visualization and Integrated Discovery i.e. DAVID (Dennis et al., 2003; Huang et al., 2008b), look at relationships between different terms and integrate annotation terms from various different sources and lower the redundancy which provides a more biology centric rather than gene centric approach (Huang et al., 2008a; Khatri and Drăghici, 2005).

From a list of various excellent functional enrichment tools available (Ramanan et al., 2012), the pathway annotation tools I considered for my RNA-Seq data were IPA and PANTHER. Using the gene-expression dataset from my RNA-Seq study, I wished to explore the biological pathways and functions represented by the transcriptomic data as well as observe the predicted upstream regulators and diseases processes.

The causal network underlying IPA algorithms is based on the Ingenuity Knowledge Base (Krämer et al., 2013), with extensive findings manually curated as well as a huge number of nodes and molecules.

I also considered Cytoscape and MetaCore. However, there are both advantages and disadvantages of using Cytoscape versus IPA. While IPA is easier to learn than

Cytoscape, and learning curve is subjective; it provides less information about the 'networks' (Thomas and Bonchev, 2010). Cytoscape lets researchers carry out the statistical assessment of network properties based on graph theory, while IPA only provides graphical representation of biological pathways as networks of interacting genes and emphasizes predominantly the biological nature of the pathways and not their graph theoretical properties (Thomas and Bonchev, 2010). Therefore, I considered IPA a good resource for specific molecular/cellular pathways based on known biological interactions, as opposed to the more theoretical approach to network analysis provided by Cytoscape. MetaCore requires a paid subscription and unfortunately not procured by University of Southern California, unlike IPA. A study that compared 10 different pathway databases, including IPA and MetaCore, concluded that different pathway analysis tools and software programs will provide slightly different results and therefore biological relevance and cross-validation with existing data are prerequisites for choosing a pathway database or tool (Shmelkov et al., 2011). In order to retain a more unbiased and holistic view of my dataset, I also utilized PANTHER. IPA functional enrichment assesses for pathways based on IPA's proprietary 'knowledge base'. This knowledge base is based upon manually-curated descriptions of gene-gene (or protein-protein) interactions from the literature and IPA is therefore able to provide gene interaction pathways and upstream regulators. PANTHER on the other hand assesses for functional enrichment into known GO categories which are publicly accessible (Mi et al., 2013). Using both IPA and PANTHER thus provided curated knowledge from two completely different unrelated sources. According to authors of a published study that evaluated multiple different analysis tools, researchers should use at least two different analysis tools or software and then base their

conclusions on the common findings from the two different tools (Thomas and Bonchev, 2010).

In brief, I chose the analysis pipeline for RNA-Seq data that delivered results most consistent with our previously published data (Yin et al., 2015), which is in agreement with a recent review on multiple sources of bias that could confound functional enrichment analysis of -omics data (Timmons et al., 2015).

2.4 Results

2.4.1 DEVELOPING RNA-SEQ ANALYISIS PIPELINE

It was initially challenging to develop an analysis pipeline for the RNA-Seq data as we possessed previously published data from the perimenopausal rat model and our goal

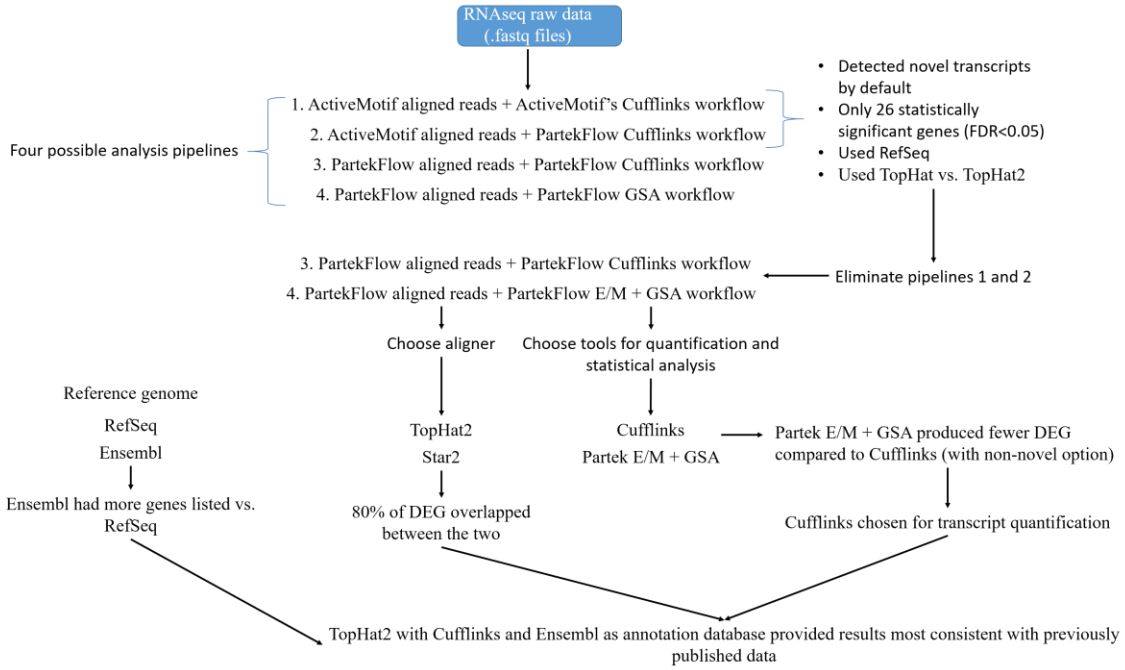

Figure 2.1 **Flow chart of data analysis for RNA-Seq bioinformatics pipeline**. RNA-Seq was carried out by Active Motif but their bioinformatics pipeline did not meet our needs. I developed a customized data analysis pipeline for analyzing the data from the hippocampal RNA-Seq based on two factors: cross-validation with published biologically releavnt data and using latest versions of well-referenced bioinformatic tools.

was data consistency and cross-validation. The sequencing of RNA was carried out by Active Motif (AM) and the company provided us with a list of differentially expressed genes (DEG) for each comparison between the six groups. However, the analysis pipeline carried out by the company to obtain the DEG was standardized, detected novel transcripts by default and provided 26 statistically significant genes (FDR<0.05). I therefore developed a customized fine-tuned workflow with more updated gene annotation to produce biologically relevant results compared to those from AM's generic pipeline.

I followed a method of trial and error in analyzing the RNA-Seq data from raw reads stage (.fastq files) to establish an analysis pipeline that provided biologically consistent results. With that goal in mind I attempted multiple permutations and combinations to construct an analysis pipeline that delivered results consistent with published data.

Each of my analysis focused on a single DEG list obtained when comparing two groups: Irregular 9-10m and Regular 9-10m in order to evaluate multiple pipelines for the identical comparison. For the process of alignment of raw reads I used three different options available to me: using aligned files (.bam) provided by AM using TopHat, aligning

Figure 2.2 **Developing RNA-Seq data analysis pipeline: First iteration.**
In the first iteration, multiple different permutations and combinations of two aligner tools, two sets of rat reference genomes and two different tools for transcript quantification were conducted to select the most appropriate bioinformatic pipeline.

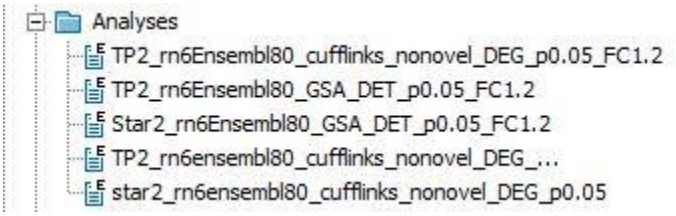

Figure 2.3 **Developing RNA-Seq data analysis pipeline: Second iteration**.
After narrowing down the number of analysis pipelines to five, in the second iteration results from all five pipelines were cross-validated with published data from the perimenopausal model.

raw reads myself using an aligner called TopHat2 (Kim et al., 2013a) and aligning reads using a different aligner called Star2. At the next step, aligned raw reads need to be quantified and statistical analysis must be carried out to generate DEG, for which I decided to use both Cufflinks (Trapnell et al., 2013; Trapnell et al., 2010) and Gene Specific Analysis (GSA). Cufflinks has its own tools for statistical analysis called Cuffmerge and Cuffdiff (Trapnell et al., 2012) to generate lists of DEG and differentially expressed transcripts (DET) after transcript quantification. However, GSA is a statistical analysis tool and must be used in conjunction with Partek E/M (Partek Flow's optimization of the expectation-maximization algorithm) for transcript quantification. I also found that using the right annotation for the rat reference genome could vary results. I considered two annotation tools, RefSeq and Ensembl, but ultimately decided in favor of Ensembl since Ensembl annotates many more genes than RefSeq (Zhao and Zhang, 2015). Based on the initial evaluation of different pipelines (Figure 2.2 – screenshot of all pipelines from IPA) I determined that for RNA quantification and DEG analyses, Cufflinks + Cuffdiff and Partek E/M + GSA were the most appropriate methods, but I was still considering both aligners Star2 and TopHat2. When all other parameters were the same, Partek E/M + GSA produced 30% fewer DEG than Cufflinks. About 60% of the former overlapped with the latter, but less than 35% of the latter overlapped with the former. When all other parameters were the same, the choice of different alignment methods (TopHat2 vs Star2) had limited impact on the DEG results as over 80% of DEG

overlapped. Based on these results, I narrowed down the bioinformatics pipeline to five (Figure 2.3 – screenshot of all pipelines from IPA) and used the newest available version of the annotation tool Ensembl (Ensembl 80). Next, I looked at functional data from all five pipelines in IPA which included canonical pathways, upstream regulators and disease and functions (Figures 2.4 and 2.5 – images exported from IPA).

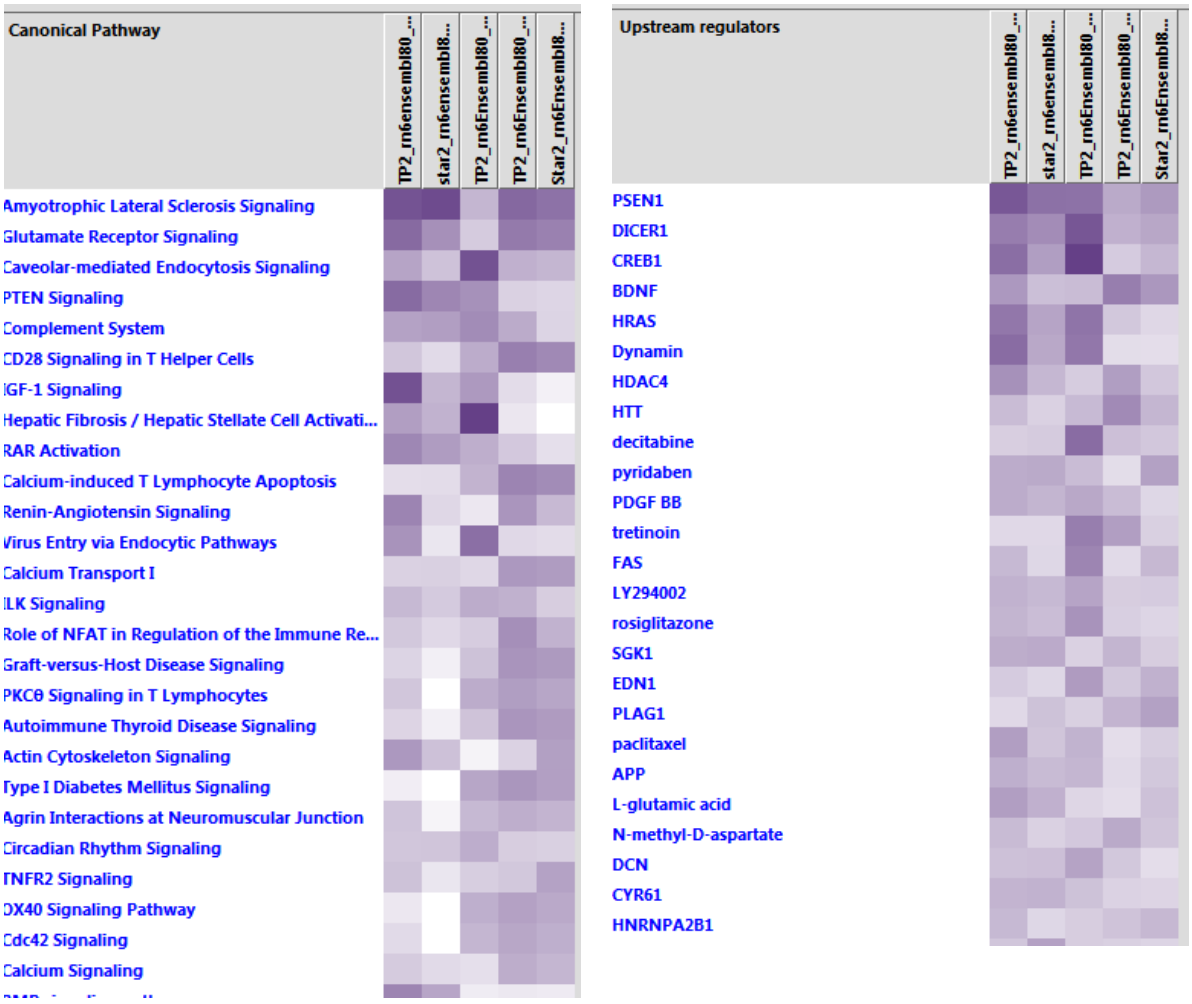

Figure 2.4 **Functional analyses results of the second iteration with five DEG lists**. As seen in this image exported from IPA, the final five bioinformatic analysis pipelines were tested for functional data in IPA cross-validated with published literature on perimenopausal model. Overall, they exhibit similarity, especially for the top ranked items in canonical pathways and upstream regulators (ranked by p-value of overlap).

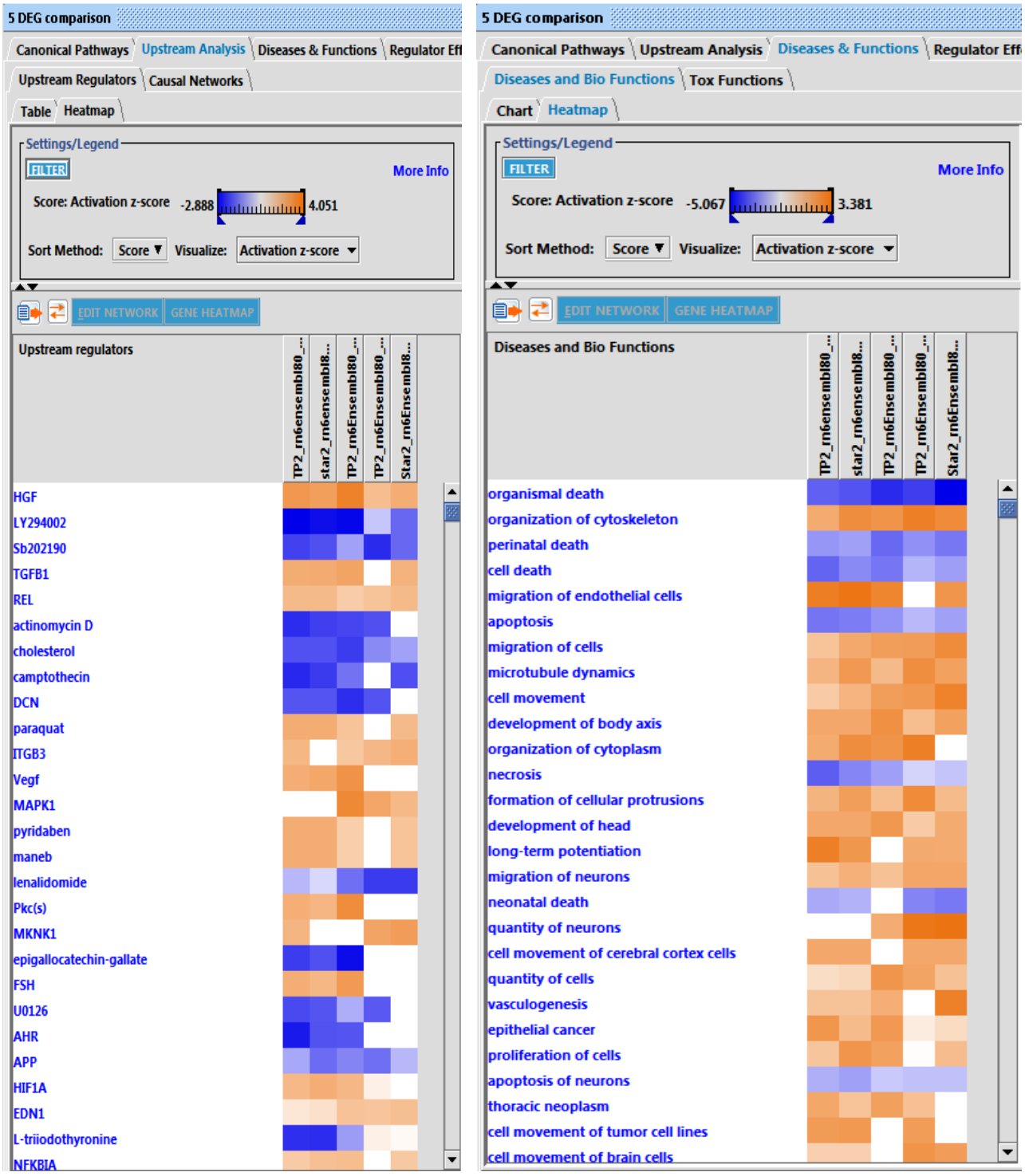

Figure 2.5 **Functional data used to develop bioinformatics pipeline**.
As seen in this image exported from IPA, diease and biofunctions, and upstream regulators obtained using five DEG lists of second iteration used to develop bioinformatics analysis pipeline. Overall, they exhibit similarity.

To help determine which DEG list makes the most sense, I created 20 gene lists for the key functional concepts mentioned in Yin et al., 2015 and conducted the functional analyses considering these gene lists (Fig 2.6 – image exported from IPA). Based on this evaluation, the TP2_rn6Ensembl80_Cufflinks_nonovel was found to be the best method

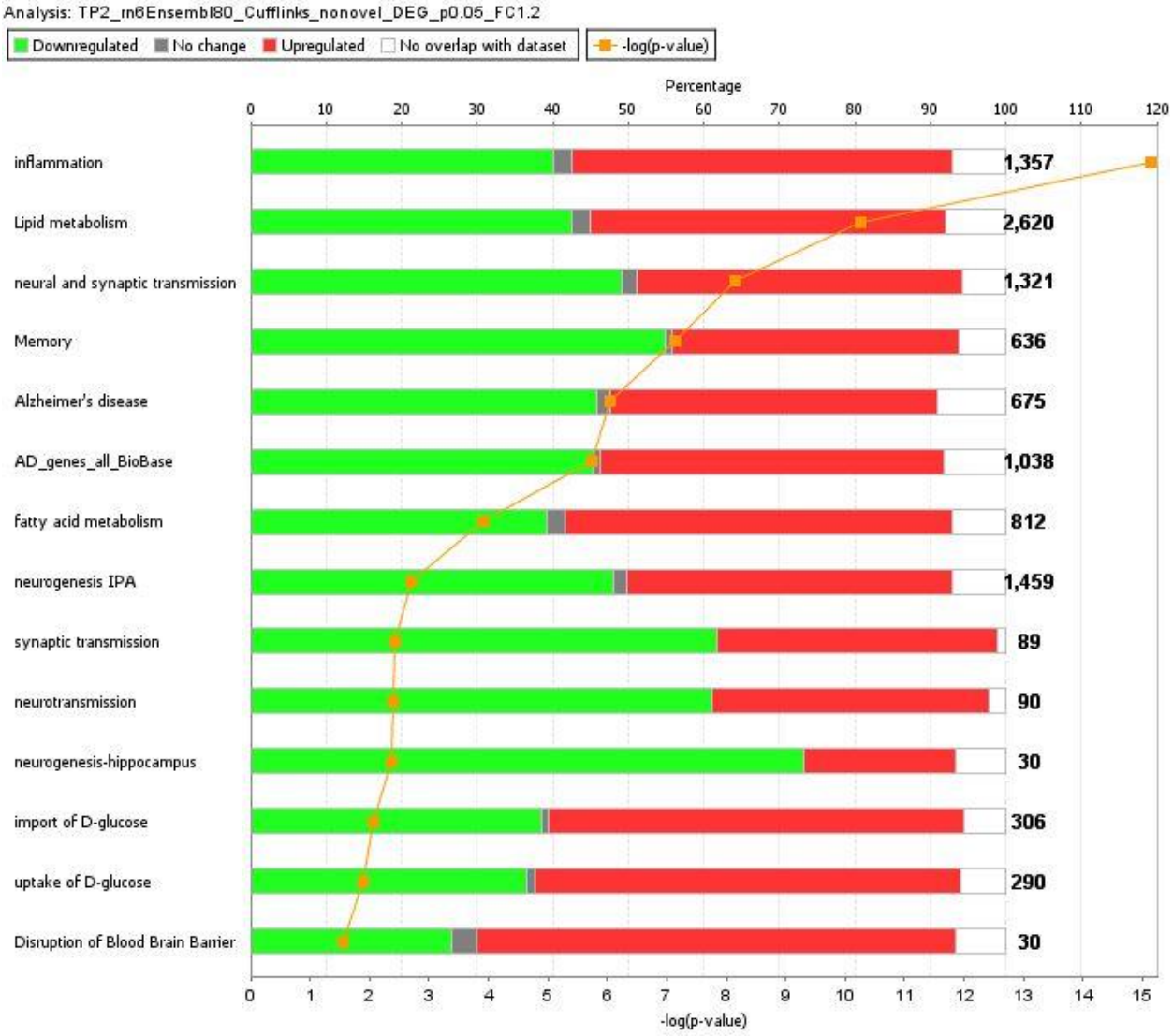

Figure 2.6 **RNA-Seq data analysis: Cross validation with pathways published previously**.
As seen in this image exported from IPA, final five bioinformatics pipelines under consideration were cross-validated with previously published findings from Yin et al., 2015.

with biologically relevant results and was chosen for all subsequent analysis. The novel

transcript option does not require any annotation reference, it will carry out de novo assembly to reconstruct transcripts and estimate their abundance. I instead chose the non-novel (or annotated transcripts) option for transcript quantification when running Cufflinks to focus on mapping known genes and transcripts.

For additional cross-validation, the 8 down-regulated genes (Atpaf2, Esrra, Nfkb2, Il1rl1, Mapk3, Plcb3, Thop1, Map2) reported in Yin et al., 2015 were checked against DEG results from the chosen method and except Map2, all other genes were found to be consistently down-regulated, similar to published findings. Map2 has three different isoforms, only one of which was down-regulated. This bioinformatic pipeline was used to analyze the hypothalamic RNA-Seq data published this year (Bacon et al., 2018).

2.4.2 MAPPED TRANSCRIPTS FOR EACH COMPARISON GROUP

The Differentially Expressed Gene (DEG) list generated by Cufflinks enumerated more than 32,000 transcripts out of which 20,493 were mapped to genes in the rat genome within IPA. Only a tiny fraction (ranging from 0.27% - 1.93%) of the total number of hippocampal genes mapped by IPA to the rat reference genome met the FDR<0.05 cut-off for significantly up- or down regulated genes in all of the one-on-one comparison between the six groups (Figure 2.7). Very few genes were significantly up- or down-regulated when female SD rats transitioned from Irregular cyclers 9-10m to Acyclic 9-10m (31 upregulated and 25 downregulated genes), whereas more than 650 genes were significantly changed between Regular cyclers 9-10m and Acyclic 9-10m (493 upregulated and 176 downregulated). Almost 400 genes were significantly differentially expressed between Acyclic 16m and Regular cyclers 6m (285 upregulated and 103 downregulated) and Irregular 9-10m and Acyclic 16m (219 upregulated and 177 downregulated). Upwards of 250 genes were differentially expressed between Regular 9-10m and Regular 6m (140

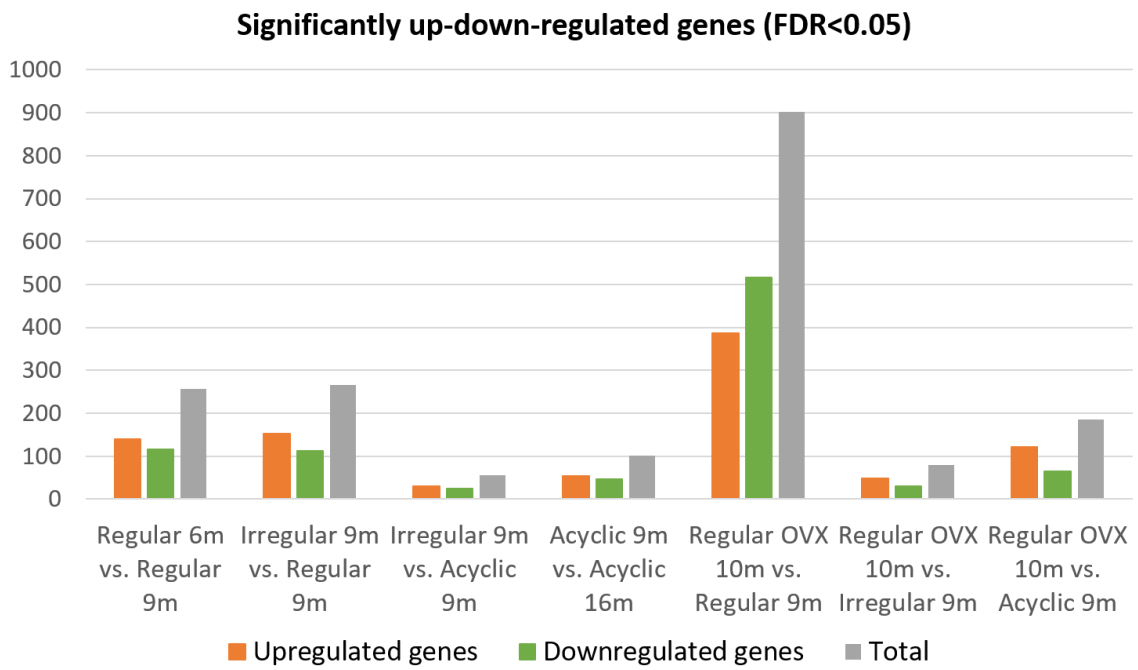

Figure 2.7 **Number of genes significantly up- and down-regulated between different perimenopausal groups**.
Excluding the surgical menopausal group of Regular OVX 10-10.5m, the highest number of genes changed significantly between groups involved in intital chronological and endocrinological aging i.e. Regular cyclers 9-10m vs. Regular cyclers 6m and Irregular cyclers 9-10m vs. Regular cyclers 9-10m (cut-off: q=FDR= False Discovery Rate<0.05).

upregulated and 116 downregulated) as well as between Regular 9-10m and Irregular 9-10m (153 upregulated and 113 downregulated).

When hippocampal gene expression was compared between Regular cyclers 9-10m and Regular Ovariectomized 10-10.5m, the highest number of significantly differentially expressed genes (more than 900 genes total) were observed (Fig. 2.8). Abrupt removal of ovaries and cessation of a functional HPA axis in female rats has demonstrable impact on the hippocampus as seen from the differential regulation of hippocampal gene expression.

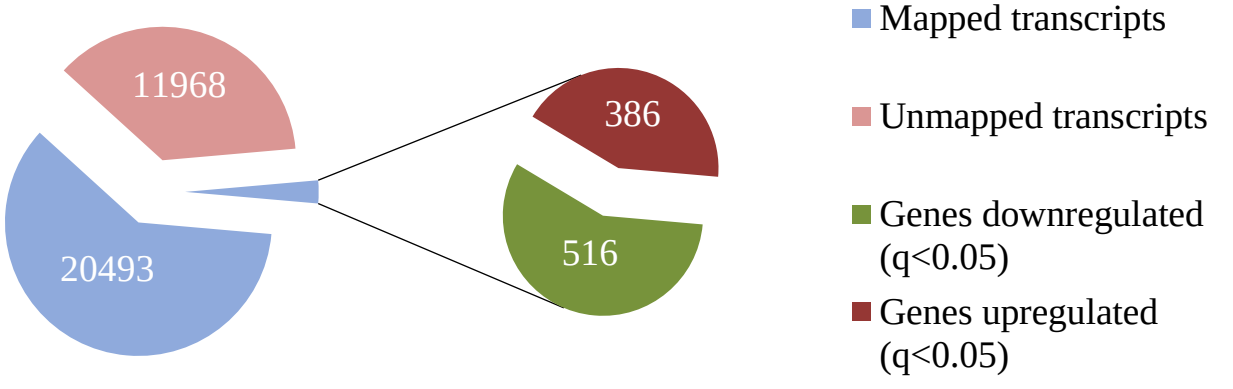

Figure 2.8

Figure 2.8 **Number of hippocampal genes up- and down-regulated due to ovariectomy**. Female SD rats that exhibited regular estrus cycles had their ovaries removed at 9 months and were sacrificed at 10-10.5 months to determine the effect ovariectomy had on hippocampal gene expression.

2.4.3 FUNCTIONAL CLASSIFICATION OF DIFFERENTIALLY EXPRESSED GENES OF FIRST ENDOCRINE TRANSITION

Figure 2.9a Number of genes in each category

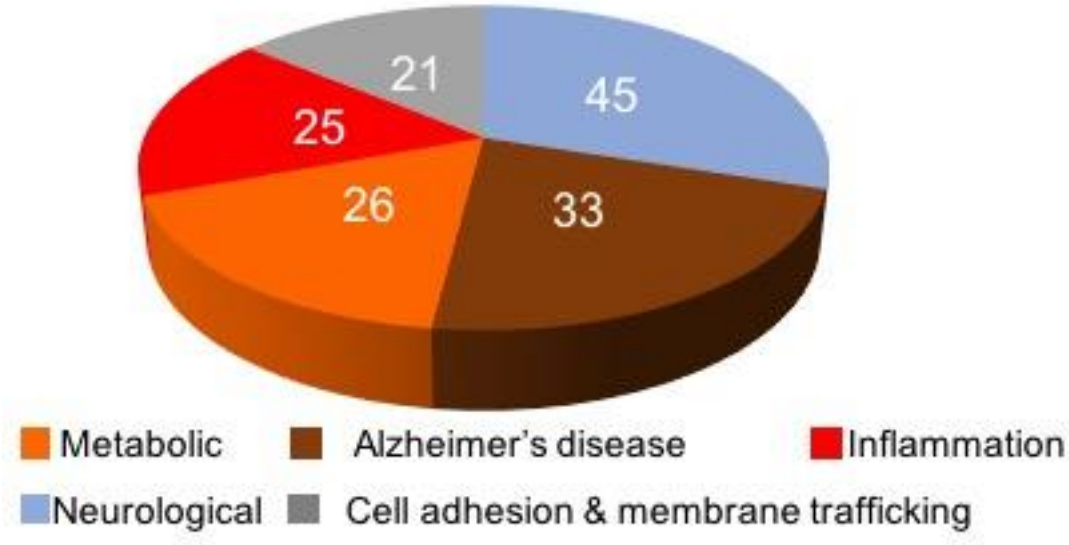

Figure 2.9b

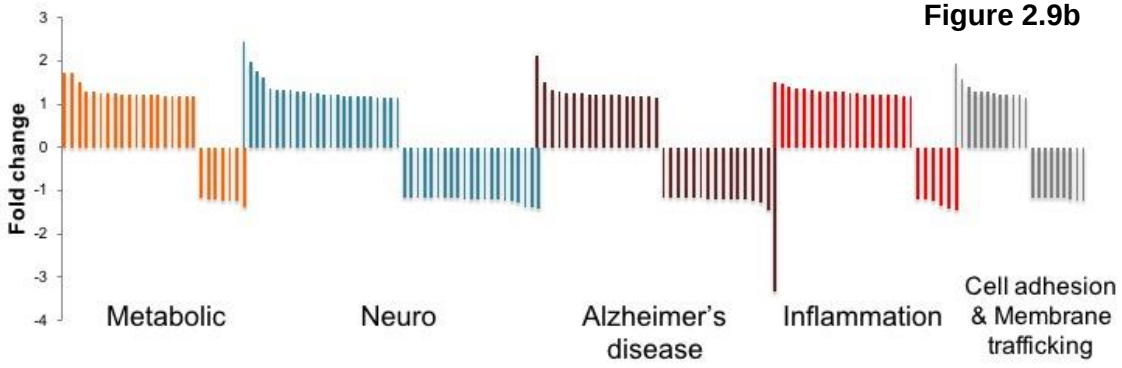

Figure 2.9 **Functional classification of genes**.
This figure illustrates the functional classification of significantly up- and down-regulated genes (number of genes in each category), along with their fold change, for the first endocrinological transition from Regular cyclers 9-10m to Irregular cyclers 9-10m (FDR<0.05).

Previously our lab has established that an important period during the entire perimenopausal transition was the progression from regular to irregular estrus cycling at 9-10 months of age in female SD rats (Yin et al., 2015). The sequencing of hippocampal genes found that 266 genes that were significantly differentially regulated during this transition period (FDR<0.05) out of which 150 genes had known functions in the NCBI database and were classified into functional groups (metabolic, neurological, cell adhesion and membrane

Figure 2.10a

Regular 9-10 months vs. Regular 6 months
UCP2 transcript significantly increased in the hippocampus

ID	Fold Ch...	p-value	Fals...
Gjc2	↑1.205	5.00E-05	5.70E-03
Grin3a	↓-1.386	5.00E-05	5.70E-03
LOC287167	↑1.815	5.00E-05	5.70E-03
Lpar1	↑1.220	5.00E-05	5.70E-03
Myo5b	↓-1.202	5.00E-05	5.70E-03
Npas4	↓-1.533	5.00E-05	5.70E-03
Ntrk1	↑2.100	5.00E-05	5.70E-03
Reln	↓-1.233	5.00E-05	5.70E-03
Sstr1	↓-1.276	5.00E-05	5.70E-03
Tgfa	↑1.228	5.00E-05	5.70E-03
Ucp2	↑1.293	5.00E-05	5.70E-03
Erbb4	↓-1.238	1.50E-04	1.32E-02
Dusp1	↓-1.234	2.00E-04	1.67E-02
Chrm5	↓-1.295	2.50E-04	2.01E-02
Nos1	↓-1.245	3.00E-04	2.28E-02
Sulf1	↓-1.325	5.00E-04	3.32E-02
Hspb1	↑1.251	6.50E-04	4.05E-02
Nnmt	↓-1.529	6.50E-04	4.05E-02
Tyrobp	↑1.223	7.50E-04	4.50E-02
Tp73	↑1.310	8.50E-04	4.93E-02

trafficking, inflammation and Alzheimer's disease). The genes in these functional groups are shown in Figure 2.9a-b along with fold change for each group. From the above data (Fig. 2.9) it is evident that at 9-10 months of age, the female rat hippocampus experiences significant changes in expression of certain genes during two transitions. However, expression of most numbers of genes is significantly altered during the first endocrine transition from Regular cyclers 9-10m to Irregular cyclers 9-10m (total 266 genes significantly differentially expressed) compared to the second endocrine transition from Irregular 9-10m to Acyclic 9-10m (total 56 genes significantly differentially expressed), whereas expression of a total of 669 genes is significantly altered when Regular cyclers 9-10m are compared to Acyclic 9-10m. These observations and data presented by our lab previously (Yin et al., 2015) suggests that the Regular to Irregular endocrine transition likely has significant impact on hippocampal gene expression in perimenopausal female rats.

Irregular 9-10 months vs. Regular 9-10 months **Figure 2.10b**
UCP2 transcript significantly decreased in the hippocampus

ID	Fold Ch...	p-value	Fals...
Adcy1	↑1.281	5.00E-05	7.13E-03
Atp8a2	↑1.265	5.00E-05	7.13E-03
Cit	↑1.228	5.00E-05	7.13E-03
Dusp1	↑1.298	5.00E-05	7.13E-03
Kitlg	↑1.228	5.00E-05	7.13E-03
Myo5a	↑1.222	5.00E-05	7.13E-03
Nr2f6	↓-1.234	5.00E-05	7.13E-03
Orai1	↓-1.365	5.00E-05	7.13E-03
Plxna4a	↑1.203	5.00E-05	7.13E-03
Reln	↑1.215	5.00E-05	7.13E-03
Scn1b	↓-1.275	5.00E-05	7.13E-03
Shc3	↑1.356	5.00E-05	7.13E-03
Slc1a2	↑1.314	5.00E-05	7.13E-03
Slc5a7	↑2.109	5.00E-05	7.13E-03
Ucp2	↓-1.278	5.00E-05	7.13E-03
Fzd3	↑1.232	2.50E-04	2.34E-02
Foxo6	↓-1.208	3.50E-04	2.86E-02
Ecel1	↓-1.424	4.00E-04	3.00E-02
Gabrb2	↑1.209	6.00E-04	3.80E-02
Hras	↓-1.163	7.50E-04	4.49E-02

As an example of a neurological gene significantly differentially expressed during Regular 9-10 to Irregular 9-10m transition, consider uncoupling protein 2 (UCP2). UCP2 is found in the membrane of mitochondria that serves to disconnect oxidative phosphorylation from ATP synthesis furnishing neuroprotection (Sans et al., 2000). In perimenopausal female rats, hippocampal transcriptome shows statistically significant (FDR<0.05) upregulation of UCP2 during the Regular 6 to Regular 9-month transition but its expression is downregulated during the Regular to Irregular transition (first endocrine transition) and from Regular to Acyclic transition (Figs. 2.10a-c).

Figure 2.10c Acyclic 9-10 months vs. Regular 9-10 months
UCP2 transcript significantly decreased in the hippocampus

ID	Fold Ch...	p-value	Fals...
Adcy1	↑1.290	5.00E-05	2.67E-03
Atp8a2	↑1.311	5.00E-05	2.67E-03
Cdkl5	↑1.292	5.00E-05	2.67E-03
Cpeb3	↑1.219	5.00E-05	2.67E-03
Creb1	↑1.447	5.00E-05	2.67E-03
Dgkh	↑1.306	5.00E-05	2.67E-03
Efnb2	↑1.202	5.00E-05	2.67E-03
Ep300	↑1.292	5.00E-05	2.67E-03
Erbb4	↑1.326	5.00E-05	2.67E-03
Fn1	↑1.208	5.00E-05	2.67E-03
Fzd3	↑1.375	5.00E-05	2.67E-03
Gabrb2	↑1.388	5.00E-05	2.67E-03
Gda	↑1.217	5.00E-05	2.67E-03
Gjc2	↓-1.320	5.00E-05	2.67E-03
Grin2a	↑1.316	5.00E-05	2.67E-03
Hspb1	↓-1.372	5.00E-05	2.67E-03
Lpar1	↓-1.263	5.00E-05	2.67E-03
Mecp2	↑1.255	5.00E-05	2.67E-03
Met	↑1.393	5.00E-05	2.67E-03
Myo5a	↑1.299	5.00E-05	2.67E-03
Nos1	↑1.251	5.00E-05	2.67E-03
Plxna4a	↑1.236	5.00E-05	2.67E-03
Prkacb	↑1.216	5.00E-05	2.67E-03
Reln	↑1.251	5.00E-05	2.67E-03
Shc3	↑1.363	5.00E-05	2.67E-03
Slc1a2	↑1.315	5.00E-05	2.67E-03
Ucp2	↓-1.275	5.00E-05	2.67E-03
Xylt1	↑1.221	5.00E-05	2.67E-03
Grin3a	↑1.283	2.50E-04	9.90E-03
Orai1	↓-1.247	4.50E-04	1.50E-02
Tyrobp	↓-1.226	5.00E-04	1.64E-02
Itga4	↑1.282	1.15E-03	3.16E-02

Figure 2.10a-c **UCP2 expression in the hippocampal transcriptome of perimenopausal rats**.
A neuroprotective gene, UCP2, is significantly upregulated during the Regular 6 to Regular 9-10m transition but downregulated during subsequent endocrine transition from Regular 9-10 to Irregular 9-10m, as well as from Regular 9-10 to Acyclic 9-10m.

2.4.4 PATHWAY ANALYSIS USING IPA AND PANTHER

Pathway analysis was performed using IPA and PANTHER. For pathway analysis all the genes that were differentially expressed at FDR<0.2 were included in order to obtain meaningful data using the pathway analysis tools. In figure 2.11a-b, the three different colors represent the number of genes in a pathway (in blue), percent of genes out of the total number of significant genes in a pathway (in orange) and percent of genes to the total number of pathways (in green). Comparing the hippocampal transcriptome of Regular cyclers 6m to Regular cyclers 9-10m suggested that the genes that were significantly altered between these two groups were associated with PDGF signaling pathway which is important for BBB permeability, AD (presenilin and amyloid secretase pathways) and proinflammatory cytokines pathways.

Comparing significantly differentially regulated genes between Irregular cyclers 9-10m and Regular cyclers 9-10m, using PANTHER it was discovered that this set of genes were associated with T cell activation and AD amyloid secretase pathways (Figures 2.12a-b), whereas comparing significantly differentially regulated genes between Regular OVX 10-10.5m and Regular cyclers 9-10m (Fig. 2.13a-b) found these set of genes to be associated with T cell activation and two AD pathways as well. While surgical menopause (OVX group) and transition group (Irregular 9-10m) to natural reproductive senescence both show altered expression of genes, the absolute quantity of genes significantly differentially expressed in the OVX group support the abrupt nature of menopause achieved by surgical removal of ovaries. At the same time similar pathways are altered in the hippocampus between both Regular to Irregular perimenopausal transition at 9-10m as well as the Regular to Regular OVX surgically achieved abrupt menopause: T cell activation and AD pathways.

Figure 2.11a

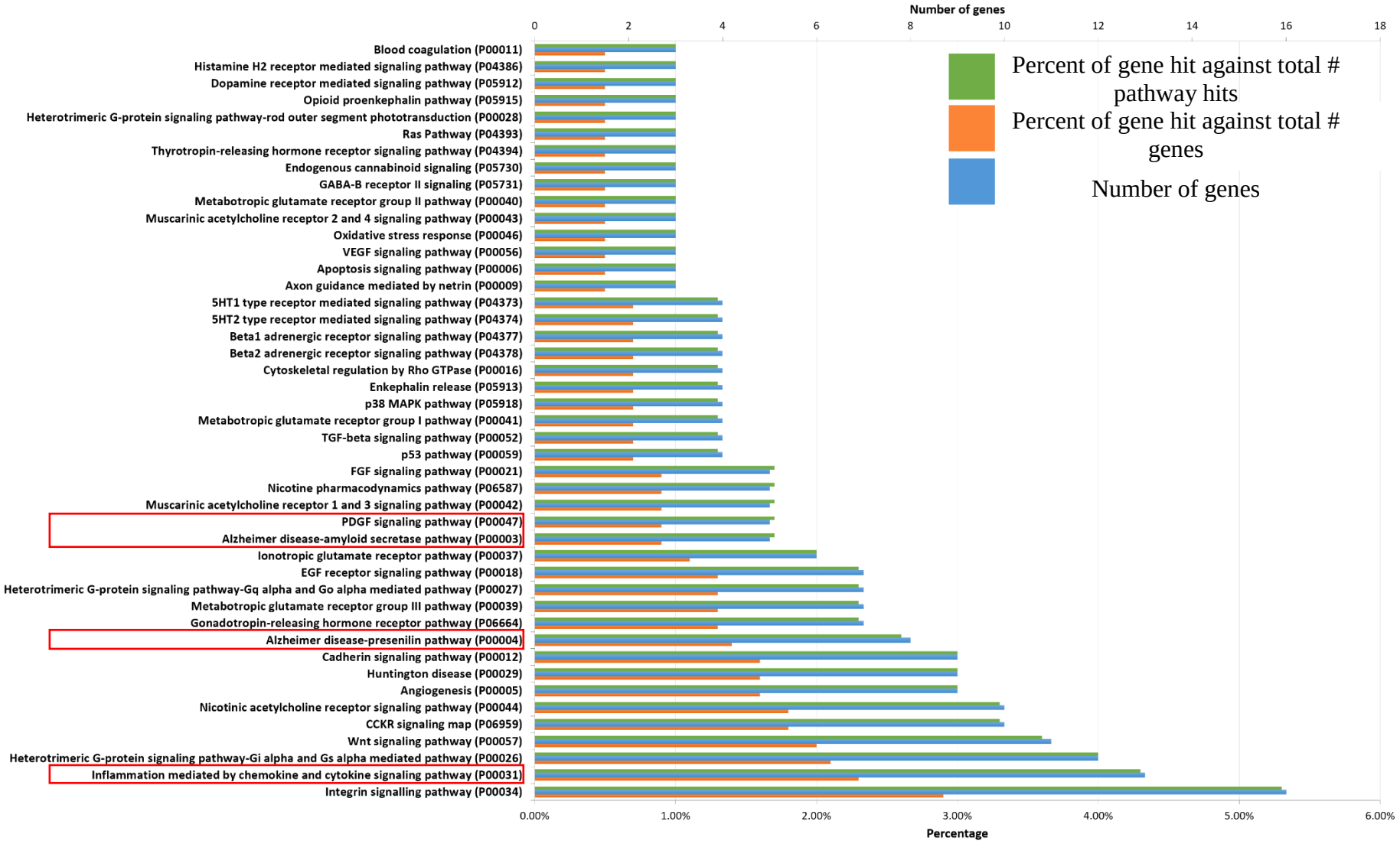
Number of genes
0
2
4
6
8
10
12
14
16
18
Blood coagulation (P00011)
Histamine H2 receptor mediated signaling pathway (P04386)
Dopamine receptor mediated signaling pathway (P05912)
Opioid proenkephalin pathway (P05915)
Heterotrimeric G-protein signaling pathway-rod outer segment phototransduction (P00028)
Ras Pathway (P04393)
Thyrotropin-releasing hormone receptor signaling pathway (P04394)
Endogenous cannabinoid signaling (P05730)
GABA-B receptor II signaling (P05731)
Metabotropic glutamate receptor group II pathway (P00040)
Muscarinic acetylcholine receptor 2 and 4 signaling pathway (P00043)
Oxidative stress response (P00046)
VEGF signaling pathway (P00056)
Apoptosis signaling pathway (P00006)
Axon guidance mediated by netrin (P00009)
5HT1 type receptor mediated signaling pathway (P04373)
5HT2 type receptor mediated signaling pathway (P04374)
Beta1 adrenergic receptor signaling pathway (P04377)
Beta2 adrenergic receptor signaling pathway (P04378)
Cytoskeletal regulation by Rho GTPase (P00016)
Enkephalin release (P05913)
p38 MAPK pathway (P05918)
Metabotropic glutamate receptor group I pathway (P00041)
TGF-beta signaling pathway (P00052)
p53 pathway (P00059)
FGF signaling pathway (P00021)
Nicotine pharmacodynamics pathway (P06587)
Muscarinic acetylcholine receptor 1 and 3 signaling pathway (P00042)
PDGF signaling pathway (P00047)
Alzheimer disease-amyloid secretase pathway (P00003)
Ionotropic glutamate receptor pathway (P00037)
EGF receptor signaling pathway (P00018)
Heterotrimeric G-protein signaling pathway-Gq alpha and Go alpha mediated pathway (P00027)
Metabotropic glutamate receptor group III pathway (P00039)
Gonadotropin-releasing hormone receptor pathway (P06664)
Alzheimer disease-presenilin pathway (P00004)
Cadherin signaling pathway (P00012)
Huntington disease (P00029)
Angiogenesis (P00005)
Nicotinic acetylcholine receptor signaling pathway (P00044)
CCKR signaling map (P06959)
Wnt signaling pathway (P00057)
Heterotrimeric G-protein signaling pathway-Gi alpha and Gs alpha mediated pathway (P00026)
Inflammation mediated by chemokine and cytokine signaling pathway (P00031)
Integrin signalling pathway (P00034)
Percent of gene hit against total # pathway hits
Percent of gene hit against total # genes
Number of genes
0.00%
1.00%
2.00%
3.00%
4.00%
5.00%
6.00%
Percentage

Figure 2.11b

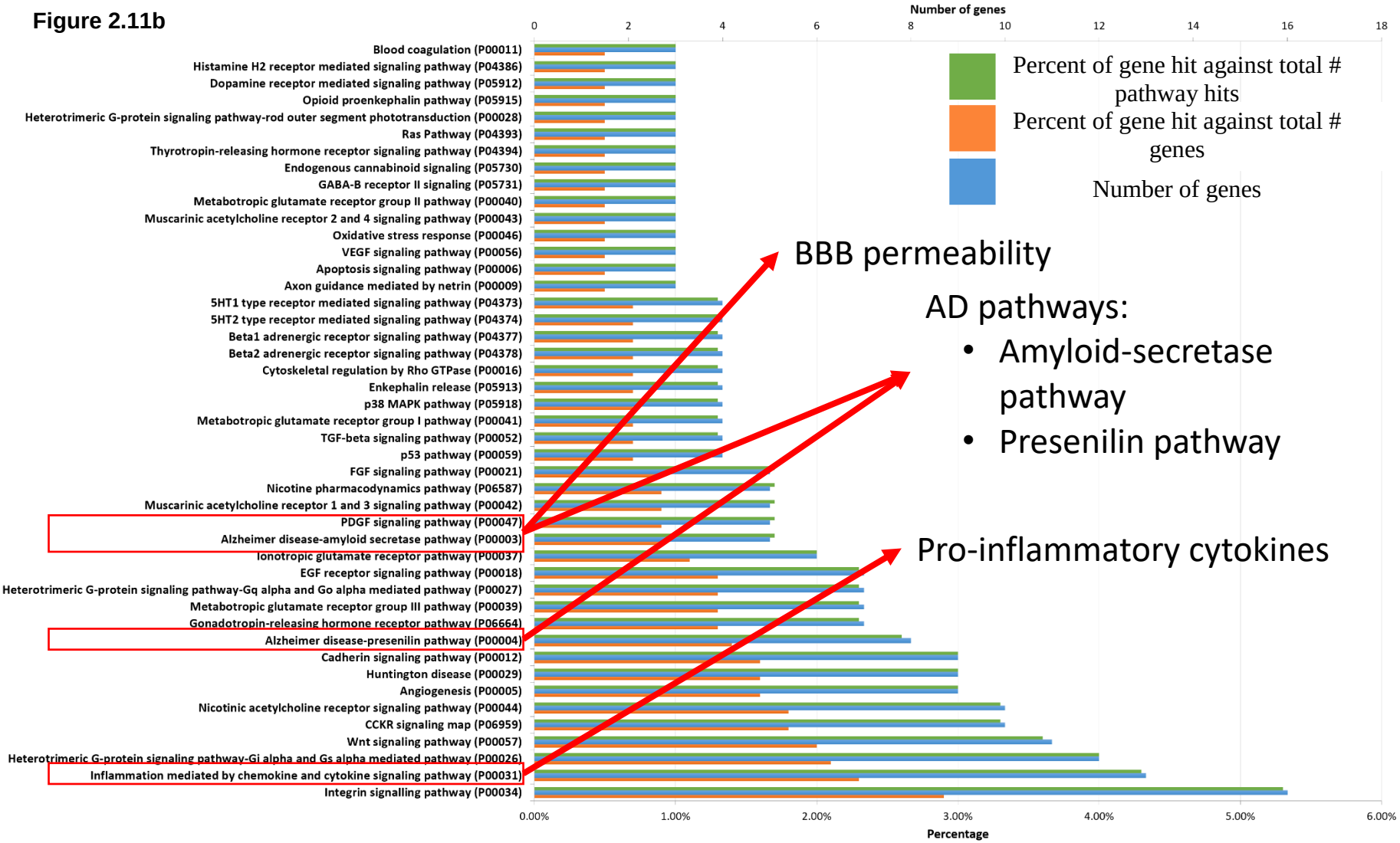

Figure 2.11a-b **PANTHER classification system: Regular cyclers 6m vs. Regular cyclers 9-10m**.
The significance cut-off used for genes was FDR<0.2. When genes that were significantly differentially expressed in hippocampi of Regular cyclers 6m and Regular cyclers 9-10m female rats were compared, genes that were significantly altered between these two groups were associated with Platelet Derived Growth Factor (PDGF) signaling pathway which is important for BBB permeability, Alzheimer's disease (presenelin and amyloid secretase pathways) and proinflammatory cytokines pathways.

Figure 2.12a

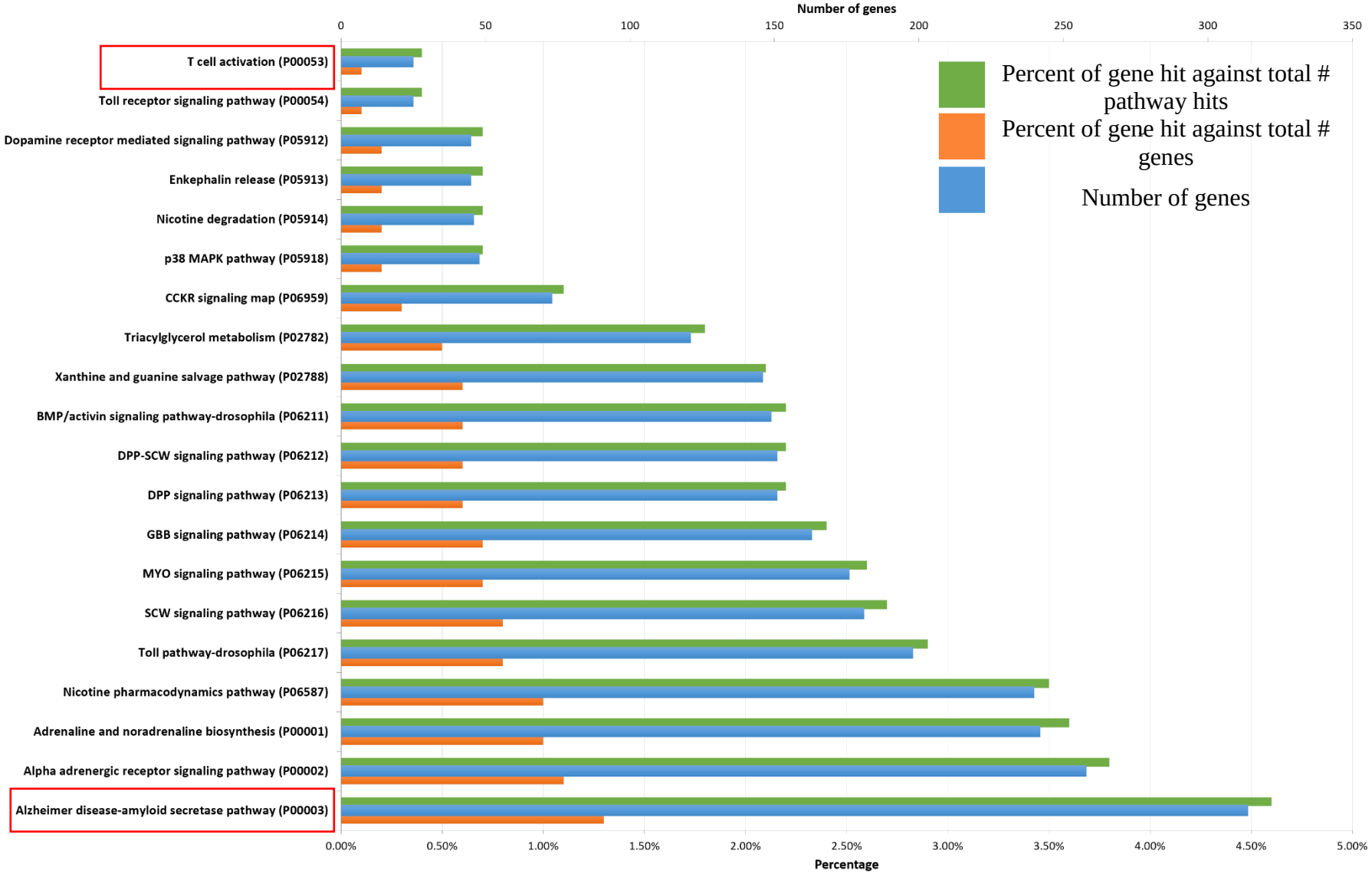
Number of genes
0
50
100
150
200
250
300
350
T cell activation (P00053)
Toll receptor signaling pathway (P00054)
Dopamine receptor mediated signaling pathway (P05912)
Enkephalin release (P05913)
Nicotine degradation (P05914)
p38 MAPK pathway (P05918)
CCKR signaling map (P06959)
Triacylglycerol metabolism (P02782)
Xanthine and guanine salvage pathway (P02788)
BMP/activin signaling pathway-drosophila (P06211)
DPP-SCW signaling pathway (P06212)
DPP signaling pathway (P06213)
GBB signaling pathway (P06214)
MYO signaling pathway (P06215)
SCW signaling pathway (P06216)
Toll pathway-drosophila (P06217)
Nicotine pharmacodynamics pathway (P06587)
Adrenaline and noradrenaline biosynthesis (P00001)
Alpha adrenergic receptor signaling pathway (P00002)
Alzheimer disease-amyloid secretase pathway (P00003)
Percent of gene hit against total # pathway hits
Percent of gene hit against total # genes
Number of genes
0.00%
0.50%
1.00%
1.50%
2.00%
2.50%
3.00%
3.50%
4.00%
4.50%
5.00%
Percentage

Figure 2.12b

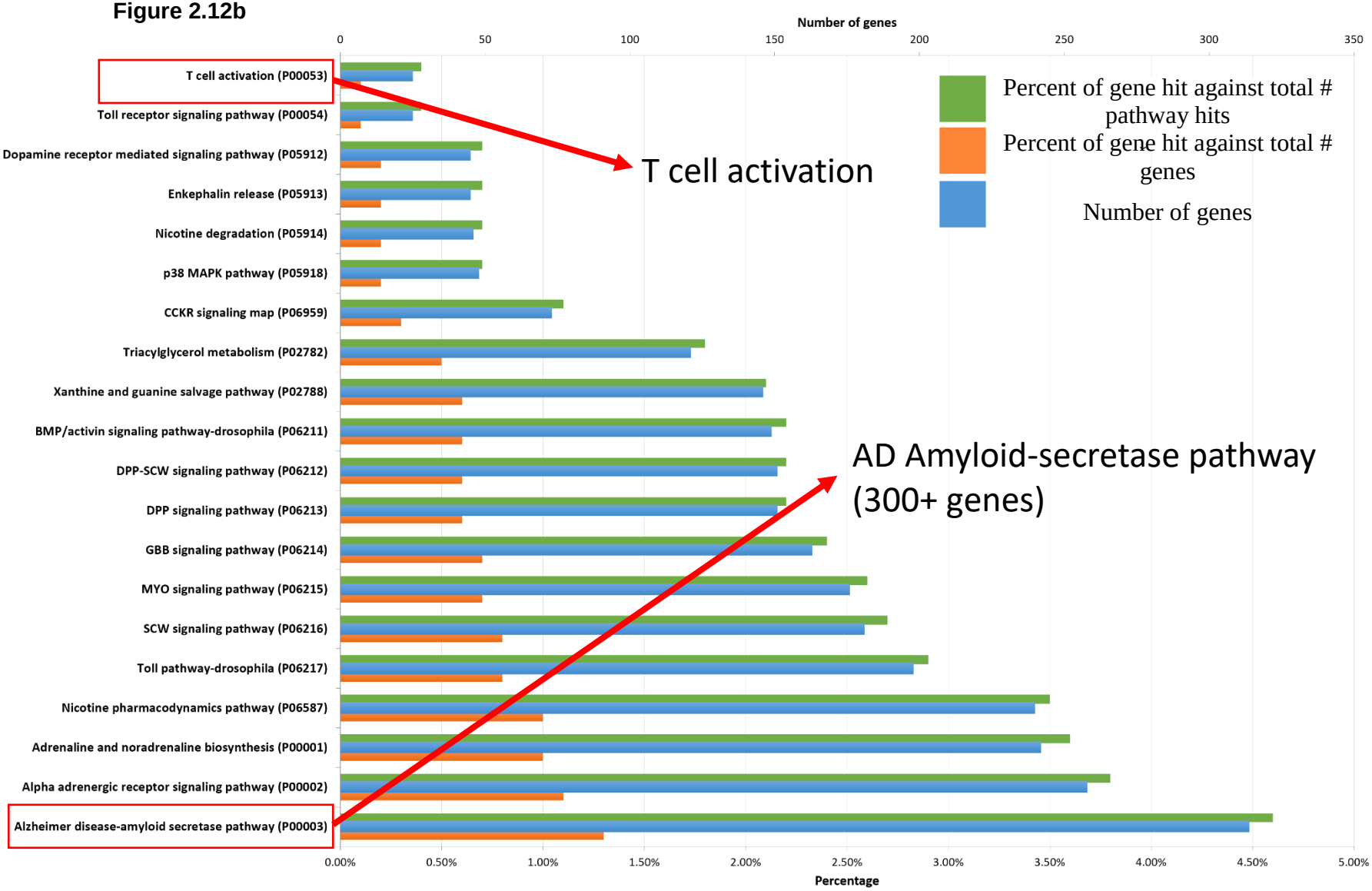

Figure 2.12a-b **PANTHER classification system: Regular cyclers 9-10m vs. Irregular cyclers 9-10m**.
The significance cut-off used for genes was FDR<0.2. When genes that were significantly differentially expressed in hippocampi of Irregular cyclers 9-10m and Regular cyclers 9-10m female rats were compared, genes that were significantly altered between these two groups were associated with were T cell activation and AD amyloid secretase pathways.

Figure 2.13a

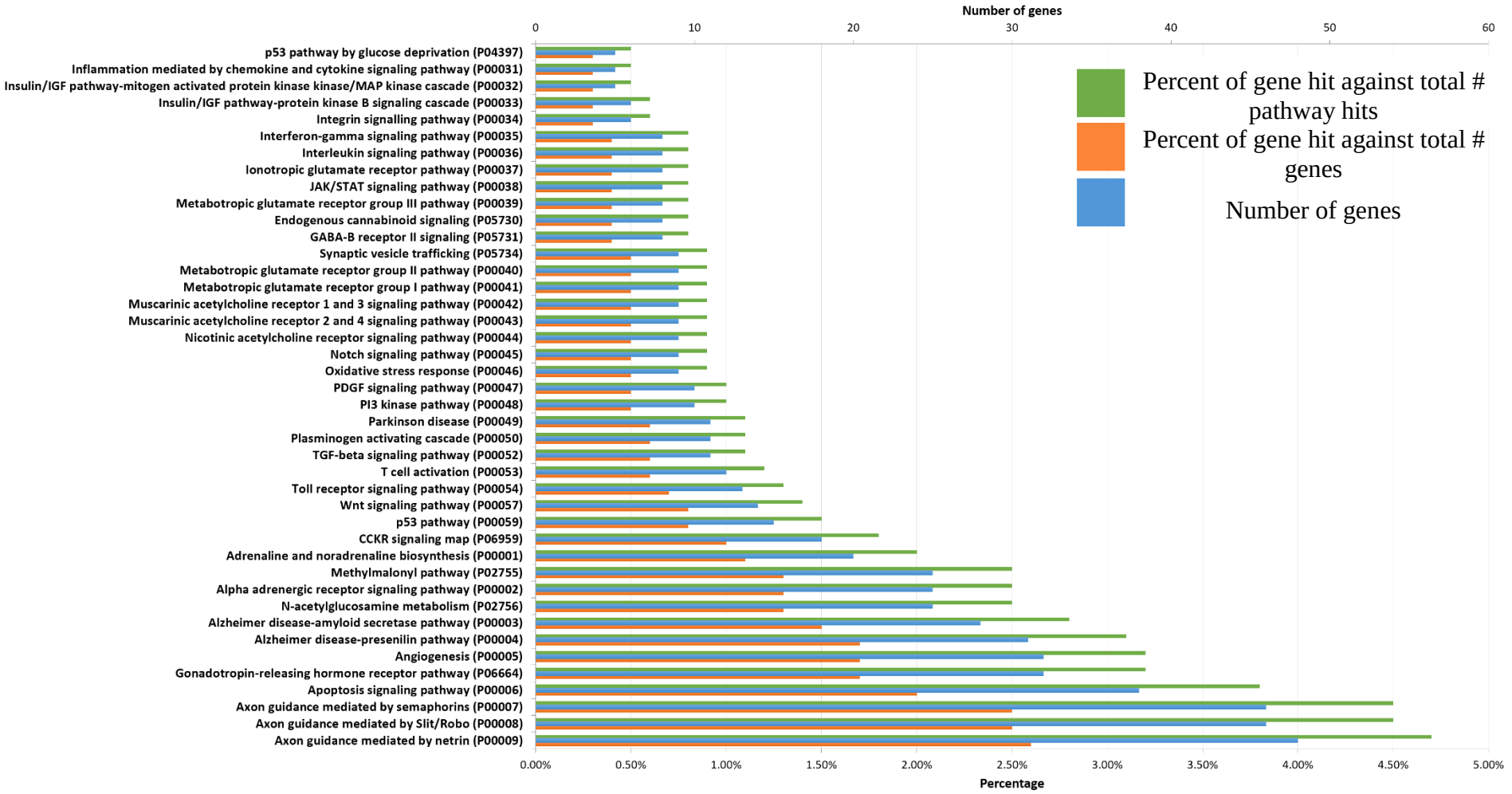
Number of genes
0
10
20
30
40
50
60
p53 pathway by glucose deprivation (P04397)
Inflammation mediated by chemokine and cytokine signaling pathway (P00031)
Insulin/IGF pathway-mitogen activated protein kinase kinase/MAP kinase cascade (P00032)
Insulin/IGF pathway-protein kinase B signaling cascade (P00033)
Integrin signalling pathway (P00034)
Interferon-gamma signaling pathway (P00035)
Interleukin signaling pathway (P00036)
Ionotropic glutamate receptor pathway (P00037)
JAK/STAT signaling pathway (P00038)
Metabotropic glutamate receptor group III pathway (P00039)
Endogenous cannabinoid signaling (P05730)
GABA-B receptor II signaling (P05731)
Synaptic vesicle trafficking (P05734)
Metabotropic glutamate receptor group II pathway (P00040)
Metabotropic glutamate receptor group I pathway (P00041)
Muscarinic acetylcholine receptor 1 and 3 signaling pathway (P00042)
Muscarinic acetylcholine receptor 2 and 4 signaling pathway (P00043)
Nicotinic acetylcholine receptor signaling pathway (P00044)
Notch signaling pathway (P00045)
Oxidative stress response (P00046)
PDGF signaling pathway (P00047)
PI3 kinase pathway (P00048)
Parkinson disease (P00049)
Plasminogen activating cascade (P00050)
TGF-beta signaling pathway (P00052)
T cell activation (P00053)
Toll receptor signaling pathway (P00054)
Wnt signaling pathway (P00057)
p53 pathway (P00059)
CCKR signaling map (P06959)
Adrenaline and noradrenaline biosynthesis (P00001)
Methylmalonyl pathway (P02755)
Alpha adrenergic receptor signaling pathway (P00002)
N-acetylglucosamine metabolism (P02756)
Alzheimer disease-amyloid secretase pathway (P00003)
Alzheimer disease-presenilin pathway (P00004)
Angiogenesis (P00005)
Gonadotropin-releasing hormone receptor pathway (P06664)
Apoptosis signaling pathway (P00006)
Axon guidance mediated by semaphorins (P00007)
Axon guidance mediated by Slit/Robo (P00008)
Axon guidance mediated by netrin (P00009)
Percent of gene hit against total # pathway hits
Percent of gene hit against total # genes
Number of genes
0.00%
0.50%
1.00%
1.50%
2.00%
2.50%
3.00%
3.50%
4.00%
4.50%
5.00%
Percentage

Figure 2.13b

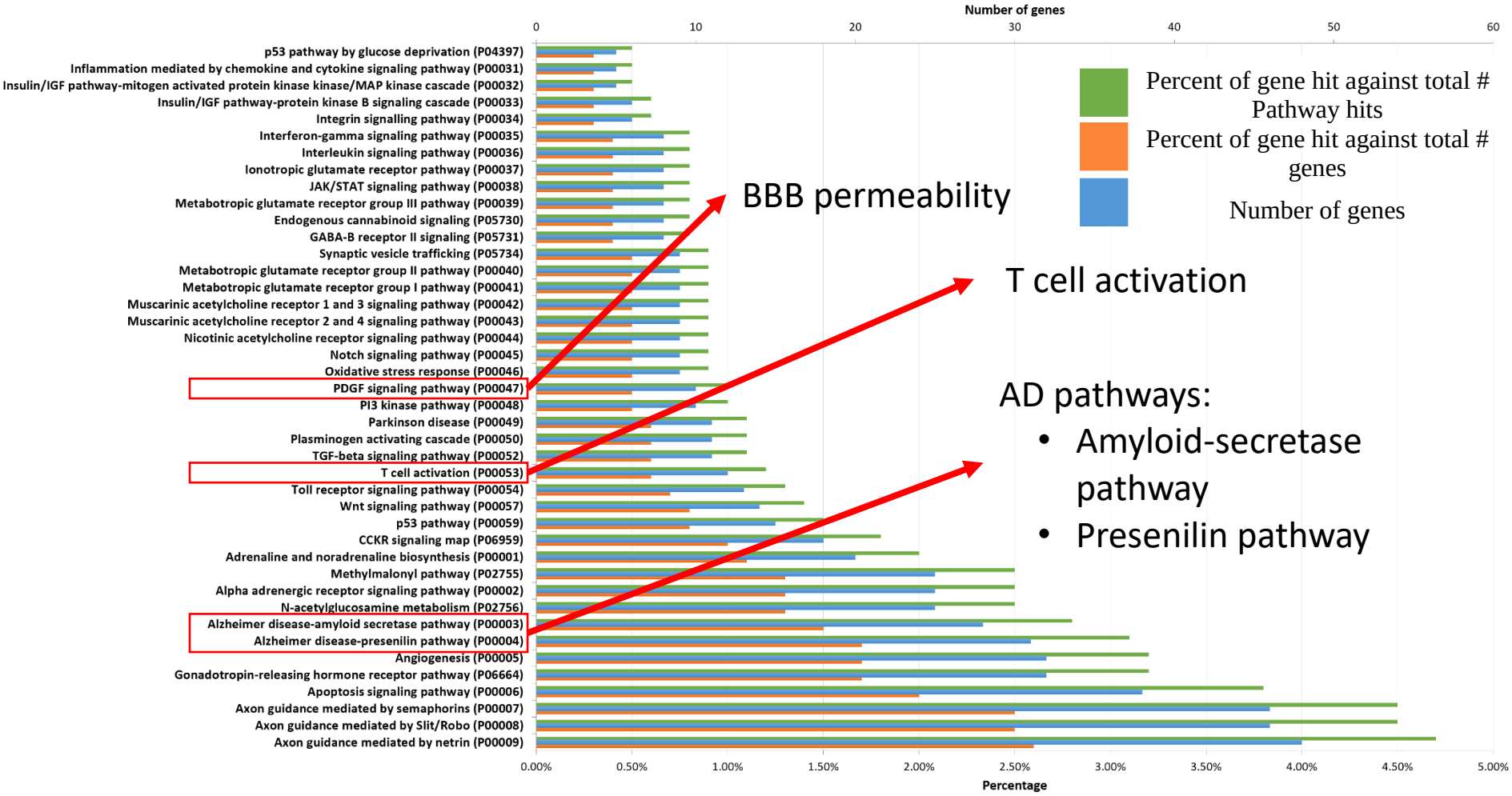

Figure 2.13a-b **PANTHER classification system: Regular OVX 10-10.5m vs. Regular cyclers 9-10m**.
The significance cut-off used for genes was FDR<0.2. When genes that were significantly differentially expressed in hippocampi of Regular OVX 10-10.5m and Regular cyclers 9-10m female rats were compared, genes that were significantly altered between these two groups were associated with were T cell activation and two AD pathways.

Figure 2.14a

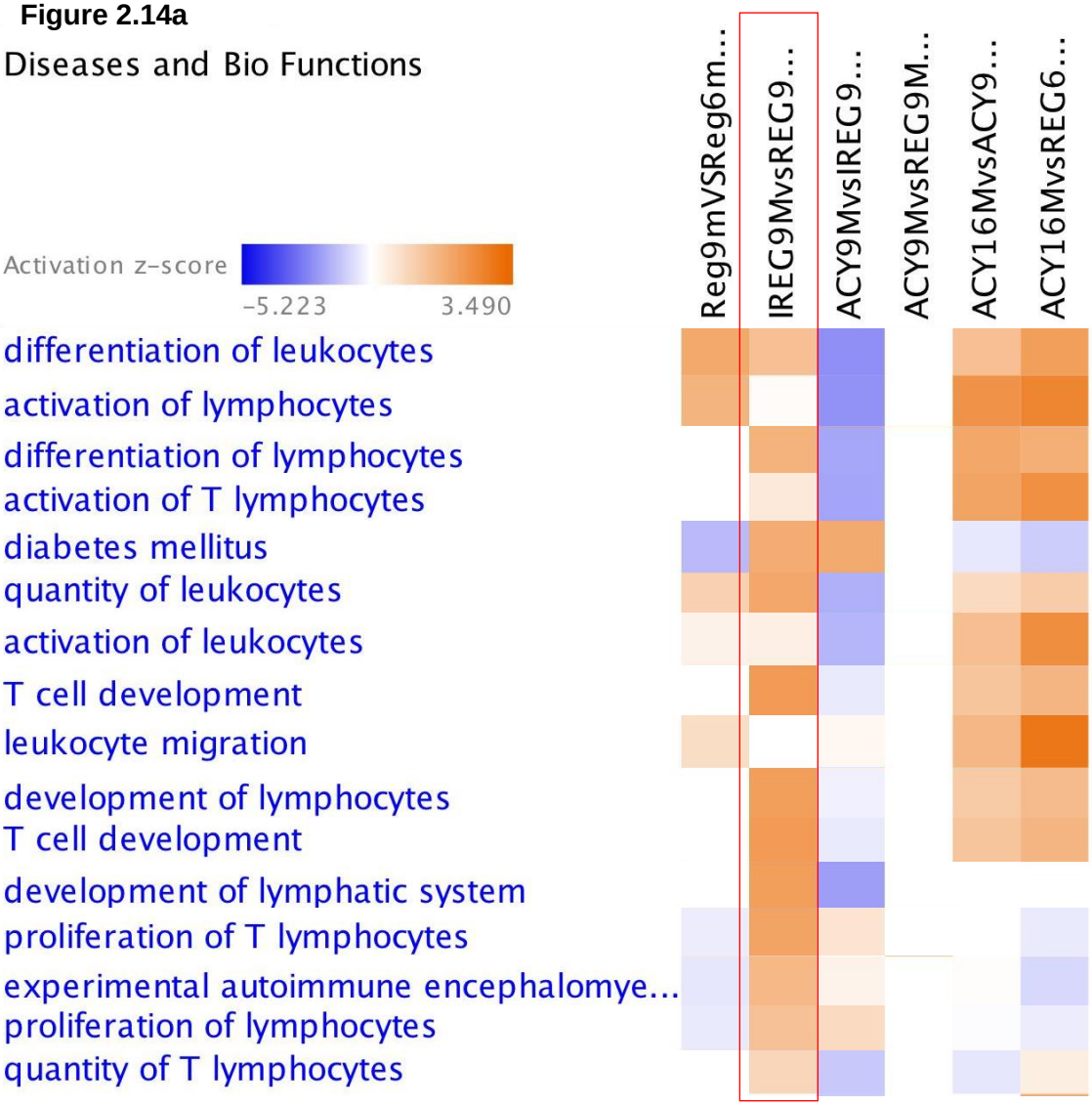
Diseases and Bio Functions
Activation z-score
-5.223
3.490
Reg9mVSReg6m...
IREG9MvsREG9...
ACY9MvsIREG9...
ACY9MvsREG9M...
ACY16MvsACY9...
ACY16MvsREG6...
differentiation of leukocytes
activation of lymphocytes
differentiation of lymphocytes
activation of T lymphocytes
diabetes mellitus
quantity of leukocytes
activation of leukocytes
T cell development
leukocyte migration
development of lymphocytes
T cell development
development of lymphatic system
proliferation of T lymphocytes
experimental autoimmune encephalomye...
proliferation of lymphocytes
quantity of T lymphocytes

Figure 2.14b

Categories	Diseases or Functions Annotation	p-Value	Predicted Ac	Activation z-scor
Cell-mediated Ir	T cell development	1.93E-05	Increased	2.339
Embryonic Deve	development of head	6.06E-05	Increased	2.329
Tissue Morpholo	quantity of cells	3.20E-06	Increased	2.323
Cell Cycle	interphase	7.64E-04	Increased	2.281
Cellular Assemb	organization of cytoskeleton	6.26E-06	Increased	2.280
Cellular Assemb	organization of cytoplasm	1.60E-05	Increased	2.280
Cancer, Cellular	proliferation of tumor cells	1.35E-03	Increased	2.250
Cellular Develop	development of lymphocytes	4.86E-05	Increased	2.246
Embryonic Deve	development of lymphatic systen	2.17E-04	Increased	2.245
Cellular Growth	outgrowth of cells	8.83E-06	Increased	2.212
Cellular Moveme	cell movement of leukemia cell li	1.22E-03	Increased	2.209
Organismal Injur	angiogenesis of lesion	3.51E-06	Increased	2.201
Cell-To-Cell Sigi	signaling of cells	6.98E-04	Increased	2.187
Cell Signaling, M	concentration of Ca2+	7.68E-04	Increased	2.180
Cellular Develop	proliferation of hematopoietic pr	1.79E-03	Increased	2.177
Cancer, Organis	malignant solid tumor	2.92E-05	Increased	2.142
Cellular Moveme	cell movement	5.03E-08	Increased	2.138
Cellular Moveme	migration of cells	4.33E-06	Increased	2.133
Cellular Develop	proliferation of T lymphocytes	2.32E-04	Increased	2.128
Hematological Sy	quantity of leukocytes	6.05E-06	Increased	2.047

Categories	Diseases or Functions Annotation	p-Value	Predicted Ac	Activation z-sco
Organismal Surv	organismal death	3.29E-06	Decreased	-4.245
Organismal Surv	perinatal death	1.97E-03	Decreased	-3.013
Cell Death and S	cell death	5.54E-06	Decreased	-2.783
Cell Death and S	apoptosis	9.56E-06	Decreased	-2.285
Cell Death and S	apoptosis of leukocytes	8.17E-04	Decreased	-2.156
Cell Death and S	apoptosis of lymphocytes	2.79E-04	Decreased	-2.154

Figure 2.14a-b **Up-regulation of T lymphocyte related process: Irregular 9-10m vs. Regular 9-10m**.
When genes that were significantly differentially expressed (FDR<0.2) in hippocampi of Irregular cyclers 9-10m and Regular cyclers 9-10m female rats were analyzed by IPA it was found that this set of genes signaled an upregulation of functions such as T cell development and development of lymphocytes, and downregulation of apoptosis of lymphocytes and leukocytes.

Additionally, IPA analysis also showed upregulation of functions such as T cell development and development of lymphocytes, and downregulation of apoptosis of

lymphocytes and leukocytes in the hippocampus (Fig. 2.14a-b) during the Regular to Irregular transition at 9-10 months of age.

Figure 2.15

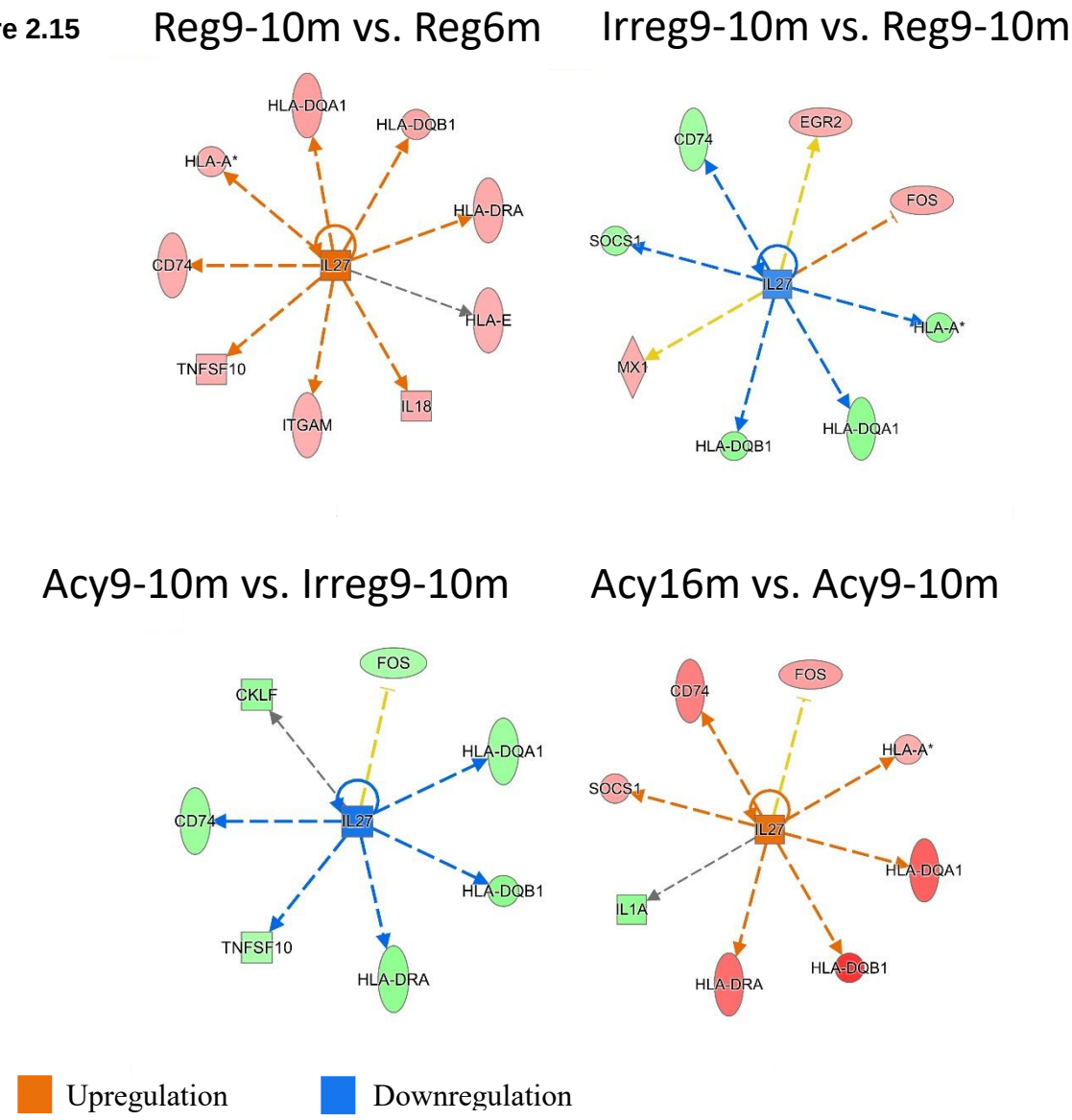

Figure 2.15 **Differential regulation of interleukin (IL)-27 between different groups of female SD rats**.
Analysis of hippocampal RNA-Seq using IPA suggests that IL-27 level increases from Regular cyclers 6m to Regular cyclers 9-10m and decreases thereafter through Irregular and Acyclic 9-10m groups, and then shows an increase in the Acyclic 16m group. IL-27 is an immunomodulatory cytokine with wide-ranging effects on all subsets of T lymphocytes

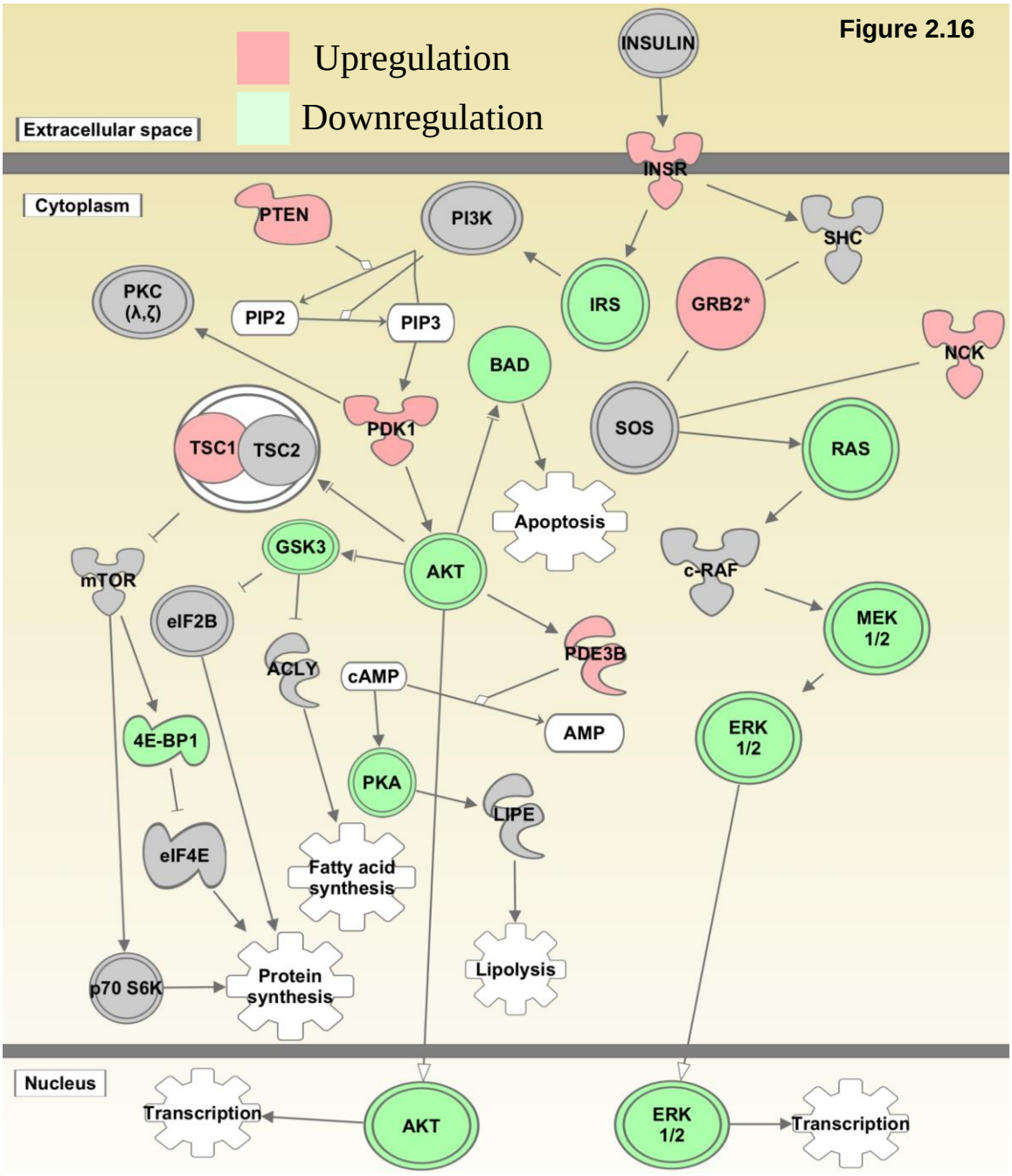

Figure 2.16 **Insulin signaling pathway in the hippocampal transcriptome during the Regular to Irregular transition at 9-10 months of age in female SD rats**.
Insulin signaling pathway is downregulated in the hippocampus during perimenopausal transition from Regular to Irregular stage in 9-10 months old female SD rats.

IL-27 is an immunomodulatory cytokine with wide-ranging effects on all subsets of T

lymphocytes (Yoshida and Hunter, 2015). IL-27 appears to be downregulated in the hippocampus during the two endocrinological transition stages and is elevated before and after the perimenopausal transition (Fig. 2.15); its downregulation may explain

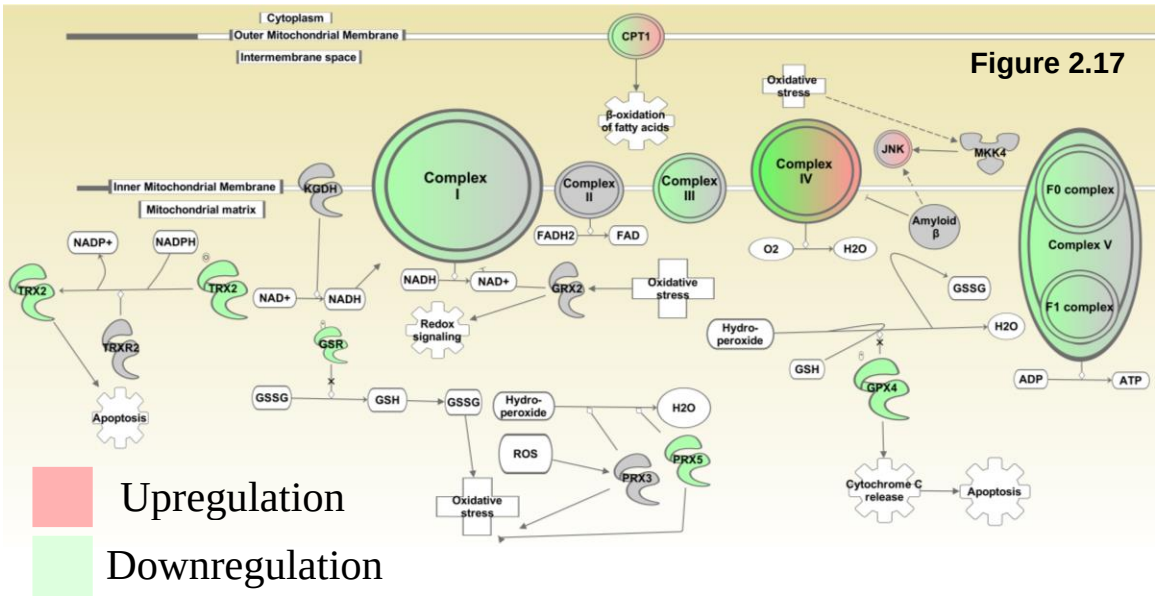

Figure 2.17 **Downregulation of mitochondrial complexes of the electron transport chian as well as Carnitine palmitoyltransferase I in the hippocampal transcriptome during the Regular to Irregular transition at 9-10 months of age in female SD rats**.
Analysis of the hippocampal transcriptome using IPA suggests downregulation of almost all the proteins and complexes of the electron transport chain, with only complex II unaffected and complex IV mildly downregulated. Additionally, carnitine palmitoyltransferase I, essential in the beta-oxidation of long chain fatty acids, too appears to be downregulated. These findings together suggest reduced bioenergetic function in the hippocampus during the transition from Regular to Irregular stage at 9-10m of age in female SD rats.

dysregulated T cell functions predicted in the hippocampus during perimenopausal transition shown by analysis of hippocampal transcriptome using IPA and PANTHER.

Besides the immune system and blood brain barrier permeability, it was also discovered that the perimenopausal transition affected the bioenergetic and metabolic pathways in the hippocampus, implying reduced utilization of glucose in the brain (Figures 2.16 and 2.17) evidence by downregulation of AKT and ERK.

Increased ROS, which possibly could be a result of downregulated UCP2 (Fig. 2.10a-c), could potentially explain downregulation of mitochondrial complexes in the hippocampus seen in Figure 2.17 and ROS can also inhibit Carnitine palmitoyltransferase I (CPT1) enzymatic activity (Setoyama et al., 2013). All these confirm the deleterious effect of ROS, which could be the result of statistically significantly reduced expression of UCP2, in the

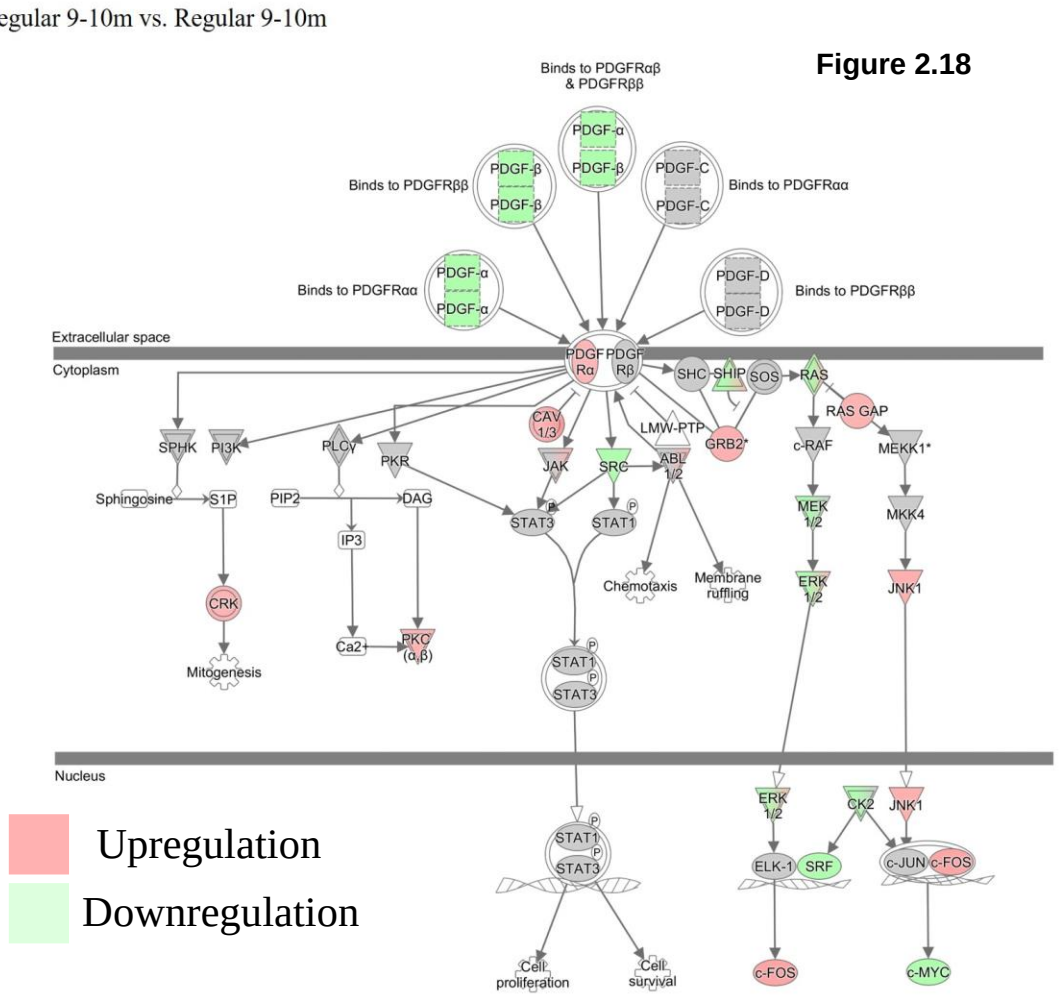

Figure 2.18 **Downregulation of PDGF signaling pathway during the perimenopausal transition**.
Transcriptomic expression obtained through RNA-Seq demonstrates downregulation of PDGF signaling pathway during the endocrinological transition from Regular 9-10-month to Irregular 9-10-month.

downregulation of fatty acid oxidation via inhibition of CPT1. In the mitochondria (Fig. 2.17)

almost all the proteins and complexes of the electron transport chain are predicted to be

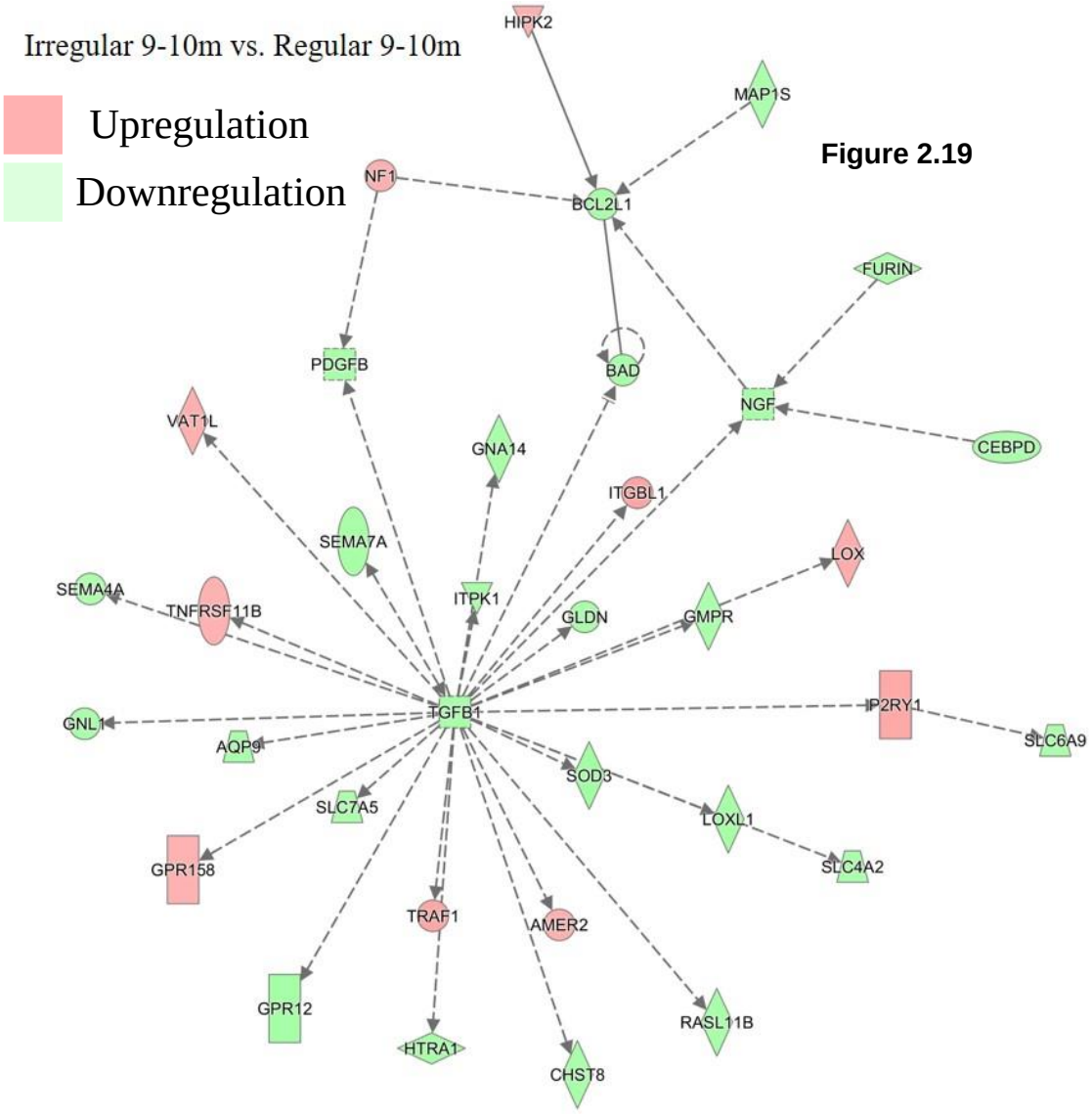

Figure 2.19

Figure 2.19 **TGFB1 gene network showing downregulation of PDGF, solute carriers and integrin binding proteins in the hippocampal transcriptome during the perimenopausal transition**.
Transcriptomic expression obtained through RNA-Seq demonstrates downregulation of TGFB1 gene, which is a central node in the network accompanied by downregulation of PDGF, solute carriers, integrin binding proteins and pro-apoptotic proteins during the endocrinological transition from Regular 9-10-month to Irregular 9-10-month in the hippocampal transcriptome.

downregulated with only complex II unaffected and complex IV mildly downregulated.

Moreover, the insulin signaling pathway, which is an important metabolic pathway is downregulated with predicted reduction in transcription during Regular to Irregular transition (Fig. 2.16), which could be due to chronic oxidative stress induced by decreased UCP2 that impedes the function of ROS in insulin secretion (Diano and Horvath, 2012). PDGF signaling pathway (Fig. 2.18), an important pathway with respect to blood brain barrier, appears to be downregulated in the hippocampal transcriptome during the first endocrine transition, but PDGFRα is upregulated. According to IPA, PDGFB is part of a network of genes with Transforming growth factor beta-1 (TGFB1) as a central node (Fig. 2.19). During transition from Regular to Irregular stage, TGFB1 is downregulated in the hippocampal transcriptome which seems to downregulate PDGF, transport proteins such as SLC7A5, AQP9, SLC4A2 (via LOXL1), integrin binding proteins such as SEMA7A, SEMA4A and SOD3, member of the superoxide dismutase family. Downregulation of TGFB1 and other associated proteins during the Regular to Irregular transition in the hippocampus indicates reduced cell growth and proliferation which may directly impact the blood brain barrier integrity. Integrins, seen downregulated in Fig. 2.19, serve to keep the extra-cellular matrix adherent and their downregulation suggests reduced attachment of cells to the ECM which in the context of BBB coupled with reduced PDGF and TGFB1 can be interpreted to indicate downregulation of pericytes and endothelial cells leading to lower cell growth and survival and cellular differentiation. On the other hand, downregulation of BCL2L1 and BAD indicate reduced cell apoptosis since BAD downregulation reduces proapoptotic activity. SOD3 downregulation impairs the ability to neutralize superoxide free radicals. Taken together these results suggest reduced growth and cell proliferation, reduced apoptosis and decreased integrity of ECM in the hippocampus which could result in compromised BBB.

2.5 Discussion

Perimenopausal transition is known to increase risk of cognitive decline, AD and immune dysregulation as discussed earlier. A systems biology study of the perimenopausal hippocampal transcriptome was carried out to understand transcript-level changes in the hippocampi of female SD rats during chronological and endocrinological aging. The data in this study were obtained from the sequencing of messenger RNA (protein-coding RNA) extracted from homogenized hippocampi of female rats in various stages of chronological and endocrinological transition. These data represent transcriptomic changes in the hippocampus as a whole, and consequently it is challenging to attribute transcriptomic alterations to specific cell types found in the hippocampus. The complexity of the data allows only a broad overview of the alterations in hippocampal transcriptome. In this section I discuss the general findings of the RNA-Seq and their interpretations in light of published literature.

Differentially expressed genes obtained through RNA-Seq must be analyzed with respect to specific statistical cut-offs. A standard cut-off of $p<0.05$ will result in a large number of false positives due to the tens of thousands of genes being involved in the study. Therefore, the most stringent cut-off of $FDR<0.05$ was used that guarantees less than five percent false positive genes among the list of genes deemed to be significant. For each comparison, only those genes that met this stringent cut-off were termed as significantly differentially expressed genes.

From the results it is evident that both age and endocrine changes play a significant role on gene expression in the hippocampus of female rats. The first aging and endocrine transitions - Regular cyclers 6m to Regular cyclers 9-10m and Regular cyclers 9-10m to

Irregular cyclers 9-10m respectively show similar number of genes significantly altered (FDR<0.05). The second endocrine transition from Irregular 9-10m to Acyclic 9-10m has very few genes significantly altered. This phenomenon demonstrates that hippocampal transcriptomic expression alters the most from the age of 6 to 9 months in female rats and again when they transition from Regular to Irregular estrus cycling status at 9-10m, but very few genes are significantly differentially expressed during the transition from Irregular to Acyclic 9-10m, during which the perimenopausal transition is almost over and menopause begins.

However, the greatest number of genes significantly differentially expressed in the hippocampi are observed when Regular 9-10m and Regular OVX 10-10.5m are compared. This reinforces the belief that sudden loss of ovarian steroids (such as during surgical menopause) could result in dramatic alterations in the hippocampus based on changes observed in the hippocampal transcriptome of perimenopausal female rats. Surgical menopause is not representative of the majority of human females that undergo natural reproductive senescence and abrupt cessation of ovarian hormones in rodent females is dissimilar to the reproductive senescence experienced by the postmenopausal ovary in humans (Mayer et al., 2004; Mayer et al., 2002). Data from the RNA-Seq also supports natural reproductive senescence model as the least disruptive model of perimenopause. At the same time similar pathways are altered between both Regular to Irregular perimenopausal transition at 9-10m as well as the Regular 9-10m to Regular OVX 10-10.5m surgically achieved abrupt menopause: T cell activation and AD pathways as predicted by PANTHER, which supports the idea that changes happening during menopause could influence the immune system and risk of AD.

Based on the concurrence data published previously by our lab (Yin et al., 2015) and currently presented data analysis of the hippocampal transcriptome, it is likely that the Regular to Irregular endocrine transition at 9-10 months of age is a critical period in the natural rodent perimenopause. Functional classification of genes significantly differentially expressed during the Regular to Irregular transition at 9-10 months of age in female rat hippocampus revealed that majority of genes (30%) performed functions that I could classify as the Neurological genes category, 22% were in Alzheimer's disease category and the rest are in Metabolic, Inflammation and Cell adhesion & membrane trafficking category, in a descending order of the number of genes. These findings uncover the extent to which hippocampal transcriptome diverges during the Regular to Irregular transition in female rats with significant implications for cognitive decline, reduction in bioenergetic gene expression and suboptimal mitochondrial function demonstrated earlier (Yin et al., 2015). An example to support this is the expression of UCP2 during the perimenopausal transition. Absence of UCP2 results in deficits in procedural memory and spatial cognition (Hermes et al., 2016). UCP2 downregulation has been found to be associated with increased oxidative stress, atherosclerosis, vascular damage and shorter lifespan in mice (Andrews and Horvath, 2009; Ma et al., 2010; Ma et al., 2014; Moukdar et al., 2009). Increased UCP2 reduced ROS and protected endothelial cells against damage from ROS (Ma et al., 2013; Tian et al., 2012). Neuroprotective function of UCP2 has been demonstrated both *in vitro* and *in vivo* in multiple different studies (Haines et al., 2010; Hass and Barnstable, 2016; Mattiasson et al., 2003; Normoyle et al., 2015). One group also demonstrated that UCP2 conferred protection against stroke (Rubattu et al., 2017). It is therefore worrisome to observe UCP2 downregulation in the hippocampal transcriptome during endocrine transition in 9-10m old female SD rats, after its

upregulation from Regular 6m to Regular 9-10m old rats. However, direct increase in ROS due to decrease in UCP2 expression was not measured in this study and therefore a clearer correlation of UCP2 expression with ROS production in the hippocampus in the perimenopausal model is required. If extrapolatable to humans, this data from hippocampi of female rats would mean that during perimenopause women may lose the neuroprotective effect of UCP2 which in turn would increase their risk for neurodegenerative diseases.

Additionally, IPA analysis of differentially expressed genes between Regular cyclers 9-10m and Irregular cyclers 9-10m shows a differential regulation of IL-27 transcript, which is a cytokine (Hunter and Kastelein, 2012b). IL-27 has exhibited both pro- and anti-inflammatory properties, not only based on cell type it affects but also based on the context of the entire immune system milieu and type of infection or disease under study (Yoshida and Hunter, 2015). IL-27 has been shown to both reduce (Huber et al., 2007; Neufert et al., 2007; Stumhofer et al., 2007) and promote (Hall et al., 2012; Kim et al., 2013b; Moon et al., 2013) population of regulatory T cells, while it controls proinflammatory T cell responses of Th2 and Th17 cells (Hunter and Kastelein, 2012a). A neuroprotective role of IL-27 has been described but it is unclear whether these effects of IL-27 are mediated locally within the CNS or are CNS manifestations of events in the periphery or both (Yoshida and Hunter, 2015). Considering the complex role of IL-27 in regulating various aspects of the immune system, predicted downregulation of IL-27 in the hippocampal transcriptome during perimenopause in female SD rats suggests dysregulation of the immune system. IL-27 has been found to be associated with estrogen and progesterone levels during pregnancy in women and increases throughout gestation, before dropping dramatically postpartum (Enninga et al., 2015), the significance of which is unclear but this

observation hints at a role of sex steroids in IL-27 regulation. Therefore, it is difficult to ascertain the role of IL-27 during perimenopause in the hippocampus but its downregulation in the hippocampal transcriptome during the endocrine transition at 9-10m suggests a role of both innate and adaptive immune system in the hippocampus during endocrinological aging. Based on these findings in our model of natural reproductive senescence, future studies exploring immune system interactions during perimenopause may wish to delineate the role of IL-27 in this endocrine transition.

Insulin signaling pathway and bioenergetic gene expression are both downregulated during the Regular to Irregular transition in 9-10-month-old female SD rats. These observations are corroborated by results of the FDG-PET and mitochondrial function our group published previously in the same model (Yin et al., 2015).

Both IPA and PANTHER predicted downregulation of PDGF signaling (Fig. 2.18) in the hippocampal transcriptome of female SD rats during the Regular to Irregular transition at 9-10m, which could be in response to reduced cortical estrogen level observed during perimenopause (Yin et al., 2015) consistent with findings in the literature outlined in Chapter 1. The isoform of PDGF called PDGF-BB has been shown to be responsible for maintaining the health of BBB (Zhao et al., 2015; Zlokovic, 2008) and is regulated by estrogen (Bake and Sohrabji, 2004; Jiang et al., 2018). Additionally, upregulation of PDGFRα signaling seen concomitantly with PDGF-BB downregulation may contribute to BBB impairment via p38 MAPK mediated pathway (Ma et al., 2011). Besides PDGF, estrogen also affects tight junction proteins as mentioned in Chapter 1. Additionally, in the RNA-Seq data the TGFB1 gene network shows downregulation of solute carriers, integrin binding proteins, SOD3 and PDGF, as well as reduced expression of pro-apoptotic proteins, suggesting reduced cell proliferation and reduced apoptosis but at the same time

decreased cell survival and maintenance. Since the RNA-Seq results reflect the transcriptome of homogenized hippocampal tissue, cell-specific pathways and functions are difficult to elucidate, and it is possible that these conflicting findings reflect pathways in two or more differing cell types. Ligand–receptor systems such as TGFB and PDGF have been implicated in maintenance of vascular stability (von Tell et al., 2006) and TGFB signaling plays a role in differentiation, maturation, proliferation, migration and attachment of endothelial cells and pericytes (Darland and D'amore, 2001; Maddaluno et al., 2013; Reyahi et al., 2015; Van Geest et al., 2010), confirmed *in vivo* in murine models (Maddaluno et al., 2013). In fact, in an *in vitro* BBB model it was shown that continuous TGFB production by pericytes increased the barrier function of BBB and treatment with anti-TGFB1 antibody inhibited this barrier function (Dohgu et al., 2005). In PDGF deficient mice lack of pericytes is the main cause of phenotype since endothelial cells in the capillaries of these mutant mice seem to be unable to attract pericyte progenitor cells (Crosby et al., 1998; Lindahl et al., 1997) and these mice exhibited morphological sings of increased vascular permeability (Hellström et al., 2001). Most recently it was discovered that PDGF-BB signaling in pericytes results in secretion of microvesicles and growth factors that may have neuroprotective and neurorestorative role (Gaceb et al., 2018). However, pericytes in a proinflammatory environment produce proinflammatory cytokines resulting in capillary leakage (Edelman et al., 2007a, b). This can further cause detachment of pericyte from the basal lamina and demonstrate structural disorganization (Nishioku et al., 2009). Thus, the proinflammatory environment of perimenopausal hippocampus (Malutan et al., 2014; Russu and Antonescu, 2018; Yin et al., 2015) may compromise BBB integrity independently from reduced cortical level of estrogen.

Therefore, these findings from the hippocampal transcriptome suggest that during the first endocrine transition from Regular to Irregular cycling status at 9-10m of age the reduced cortical levels of estrogen and a proinflammatory environment may result in increased permeability of BBB likely facilitated by PDGF and TGFB-mediated pathways.

2.6 Conclusion

Perimenopausal transition in the hippocampi of female SD rats is a period of dramatic up- and down-regulation of genes and pathways involved in blood brain barrier permeability, immune system regulation, mitochondrial bioenergetics and metabolomic changes. The most dramatic gene level changes are seen in response to abrupt cessation of ovarian hormones achieved by surgical menopause. Compromised BBB during perimenopause could potentially be a major risk factor for women to develop neurodegenerative diseases and autoimmune states and a functional confirmation of breached BBB during perimenopause in a rat model would help validate this finding from the systems biology study.

3 Blood Brain Barrier (BBB) Permeability in Perimenopausal Female Rats

3.1 Abstract

In this experiment I tested the BBB permeability in female SD rats using sodium fluorescein. I found that perimenopause is indeed a stage of increased BBB permeability in female rats and is dependent on endocrine status more than age. I also found that intra-group variability in blood brain barrier permeability increased with gradual endocrine aging rather than with chronological aging, and abrupt endocrine aging (surgical menopause) surprisingly did not lead to appreciable increase in intra-group variability of blood brain barrier permeability when compared to natural reproductive senescence group of female rats.

3.2 Introduction

To reiterate, blood brain barrier permeability is increased during aging, neurodegenerative diseases and injury such as traumatic brain injury. Mechanistically a compromised BBB requires either altered tight junction proteins, damaged endothelial cells or pericytes or astrocyte foot processes or a compromised and exposed basement membrane or a combination of all these processes (Hawkins and Davis, 2005). In females, sex steroids, mainly estrogen, play a major role in directly and indirectly regulating both tight junction proteins as well as cellular components of BBB. On the other hand, in males, testosterone maintains healthy BBB and increased BBB permeability is seen with testosterone-depletion (Atallah et al., 2017) Supplementation with testosterone ameliorated the effects of lack of testosterone on BBB permeability (Atallah et al., 2017). Women begin to lose

the protective effect of estrogen during the perimenopausal transition and this chapter explores the effect of loss of estrogenic protection on BBB integrity by measuring the amount of a fluorescent dye, sodium fluorescein, that extravasates across the BBB in a rat model of perimenopause.

3.3 Materials & Methods

3.3.1 CHOICE OF MARKER FOR BBB DISRUPTION

The use of Evans blue (EB) dye to measure BBB permeability is quite common. However, there are certain drawbacks to using EB (Saunders et al., 2015). After EB is injected, not all of the injected dye binds exclusively to albumin and free dye could enter extravascular spaces and bind to tissues, thus distorting results. It may be difficult to measure quantity of EB in some experiments since its excitation and emission wavelengths change in the presence of proteins (Saunders et al., 2015). Another marker, Horseradish Peroxidase (HRP), causes an allergic reaction and affects permeability of blood vessels (Majno et al., 1961) in some commonly used strains of rats (Cotran and Karnovsky, 1967) but not in others (COTRAN et al., 1968). HRP itself could cause membrane damage (Mazariegos et al., 1984) which may lead to less accurate measurement of BBB permeability. The third dye under consideration, sodium fluorescein (NaF) binds to proteins weakly and can serve as an effective tracer of BBB compromise compared to protein-binding EB (Wolman et al., 1981). Due to its smaller molecular size compared to EB, measurement of NaF extravasation across BBB allows detection of subtler changes in BBB integrity versus radioactive tracers (Kaya and Ahishali, 2011). No NaF induced deleterious effects on BBB have been reported so far and NaF is considerably less toxic than Evans blue or Horseradish Peroxidase (Saunders et al., 2015). Based on these observations in

literature, I chose NaF as a marker for BBB disruption from among three markers considered namely EB, NaF and HRP.

3.3.2 DYE INJECTION AND SACRIFICE

I used sodium fluorescein (Sigma-Aldrich) for detecting suspected BBB compromise in perimenopausal female rats. Utilizing daily ovarian cytology I cycled five and eight months old female SD rats and classified them into groups based on age and estrus cycles. These groups were: Regular cyclers 6m, Regular cyclers 9-10 months, Irregular cyclers 9-10 months and Acyclic 9-10 months. Additionally, I ovariectomized some rats in the Regular cyclers 6m group while some others underwent sham ovariectomy procedure where I carried out the surgical procedure without dissecting the ovaries, in order to explore the effect of ovariectomy on BBB permeability. I labeled these two groups Regular OVX 7m and Regular Sham OVX 7m, based on the fact that female SD rats in both these groups of rats were sacrificed at 7 months of age. I decided to have a one-month lag between ovariectomy and euthanasia for the effect of surgical menopause to manifest itself. After female rats were classified into specific groups and reached the necessary age, I sacrificed each rat on the day of estrus (E) as determined by microscopic analysis of daily vaginal smears.

On the day of sacrifice, I injected the animals with 10 mg of sodium fluorescein in 0.1 ml of sterile saline, administered via intraperitoneal route, adapted from the protocol published by Li *et al* (Li et al., 2015). Thirty minutes later (Kozler and Pokorny, 2003; Yen et al., 2013), I anesthetized the animals with ketamine-HCl (100–200 mg/kg). I collected cardiac blood and perfused the rats with PBS to drain blood out. I centrifuged cardiac blood at 10,000 x g for 10 min at 4°C. I removed the serum (supernatant) and stored it at -80 °C in 50 µL aliquots and discarded the cell pellet. I dissected the brain of each female

rat on ice and collected hypothalamus, cortex and hippocampus. All the brain tissue that I harvested were frozen at −80 °C for future experiments.

3.3.3 ANALYSIS OF SERUM AND BRAIN TISSUE TO DETERMINE BBB PERMEABILITY (LI ET AL., 2015)

I thawed the serum (one 50 µL aliquot) and mixed with an equal (50 µL) volume of 15% trichloroacetic acid (TCA). After centrifugation for 10 min at 10,000 × g at 4°C, I recovered the supernatant and made it up to 150 µl by adding 30 µl of 5 M sodium hydroxide (NaOH) and rest 7.5% TCA. I removed from the freezer the brain tissue dissected and stored earlier (hypothalamus, hippocampus, cortex) and weight each tissue individually. I then homogenized the brain tissues in cold 7.5% TCA and centrifuged them for 10 min at 10,000 × g at 4°C to remove insoluble precipitates. After the addition of 30 µl of 5 M NaOH to 120 µl of supernatant, I used Synergy H1 Hybrid Multi-Mode Reader (Bio-Tek Instruments, Wonooski, VT) to determine the fluorescence of each sample with excitation at 485 nm and emission at 530 nm. I used standards of NaF (125 to 4,000 µg/mL) in identical solvent to calculate the NaF content of the samples. NaF uptake into tissue is expressed as microgram (µg) of fluorescence in tissue/mg of tissue divided by µg of fluorescence in serum/mL of blood to normalize values of fluorescence detected in brain tissue of each animals to the value of fluorescence detected in the blood (Fig. 3.1).

$$\text{BBB-PI} = \frac{\dfrac{\mu g \text{ of sodium fluorescein}}{\text{mg of brain tissue}}}{\dfrac{\mu g \text{ of sodium fluorescein}}{\text{mL of serum}}}$$

Figure 3.1 Calculation of Blood Brain Barrier Permeability Index (BBB-PI).

3.3.4 STATISTICS

Statistical analysis was performed in Prism 6.0. For each tissue type (hypothalamus, hippocampus and cortex), statistical analysis was carried out using Mann-Whitney test and each group of female rats was compared to every other group. The difference between groups was considered significant if the p-value was <0.05.

3.4 Results

The results of dye extravasation are described by tissue type. Highest BBB-PI was observed in hypothalamus from all animals, whereas hippocampus had lower BBB-PI and cortex had the lowest BBB-PI.

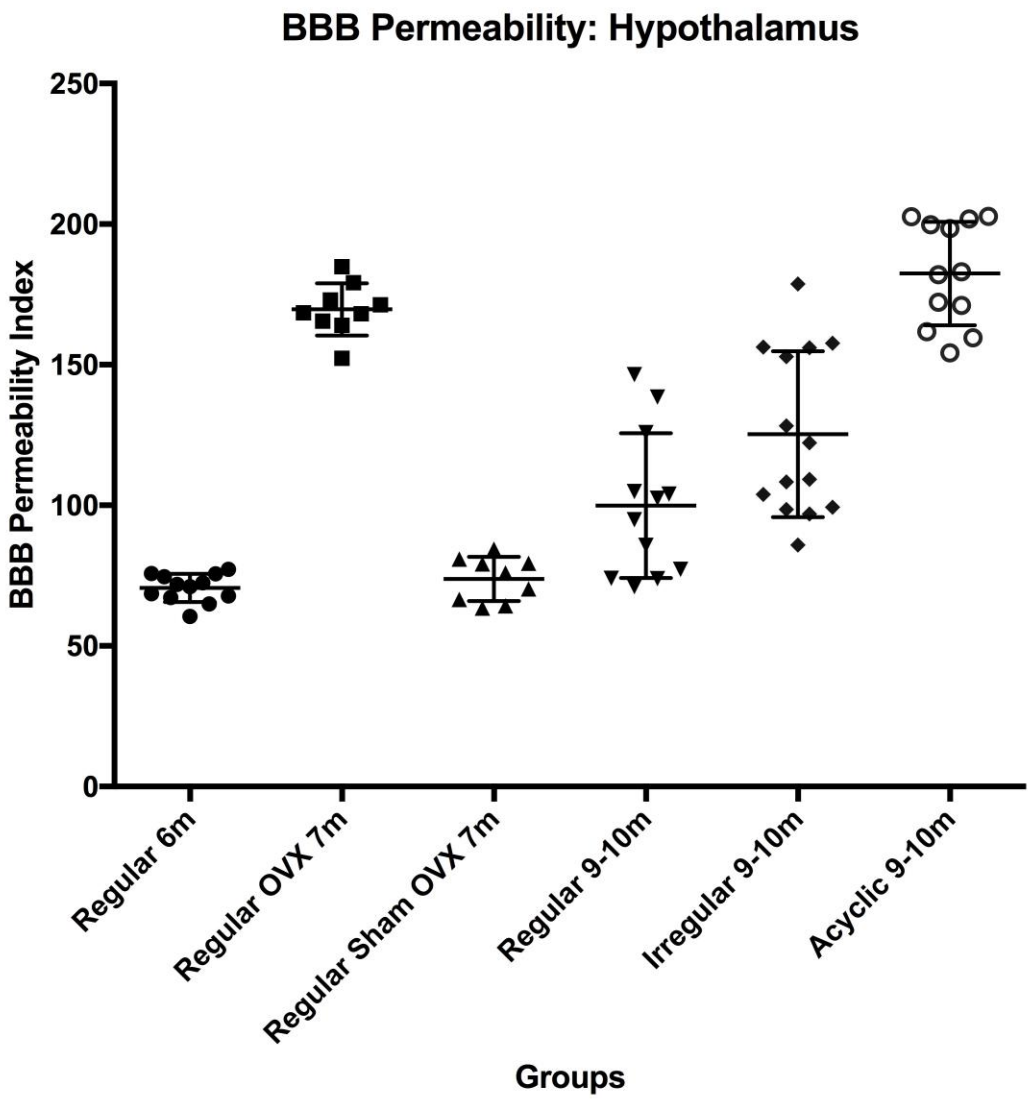

Figure 3.2 **Blood Brain Barrier Permeability Index for hypothalamus in female SD rats**.
In the hypothalamus, blood brain barrier permeability increases with increase in age and progression of endocrine status towards menopause. The magnitude of BBB permeability produced by OVX is less variable but equal in magnitude to Acyclic endocrine status.

Regular cyclers 6m group had the lowest BBB-PI among all groups in case of hypothalamic tissue, closely followed by Regular Sham OVX 7m (Fig. 3.2). BBB-PI climbed higher in the Regular cyclers 9-10m group and further increased in Irregular cyclers 9-10m. Highest BBB-PI was observed in Acyclic 9m followed by Regular OVX 7m.

It is also notable that the individual animals are more widely distributed in Regular cyclers 9-10m, Irregular cyclers 9-10m and Acyclic 9-10m with higher standard deviation than other groups, implying higher variability in these groups.

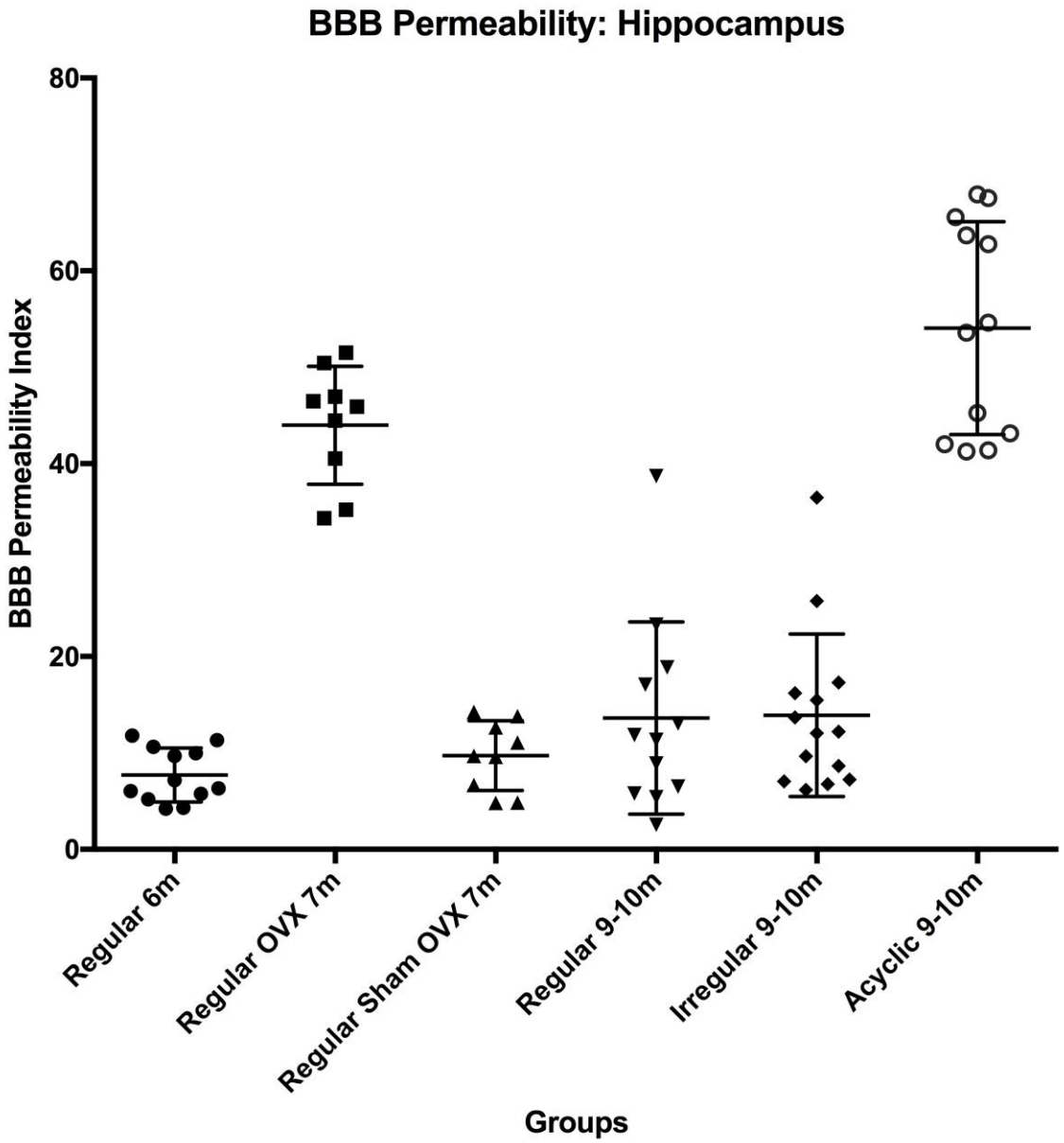

Figure 3.3 **Blood Brain Barrier Permeability Index of hippocampus in female SD rats**.
In the hippocampus, similar to hypothalamus, blood brain barrier permeability increases with increase in age and progression of endocrine status towards menopause. The variation in the magnitude of BBB permeability produced becomes apparent and animals group together into sub-populations, reflecting variability in the endocrine transition process; highest variability is exhibited in the Acyclic group.

In case of hippocampus (Fig. 3.3), a similar pattern is followed. Lowest permeability is

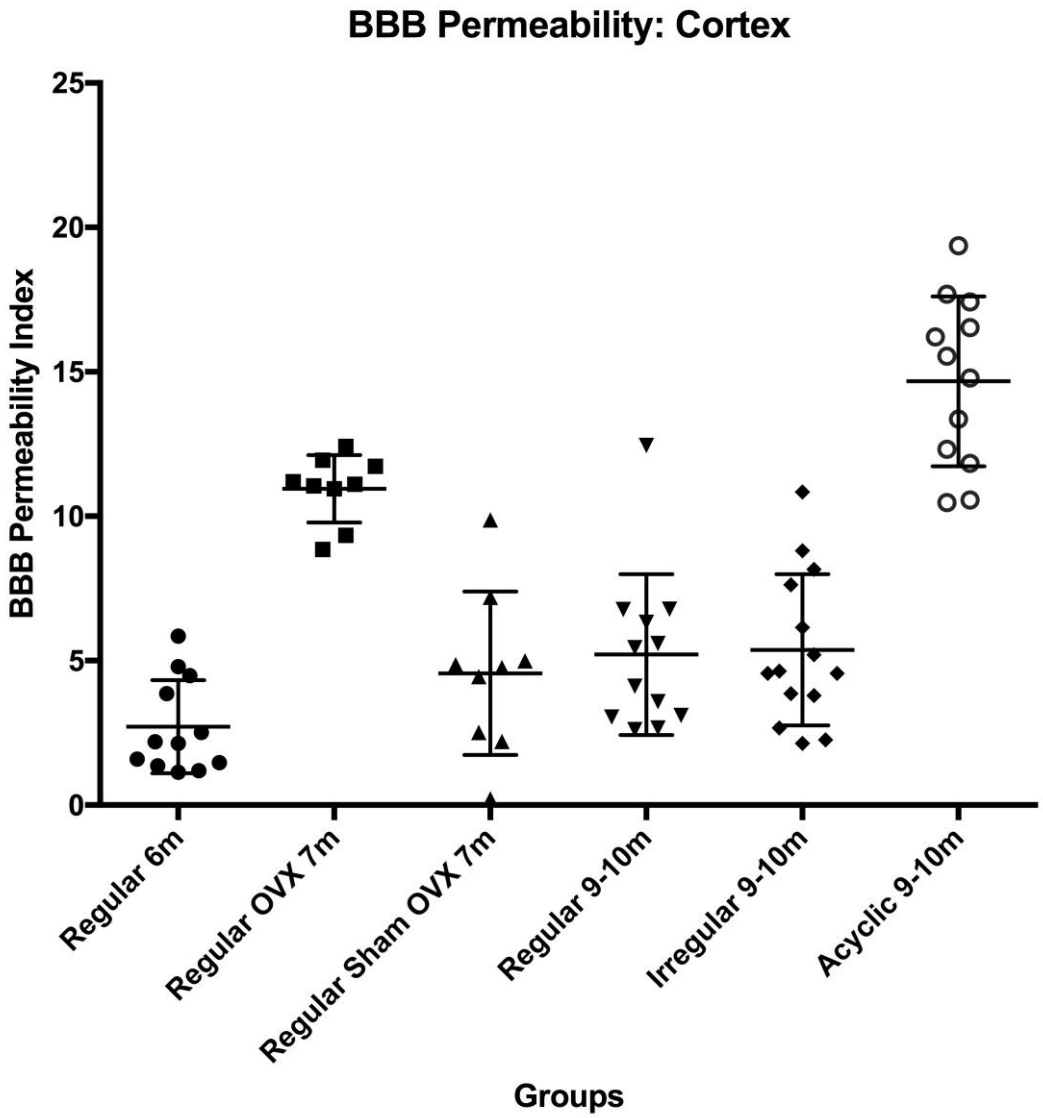

Figure 3.4 **Blood Brain Barrier Permeability Index of cortex in female SD rats**. The BBB-PI, a measurement of degree of compromise of BBB is lowest in cortical tissue. Similar to hippocampus, the variability of BBB compromise is higher in older groups progressing towards menopause.

seen in Regular cyclers 6m and Regular Sham OVX 7m, and highest permeability is seen in Acyclic 9-10m and Regular OVX 7m (Fig 3.3). It is also notable that the individual animals are more widely distributed in Regular cyclers 9-10m, Irregular cyclers 9-10m and

Acyclic 9-10m with much higher standard deviation than other groups, implying higher variability in these groups. Highest intra-group variability for hippocampus is seen in the Acyclic 9m animals.

In case of cortex (Fig. 3.4) similar pattern as seen in hippocampus is followed with some differences. All groups show higher intra-group variability compared to hippocampus, and in some groups (Regular Sham OVX 7m, Regular cyclers 9-10m and Irregular cyclers 9-10m) certain animals have a BBB-PI similar to certain Acyclic 9-10m animals.

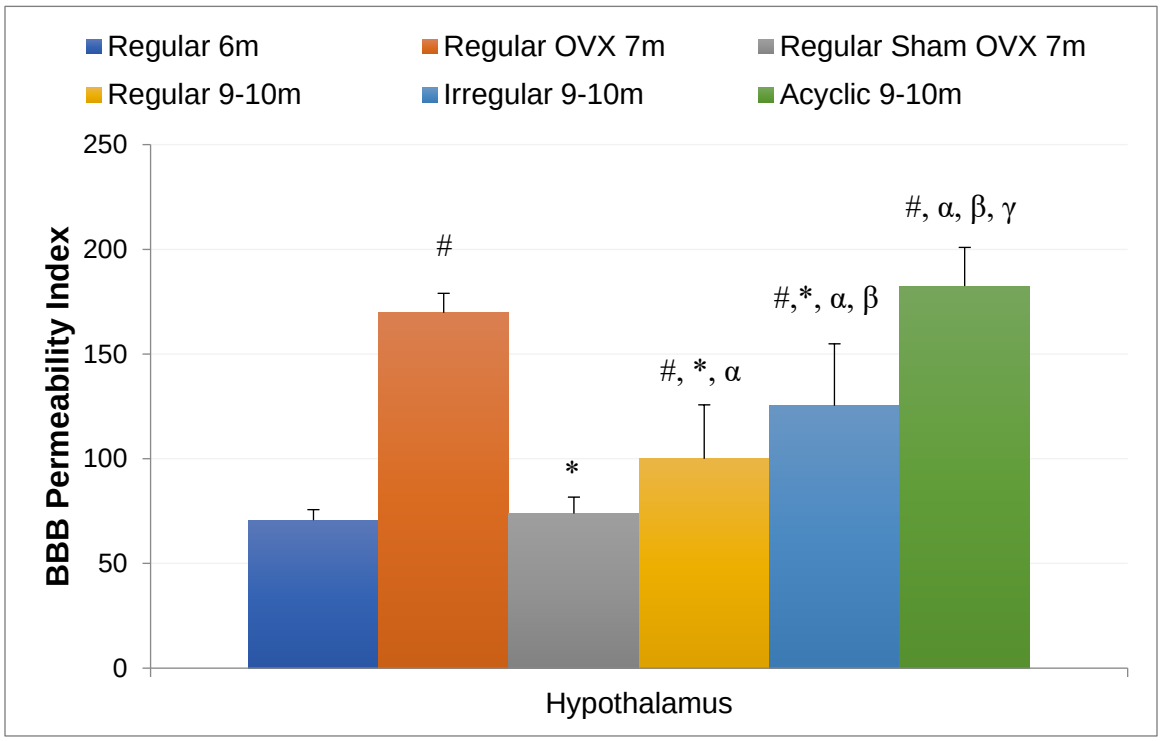

# p< 0.05 vs. Regular cyclers 6m
* p< 0.05 vs. Regular OVX 7m
α p< 0.05 vs. Regular Sham OVX 7m
β p< 0.05 vs. Regular 9-10m
γ p< 0.05 vs Irregular 9-10m

Figure 3.5 **Blood Brain Barrier Permeability Index (BBB-PI) of hypothalamus with statistical significance**.
Regular cyclers 6m and Regular Sham OVX 7m are similar and significantly different from other groups. BBB-PI in the Acyclic group is the highest and statistically significantly different from all other groups.

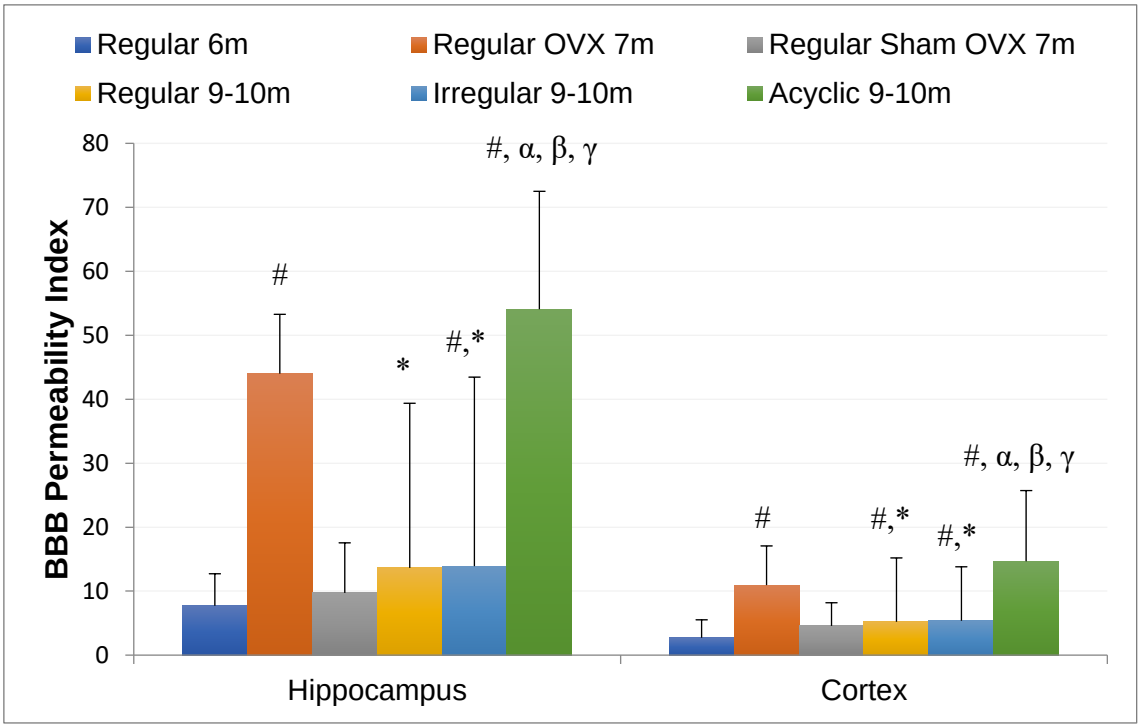

# p< 0.05 vs. Regular cyclers 6m
* p< 0.05 vs. Regular OVX 7m
α p< 0.05 vs. Regular Sham OVX 7m
β p< 0.05 vs. Regular 9-10m
γ p< 0.05 vs Irregular 9-10m

Figure 3.6 **Blood Brain Barrier Permeability Index of hippocampus and cortex with statistical significance**.
Hippocampus and cortical tissue show BBB-PI in Regular cyclers 6m and the Sham OVX groups to be similar and significantly different from the other groups. Surgical and natural reproductive senescence groups have similar BBB-PI, but the Acyclic group exhibits higher variability.

Statistically, in case of hypothalamic tissue (Fig. 3.5), Regular cyclers 6m and Regular Sham OVX 7m are similar to each other but significantly different from other groups. Also, Regular OVX 7m and Acyclic 9m are statistically similar. Acyclic 9-10m is statistically significantly different from all other groups except Regular OVX 7m. In case of hypothalamus Irregular cyclers 9-10m and Regular cyclers 9-10m are statistically different

but this is surprisingly not seen in case of hippocampus and cortex (Fig. 3.6) although the p-values are less than 0.1 and could reach a level of significance either with more animals

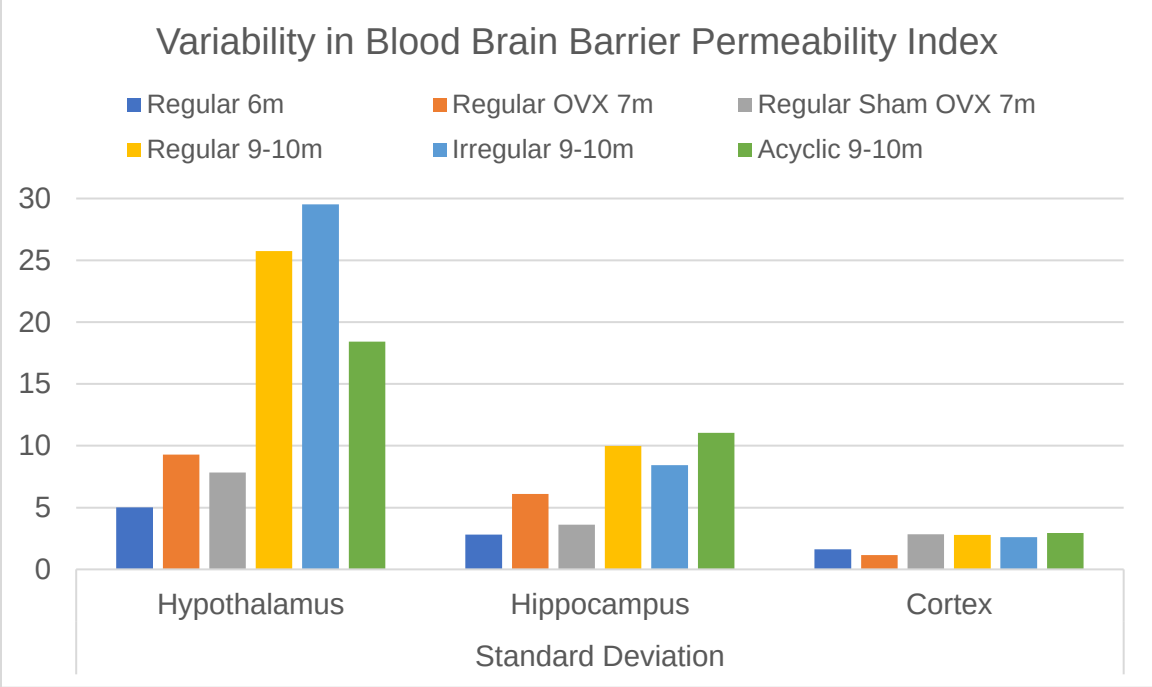

Figure 3.7 **Variability in Blood Brain Barrier Permeability Index of hypothalamus, hippocampus and cortex**.
Variability in the form of standard deviation was calculated for each group for each tissue type and suggests presence of sub-populations in each group, especially in older animals as well as endocrinologically advanced animals. The only exception is the OVX group which has lower variability compared to 9-10m groups.

or reduced intra-group variability. Even though Regular cyclers 6m and 9m in case of hippocampus are not statistically significantly different, the p-value is 0.06 and trending towards statistical significance is seen in both hypothalamus and cortex.

Figure 3.7 depicts the observed intra-group variability, in the form of standard deviation, in blood brain barrier permeability index which is a measure of how variable is the compromise of BBB among these groups. Lower variability suggests little difference in BBB permeability among the animals in the group and higher variability suggests larger difference in BBB permeability between animals of the same group. Variability varies by

tissue type, but highest variability is seen in 9-10m groups while the younger groups have lower variability.

3.5 Discussion

This set of experiments furnish functional proof of blood brain barrier permeability in three brain regions including hippocampus hypothesized by hippocampal transcriptomic analysis in perimenopausal female SD rats described in Chapter 2. This set of data taken together further support our hypothesis. Additionally, literature supports the thought that decreased level of estrogen plays a critical role in decreased integrity of BBB due to regulation of PDGF. PDGF levels decrease as a consequence of estrogen decline and subsequently reduced PDGF results in sub-optimal function of endothelial cells in cerebrovasculature (Bake and Sohrabji, 2004). Endothelial cells along with astrocyte foot processes, pericytes and basement membrane are responsible for an optimally functioning BBB (Armulik et al., 2010).

Our previous publication showed that all perimenopausal groups had varied levels of E2 in cortex and serum and that the serum and cortical levels of E2 were not correlated (Yin et al., 2015). Our group also found that cortical levels of E2 saw a statistically significant decline from 6 months to 9- to 10-month-old female SD rats, while the amount of E2 measured in acyclic rats was very small and statistically significantly lower than Regular 6 and Irregular 9-10 month groups but not dissimilar to Regular 9-10 month group (Yin et al., 2015). These previously published findings of cortical levels of E2 in the perimenopausal model of female rats correlate well with the observed BBB-PI, which is a measurement of increased extravasation of sodium fluorescein marker across the BBB and into the brain parenchyma, carried out in an identical rodent model of perimenopause.

The decrease of cortical E2 levels seen from 6-month old to 9- to 10-month old rats correspond to the increased permeability of BBB in the same groups. Cortical estrogen levels were found to rise in the Irregular 9-10m group which is reflected in a reduced increase in BBB-PI from Regular to Irregular female rats at 9-10-months of age. Highest BBB permeability is observed in Regular OVX 7m and Acyclic 9m old female rats implying that endocrine aging and cortical estrogen levels may determine the optimal functioning of BBB rather than age.

Additionally, in the Regular 6m group the female SD rats cluster closely around the mean. All the rats in this group have very similar measurements of BBB-PI with little variation. Two other groups of female rats that chronologically follow Regular 6m group, namely, Regular OVX 7m and Regular Sham OVX 7m show higher variation, as measured by standard deviation, than Regular 6m but lower than the remaining three groups. Rats in the Regular 9-10m show a much higher standard deviation and the highest standard deviation is exhibited by Irregular 9-10m female rats in case of hypothalamus. The variation among the Acyclic 9-10m group is reduced compared to the previous two groups (Fig. 3.7).

Comparatively less intra-group variability among the 6m and Sham OVX 7m old female rats suggests that the process of aging results in divergence of blood brain barrier permeability. While ovariectomy does increase permeability of the BBB in female SD rats, this increase is relatively uniform across the group due to abrupt cessation of ovarian hormone production achieved by surgical menopause. Gradual ageing of all the 9-10m groups, as opposed to sudden surgically induced menopause seen in Regular OVX 7m, results in separation of the group into distinct subpopulations. In the Regular Sham OVX 7m group in cortex and to some extent in hippocampus we can identify at least two distinct

sub-groups: those animals that have maintained BBB permeability similar 6m old animals and those with elevated BBB permeability. Such sub-populations are visible in Regular, Irregular and Acyclic 9-10m groups as well.

Since all the female rats are genetically identical and have very similar environmental exposure and handling, an alternate explanation for the variability in BBB-PI among animals in the study maybe due to differences in exposure to light in the vivarium (Emmer et al., 2018; Heywood, 1980), microbiota in the gut (Clarke et al., 2013) and potentially epigenetic differences (Bacon et al., 2018). However, these factors would likely uniformly affect all female SD rats in this study but the observed difference in variability between the different groups suggests a more group-specific cause of intra-group variability in BBB-PI. Future studies in this research area may focus on the mechanisms of increased BBB permeability in perimenopausal female rats which I suspect involves the PDGF signaling pathway, pericytes and tight junction proteins, which are all indirectly influenced by estrogen according to published literature.

3.6 Conclusion

In our model of natural reproductive senescence, BBB permeability is increased in female SD rats undergoing perimenopause. Both endocrine and chronological aging predispose to this increase, but data suggests that the increase in permeability is more dependent on gradual endocrine aging rather than pure chronological aging or abrupt endocrine aging. The divergence of BBB permeability among female SD rats as a result of chronological and endocrinological aging hints that there may be certain protective or deleterious factors besides estradiol that exert influence in modifying the permeability of BBB during the aging process in females. If found extrapolatable to humans these findings could explain the

variability seen among human females in the symptoms, onset and progression of diseases such as Multiple Sclerosis that exhibit high inter-individual variability (Kappos et al., 2015) where BBB permeability may even serve as a pathological marker of neuroinflammation (Cramer et al., 2015).

4 Allopregnanolone: A Potential Neuroregenerative Therapeutic

4.1 Abstract

This study is a translational research project that uses ApoE-Targeted Replacement (TR) mouse model to examine a promising neuroregenerative therapeutic in a genotype susceptible to AD. In this experiment, I injected mice with the human form of ApoE gene with a novel neuroregenerative therapeutic, Allopregnanolone (Allo), which is currently under clinical development in humans. I found that both males and females with ApoE 4/4 genotype demonstrated significant cognitive improvement as measured by the novel object recognition test. RNA-Seq study of the hippocampi of the Allo-treated female ApoE 4/4 mice suggested upregulation of PDGF-BB compared to saline treated counterparts, suggesting that Allo could potentially ameliorate age related increase in blood brain barrier permeability. The RNA-Seq data also suggested Allo's effect on multiple immune system, cell signaling and metabolomic pathways. Study of 185 plasma and cortex metabolites suggest major differences in glycerophospholipids, protein and lipid metabolism based on gender and genotype. *In vitro* Allo and its analogues have been shown to potentiate mitochondrial function in human neural stem cells and 30 minutes of exposure to Allo confers similar mitochondrial potentiation as 24-hour continuous exposure in these stem cells. Allo was also evaluated as a potential agonist of mitochondrial Transmembrane protein (TSPO) but found to have antagonistic-like activity in human neural stem cells.

4.2 Introduction

Apolipoprotein (Apo) E4 allele is the strongest genetic risk factor for AD (Corder et al., 1993; Farrer et al., 1997a; Genin et al., 2011; Huang and Mucke, 2012). Females bear an unequal burden of ApoE4 as a genetic risk factor with advancing age (Damoiseaux et al., 2012; Farrer et al., 1997a; Leung et al., 2012). Heterozygosity for ApoE4 allele increased AD risk by a factor of three, while homozygosity for the same allele (ApoE4/4 genotype) increased AD risk by a factor of ten (Holtzman et al., 2012; Loy et al., 2014). Those with the E4 allele are also likely to manifest AD at an earlier age compared to those with E2 or E3 allele (Spinney, 2014).

Mice whose ApoE locus contains human ApoE gene are termed as ApoE Targeted Replacement (ApoE-TR) mice. In aging ApoE4-TR mice learning and memory is significantly impaired due to loss of certain specific neurons (Andrews-Zwilling et al., 2010; Leung et al., 2012; Li et al., 2009). Tong *et al* (Tong et al., 2016) demonstrated that treatment of these mice with a molecule that acts as a $GABA_A$ receptor potentiator reduced cognitive decline and improved functional outcome in mice.

There have been multiple publications from our lab on Allopregnanolone (Allo). Allo (3α-hydroxy-5α-pregnan-20-one) activates $GABA_A$ receptor channels (Irwin and Brinton, 2014). Previously, we have established that Allo significantly increases proliferation of rat neural progenitor cells and human neural stem cells (Wang et al., 2005), reverses deficits in neurogenesis and cognition in the 3xTg mouse model of AD (Wang and Brinton, 2008; Wang et al., 2010), and improves survival of neural progenitor cells (Singh et al., 2012). In fact, Allo is currently being studied as a first-in-class neuroregenerative therapeutic for AD and mild cognitive impairment in a Phase Ib/IIa clinical trial (ClinicalTrials.gov Identifier: NCT02221622). While it is known that activation of TSPO by its ligands such as

FGIN 1-27 and PK 11195 leads to Allo production (Daugherty et al., 2013), producing anxiolytic effects in animal studies (Bitran et al., 2000), our aim was to detect if Allo itself acted as an agonist or antagonist of TSPO with respect to mitochondrial potentiation, which then would have suggested a feedback loop.

4.3 Methods:

4.3.1 ANIMALS

Animal studies were performed following National Institutes of Health guidelines on use of laboratory animals; protocols were approved by the University of Southern California Institutional Animal Care and Use Committee. Experimental and control animals had identical housing conditions from birth through euthanasia (12h light/dark cycle and PicoLab Rodent Diet 20). Female and male ApoE3-TR and ApoE4-TR homozygous mice and heterozygous female ApoE3/4-TR mice on a C57BL/6 background strain were obtained from Taconic Inc. and housed and bred at University of Southern California animal facility. I weighed the mice every week from the start of the study till euthanasia. All mice were fed identical chow and I monitored their food intake along with body weight to control for loss of body weight due to reduced consumption of food. We attempted to obtain our own ApoE 3/4 mice, however, the breeding did not succeed. I divided the mice into groups based on their genotype (ApoE3, ApoE4, ApoE 3/4), gender (male and female) as well as treatment group (Allo and Saline). Thus, the ten groups were ApoE3 Female Allo, ApoE3 Female Saline, ApoE3 Male Allo, ApoE3 Male Saline, ApoE4 Female Allo, ApoE4 Female Saline, ApoE4 Male Allo, ApoE4 Male Saline, ApoE 3/4 Female Allo and ApoE 3/4 Female Saline.

4.3.2 ALLOPREGNANOLONE INJECTIONS AND SACRIFICE

I injected the mice weekly with intramuscular injection of Allopregnanolone (1.5 mg/mL) or saline (0.9%). Allo and saline I used to treat mice were identical to the Allo and saline used in the clinical trial (ClinicalTrials.gov Identifier: NCT02221622). The amount of Allopregnanolone to be injected was calculated based on a dose of 2 mg which was identical (extrapolated to mice) to the dose that human participants received in the first cohort of the phase Ib/IIa clinical trial. I administered these weekly injections on the same day and in the same time window of nine to eleven AM for 26 weeks, starting from 10 months of age to 16 months of age. I ensured that any behavior study or blood collection procedure were separated in time from injections by at least four hours.

I sacrificed the animals after the last Allo injection. I first anaesthetized the mice using Ketamine-Xylazine cocktail (87.5 mg/kg Ketamine + 12.5 mg/kg Xylazine) 0.1mL/20g mouse weight injected intraperitoneally and collected cardiac blood in EDTA-coated tubes. I then centrifuged the tubes for 10 minutes at 2,000 x g using a refrigerated centrifuge previously adjusted to be at 4 °C. After centrifugation I immediately transferred the plasma to 1.5mL microcentrifuge tube and stored all plasma at -80 °C. The mice were not fasted before collecting this plasma and this plasma was not appropriate to carry out metabolomic analysis. Separate plasma was collected for metabolomic study as outlined later. The mice were then perfused with phosphate buffered saline (PBS) for at least 15 minutes. I then dissected the brain of each mouse on ice and separated brain stem and cerebellum first and then each cortical hemisphere laterally to dissect the hippocampus. I stored all brain tissues in -80 °C.

4.3.3 NOVEL OBJECT RECOGNITION TEST

I tested all mice for the Novel Object Recognition (NOR) test in accordance with published literature (Antunes and Biala, 2012; Ennaceur, 2010; Leger et al., 2013; Piterkin et al., 2008; Taglialatela et al., 2009). NOR was carried out after 24 once a week Allo injections. In short, I first acclimatized the mice to the NOR test room for five days during the habituation phase, taking care that the mice entered and exited the behavior room at the same time each day. I also mimicked the regular opening and closing of the room door during the habituation phase by opening and closing the room door every 15 minutes. During the second week, I allowed the mice to acclimatize to the wooden boxes in which the NOR test was to be carried out (one mouse/box) for 15 minutes, on the first three consecutive days. On the next day (fourth day of second week) I allowed the mice to explore for 10 minutes two identical objects (either two identical blue Lego pieces or two identical glass beakers) while in the wooden box and noted the specific object explored by each mouse. On the last day of NOR testing (day five of second week), I switched one of the two objects for the other and each mouse had a choice between a blue Lego piece and a glass beaker. One of the two objects had been explored by the mouse the previous day (familiar object) and the other was the novel object. Using video recording, the number of seconds spent by each mouse exploring each of the two (familiar (Tf) and novel (Tn)) objects was measured and two quantities were calculated. First, the difference in exploration time (in seconds) was calculated by subtracting the time taken to explore familiar object from that of the novel object (Tn – Tf) and denoted by Df. Second, a ratio of the difference in exploration time to the total time spent exploring was calculated (Tn-Tf/Tn+Tf) and denoted by Discrimination Index (DI).

4.3.4 SEQUENCING OF HIPPOCAMPAL RNA

The RNA I extracted from the hippocampi of ApoE mice was shipped to VANTAGE (Vanderbilt Technologies for Advanced Genomics) at Vanderbilt University and raw reads in the form of .fastq files were obtained. Before sequencing, VANTAGE analyzed RNA quantity and quality Qubit (Thermo Fisher, MA) and Bioanalysis Pico (Agilent Technologies, CA) and found the RNA to meet quality standards. VANTAGE utilized polyA-selected mRNA library preparation process and used Illumina HiSeq3000 to carry out paired end sequencing with a read length of 75 base pairs and a read depth of about 50 million reads. RNA from eight different groups of ApoE mice was sequenced with five mice per group (a total of 40 RNA samples) and initial raw data processing was carried out by Dr. Shang at UA and I analyzed the DEG list using IPA.

4.3.5 PLASMA COLLECTION AND METABOLOMIC STUDY

I collected whole blood in EDTA-coated tubes from each mouse through the eye as per the approved protocol, after subjecting the mice to an overnight fast of 14-16 hours, after 24 weeks of once a week treatment with Allo and before beginning NOR. I centrifuged the tubes for 10 minutes at 10,000 x g using a refrigerated centrifuge previously adjusted to be at 4 °C. After centrifugation I immediately transferred the plasma to 1.5mL microcentrifuge tube and stored all plasma at -80 °C. The plasma and cortex from each of the experimental mice groups were queried for 185 metabolites using ultra-performance liquid chromatography-tandem mass spectrometry [(UP)LC-MS/MS] by TGen (Phoenix, AZ).

4.3.6 *IN VITRO* STUDY IN HUMAN NEURAL STEM CELLS (HNSC)

Human embryonic brain cortical stem cells were provided as cryopreserved neurospheres by Dr. Clive Svendsen in vials and stored in -80 C. I thawed them and transferred them to

T25 flask which contained Thaw media (section 4.3.6.4). The cells were passaged (section 4.3.6.5) at least twice before being used for experiments in order to ensure cell viability after long-term storage.

4.3.6.1 Determining optimal cell density:

In preliminary experiments, optimum cell density and Allo concentration to be used were determined using identical methods as the study below. Optimal density was found to be 40,000 cells per well and optimal Allo concentration was 100 nM. Allo concentrations of 1nM, 10nM and 1000nM were used in certain experiments to obtain dose response curve of mitochondrial potentiation in hNSCs in response to Allo exposure.

4.3.6.2 Mitochondrial function measurement using Seahorse XF96 Extracellular Flux Analyzer in response to Allo and analogues:

I cultivated freshly passaged (section 4.3.6.5) Svendsen's human Neural Stem Cells (hNSC) in T25 flasks for 7 days in 100% growth factor (EGF, bFGF, Heparin) containing 'Thaw' media (section 4.3.6.4). I changed the media on day 4 post-seeding. On day 7, I passaged the cells again (section 4.3.6.5), and seeded them by columns at 40,000 cells per well in 100% growth factor containing Thaw media in Seahorse XF96 FluxPak (Agilent Technologies, Santa Clara, CA) plate coated with Matrigel hESC-qualified matrix (354277, Corning, Corning, NY) and incubated overnight (section 4.3.6.5). On day 2, I replaced the media with 0% growth factors containing Thaw media (EGF, bFGF, Heparin absent) in the morning and incubated for 4 hours. This was the starvation step. I performed a second wash step in order to minimize the residual amount of growth factors left behind in the wells of the plate, which had in earlier experiments confounded our results. After 4 hours, cells were treated with either vehicle (ethanol 0.001%) or Allopregnanolone (1nM, 10nM, 100nM or 1000nM) or an Allo Analogue (100nM). I used ethanol as a solvent for Allo and

its analogues. I measured Oxygen Consumption Rate (OCR) using Seahorse XF96 Extracellular Flux Analyzer 24 hrs. post-treatment and assessed mitochondrial respiration (section 4.3.6.6). To correct for any plating differences, I used protein readings of all wells (5000006, Bio-Rad Laboratories, Hercules, CA) to normalize measurements from all wells within the Seahorse XF96 Wave software.

I obtained the aggregated differences in mitochondrial potentiation in response to Allo and analogues treatment of hNSCs from six different experiments. All the data were normalized to protein content as described earlier and statistics were calculated by normalizing values of each plate to the average value of OCR in wells with vehicle treated hNSCs. Therefore, values of OCR for all non-vehicle treated hNSC-containing wells were calculated as a ratio of the OCR generated by the specific treatment to the OCR measured in the same cells in the same experiment by treatment with vehicle during basal respiration; an average of all six readings from all wells at basal respiration was calculated for this purpose. I only used hNSCs with passage 14 or less in these experiments. No cells in the experiment exceeded 5 freeze-thaw cycles.

4.3.6.3 Measurement of mitochondrial function at various time points in response to 30-min pulse treatment with Allo

I conducted a pulse-based experiment to determine activation time required to activate hNSCs and potentiate mitochondrial respiration by Allo. The cells were exposed to Allo only for 30-min (a 30-min Allo ‘pulse’) and mitochondrial function of hNSCs determined at multiple time points post-treatment. I chose the 30-min pulse treatment because that was the duration of exposure of the clinical trial participants of Allo phase Ib/IIa clinical trial (ClinicalTrials.gov Identifier: NCT02221622) to intravenous infusion of Allo. The pulse treatments were compared to a 24-hour continuous Allo treatment, as positive control, for

which I already had data. Pulse protocol is shown in figure. Briefly, I seeded cells in Seahorse plate as mentioned earlier and incubated them overnight. I then 'starved' the cells by removing the growth factor containing media using two washes and then after four hours of 'starvation' specific wells on the plate were treated with Allo as shown in Figure 4.1. I removed Allo after 30-min. by two washes. Only for hNSCs in one set of cells I allowed 24-hour exposure to Allo rather than 30-min and this was my positive control group. Each treatment with Allo or vehicle had at least 12 wells in each plate and this experiment was repeated six times.

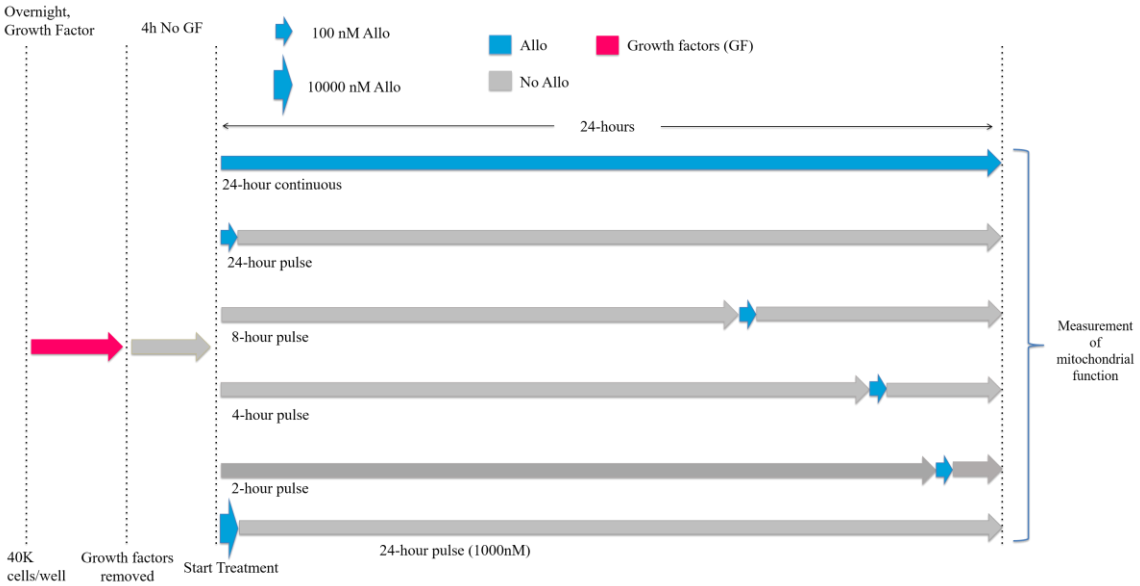

Figure 4.1 **Allo 'pulse' protocol**.
hNSCs were treated for 30-min at different time points preceding specific number of hours before measurement of mitochondrial function to understand the activation time required for and duration of, Allo's effect on mitochondria of hNSCs. The timeline of each set of wells is outlined above where grey denotes the absence of both Allo and growth factors, blue denotes the presence of Allo and pink denotes the presence of growth factors. The larger blue arrow in the last set of wells denotes the larger dose of Allo used (1000nM), while all other Allo doses were 100nM. Ethanol was used as a solvent for Allo and vehicle-treated cells were treated with 0.001% ethanol, which is the same concertation of ethanol as that of the solvent in Allo preparation.

Evaluation of Allo as an agonist or antagonist of TSPO

I carried out passaging, seeding and incubation of hNSC cells as described earlier. I treated the cells seeded into wells of Seahorse plates with either Allo, vehicle, a known agonist of TSPO (FGIN 1-27), a known antagonist of TSPO (PK 11195), a combination of Allo and antagonist and a combination of agonist and antagonist. Based on literature the I chose a concentration of 1µL for both FGIN 1-27 and PK 11195 and Allo concentration was 100nM as per earlier experiments. I used ethanol as vehicle and its concentration in the wells was 0.001%. Six independent experiments were carried out and cell passage numbers did not exceed 14. No cells in the experiment exceeded 5 freeze-thaw cycles.

4.3.6.4 Preparation of media for cell culture and Seahorse XF96 procedure

4.3.6.4.1 Thaw Media (100 percent (%) growth factor containing thaw media – 100GF):

Thaw Media with specific amount of growth factors (defined as 100% for experimental purposes) can be prepared by combining 33.9ml DMEM (Gibco/Invitrogen, Cat. # 21063-029), 14.5ml Ham's F-12 (Gibco/Invitrogen, Cat. # 11765-054), 0.5ml Penicillin/Streptomycin (Gibco/Invitrogen, Cat. # 15140-122), 1ml B27 (50X) (Gibco/Invitrogen, Cat. # 17504-044), 100µl of 10µg/ml stock bFGF (Gibco/Invitrogen, Cat. # 13256-029), 100µl of 10µg/ml stock EGF (Gibco/Invitrogen, Cat. # 13247-051) and 125µl of 2mg/ml stock Heparin

4.3.6.4.2 Thaw Media (without growth factors – zero % growth factor containing thaw media):

Thaw Media without any amount of growth factors (defined as zero % for experimental purposes) can be prepared by combining 33.9ml DMEM (Gibco/Invitrogen, Cat. # 21063-029), 14.5ml Ham's F-12 (Gibco/Invitrogen, Cat. # 11765-054), 0.5ml

Penicillin/Streptomycin (Gibco/Invitrogen, Cat. # 15140-122) and 1ml B27 (50X) (Gibco/Invitrogen, Cat. # 17504-044). No growth factors are added to this media.

4.3.6.5 Passaging hNSCs for *in vitro* experiments

First, I made sure to aspirate any Thaw medium already in the flask. I then washed the flask twice with 10mL of Hank's Balance Salt Solution (BSS) to remove any remaining serum, as this will inhibit the action of the dissociation enzyme. I then aspirated out the Hank's BSS and added 1 mL of Accutase (07920, STEMCELL Technologies, Vancouver, BC, Canada). Then I placed the flask in the incubator (37 °C) for 3 minutes. After that I neutralized the Accutase enzyme with 7 mL of 100GF Thaw Medium. I then transferred contents of the flask to a sterile 15mL conical tube. After washing the flask with another 4mL of 100GF Thaw Medium to collect any remaining cells, I added this wash to the 15mL conical tube. I then centrifuged the suspension at 300 x g (gravitational constant) for 5 minutes. After centrifugation I aspirated the supernatant, resuspend the cell pellet by gently tapping the tube, then add 5mL 100GF Thaw Medium to fully resuspend cells. I then counted the cells using a hemocytometer.

4.3.6.6 Using Seahorse XF96 Extracellular Flux Analyzer

4.3.6.6.1 Seahorse Medium

Seahorse medium can be prepared by combining 1 vial of Dulbecco′s Modified Eagle′s Medium (DMEM) powder (without glucose, L-glutamine, phenol red, sodium pyruvate and sodium bicarbonate) (D5030-1L, Sigma-Aldrich, St. Louis, MO) with 10mL of Glutamax (35050-061, Thermo Fisher Scientific, Waltham, MA), 1.85g of NaCl (0241, Amresco LLC, Solon, OH) in 1L of sterile diH2O. I measured 900mL sterile diH2O into large beaker, added DMEM powder and dissolved it with stirring. Then I added glutamax and NaCl and adjusted the pH to 7.4 at 37 °C with NaOH/HCl. I made it up to 1000mL with sterile diH2O

while stirring briefly. I filtered it with sterile filter (431096, Corning, Corning, NY), and stored it at 4 °C. On day of use, I warmed it to 37 °C and added 25mM glucose (BDH9230, VWR International, Radnor, PA).

4.3.6.6.2 Seahorse XF96 procedure:

I assessed mitochondrial function using the Seahorse XF96 Analyzer (Agilent Technologies, Santa Clara, CA). On Day 1, I plated hNSCs at a density of 40,000 cells/well in 100% growth factors containing Thaw medium on 96- well cell culture microplate from the Seahorse XF96 FluxPak previously coated with Matrigel (354277, Corning, Corning, NY). I left the plate at room temperature for 30-minutes to allow cells to settle and then I incubated the plate at 37 °C with 5% CO_2. On Day 2, I replaced the media in the wells with zero % growth factors containing Thaw medium in the morning and incubated it for 4 hours (starvation step). I performed a second wash step to minimize the residual amount of growth factors left behind in the wells of the plate which could interfere with the results. After 4 hours, I treated cells in each well with either vehicle (ethanol 0.001%) or Allopregnanolone (1nM, 10nM, 100nM or 1000nM) or an Allo Analogue (100nM). Ethanol was used as a solvent for Allo and Allo analogues. I then left the plate to incubate at 37 °C. On day 2, I also rehydrated a XF96 cartridge overnight from the Seahorse XF96 Flux Pak (102416, Agilent Technology, Santa Clara, CA) as per manufacturer's instructions. On Day 3, 24-hours after the treatment step, I changed the media in the wells to unbuffered Seahorse Medium, with 25mM glucose, warmed to 37 °C. I then incubated the plate at 37 °C without CO_2 for 60 minutes. I loaded the XF96 cartridge with the following inhibitors: Port A: Sodium Pyruvate (50mM); Port B: Oligomycin (32μM; to inhibit ATP synthase); Port C: FCCP (carbonylcyanide p-trifluoromethoxyphenylhydrazone, 9μM; to uncouple mitochondria); Port D: Rotenone (10μM; to inhibit electron transfer from complex I to

ubiquinone). Injection volumes for all ports were 25µl. The inhibitor concentrations at injection are: Sodium Pyruvate 7mM (S8636, Sigma-Aldrich, St. Louis, MO), Oligomycin 4µM (151786, MP Biomedicals, Santa Ana, CA), FCCP 1µM (0453, Tocris Cookson, Bristol, UK), Rotenone 1µM (0215015410, MP Biomedicals, Santa Ana, CA). I set the machine to carry out six baseline measurements of oxygen consumption rate (OCR) and extracellular acidification rate (ECAR) before sequential injection of mitochondrial inhibitors. I also set the machine to carry out three measurements following inhibitor addition and prior to automated addition of subsequent inhibitors. OCR and ECAR were automatically calculated and recorded by Seahorse XF96 Wave software. To correct for any plating differences, I used protein readings of all wells (5000006, Bio-Rad Laboratories, Hercules, CA) to normalize values of OCR and ECAR from all the wells within the Seahorse XF96 Wave software. I calculated the parameters of mitochondrial function as follows: Basal Respiration (Average first six OCR readings); Maximal Capacity (First reading after FCCP addition – Non-Mito Respiration); Reserve Capacity (First reading after FCCP addition – Basal Respiration). I calculated outliers with the ROUT method using Prism 6.0 and keeping FDR of 1%.

4.3.7 IMAGING

MRI study was carried out on brains of certain Allo and saline treated mice that I shipped to University of Arizona. At least two mice were selected per treatment group based on their performance in the NOR test to obtain the best visual evidence of differences due to Allo treatment compared to saline in the brain.

4.4 Results

4.4.1 BODY WEIGHTS OF MICE

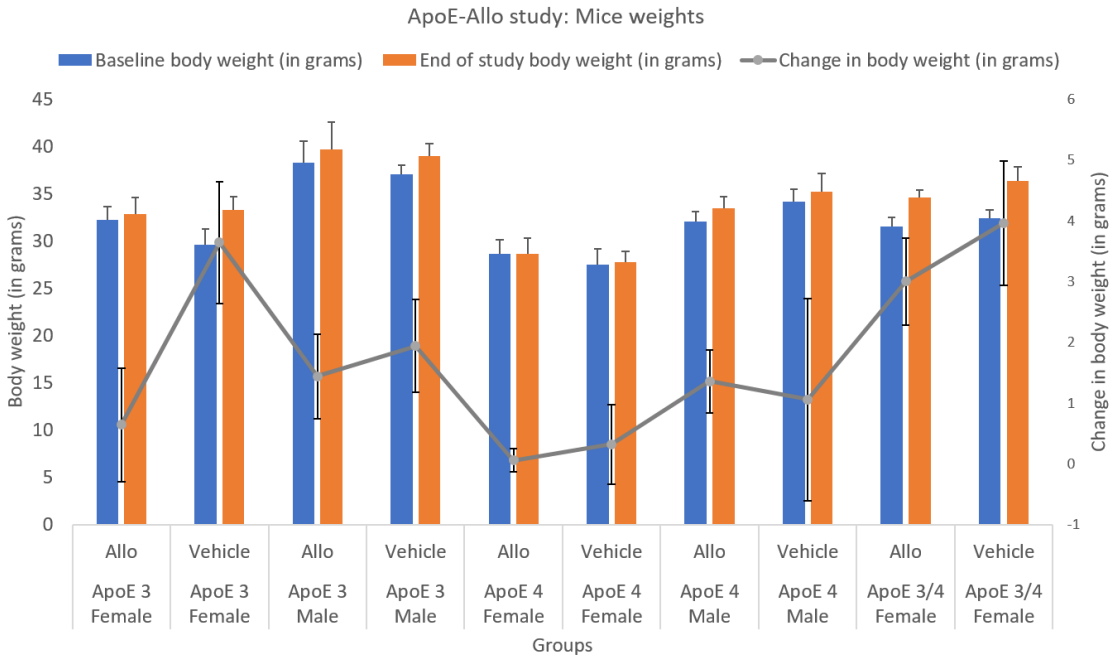

Figure 4.2 **Body weights of different groups of ApoE mice by sex, genotype and treatment**.
Body weights of mice showed a general trend of increase during the study. No statistically signficant differences were observed between Allo and saline treated mice of identical sex and genotype.

Body weights of mice showed a general trend of increase during the study. No statistically significant differences were observed between Allo and saline treated mice of identical sex and genotype. All male mice had statistically significantly

higher weight than corresponding female mice with two exceptions, male vs. female ApoE 3/3 Allo (end of study weights p-value=0.07) and male vs. female Allo ApoE 4/4 (baseline body weight p-value=0.09). By genotype, I found no statistically significant difference in body weights except between Allo treated ApoE 3/3 and ApoE 4/4 males at baseline and between vehicle treated ApoE 3/3 and ApoE 4/4 females at end of study.

4.4.2 COGNTIVE FUNCTION OF MICE

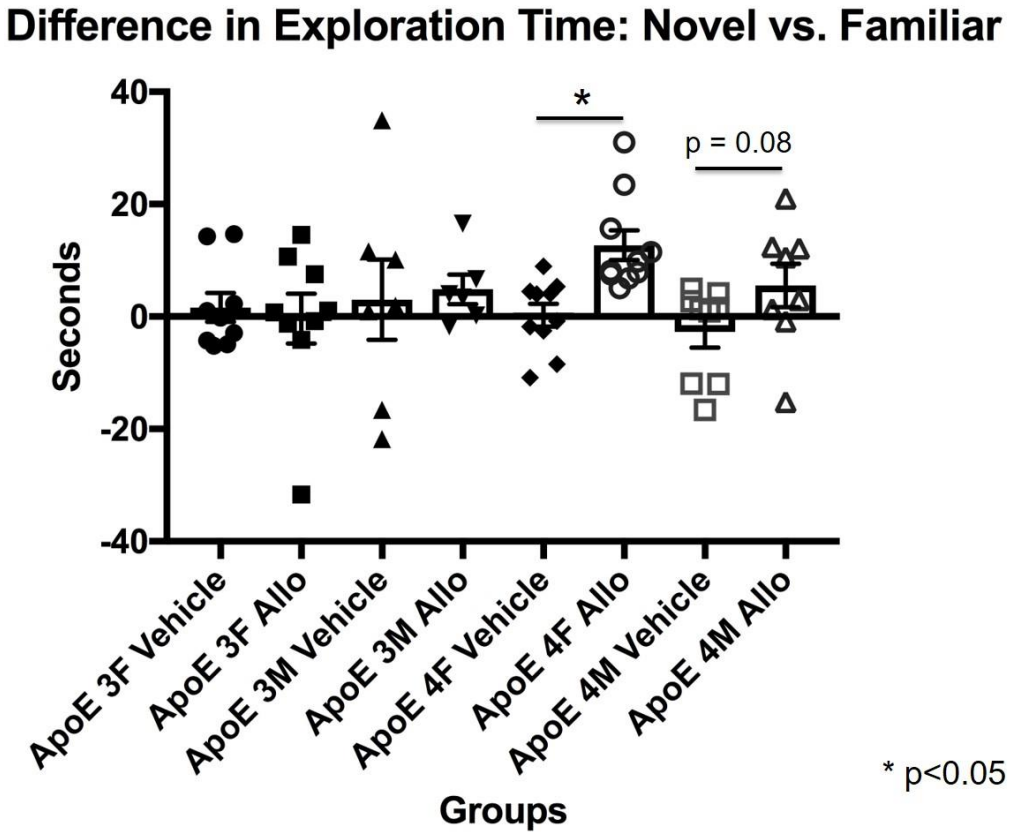

Figure 4.3 **Difference in exploration time between different groups**.
Both Allo-treated ApoE 4/4 males and females explored novel object for longer period of time compared to their saline-treated counterparts. However, only in female ApoE 4/4 mice this difference reached significance.

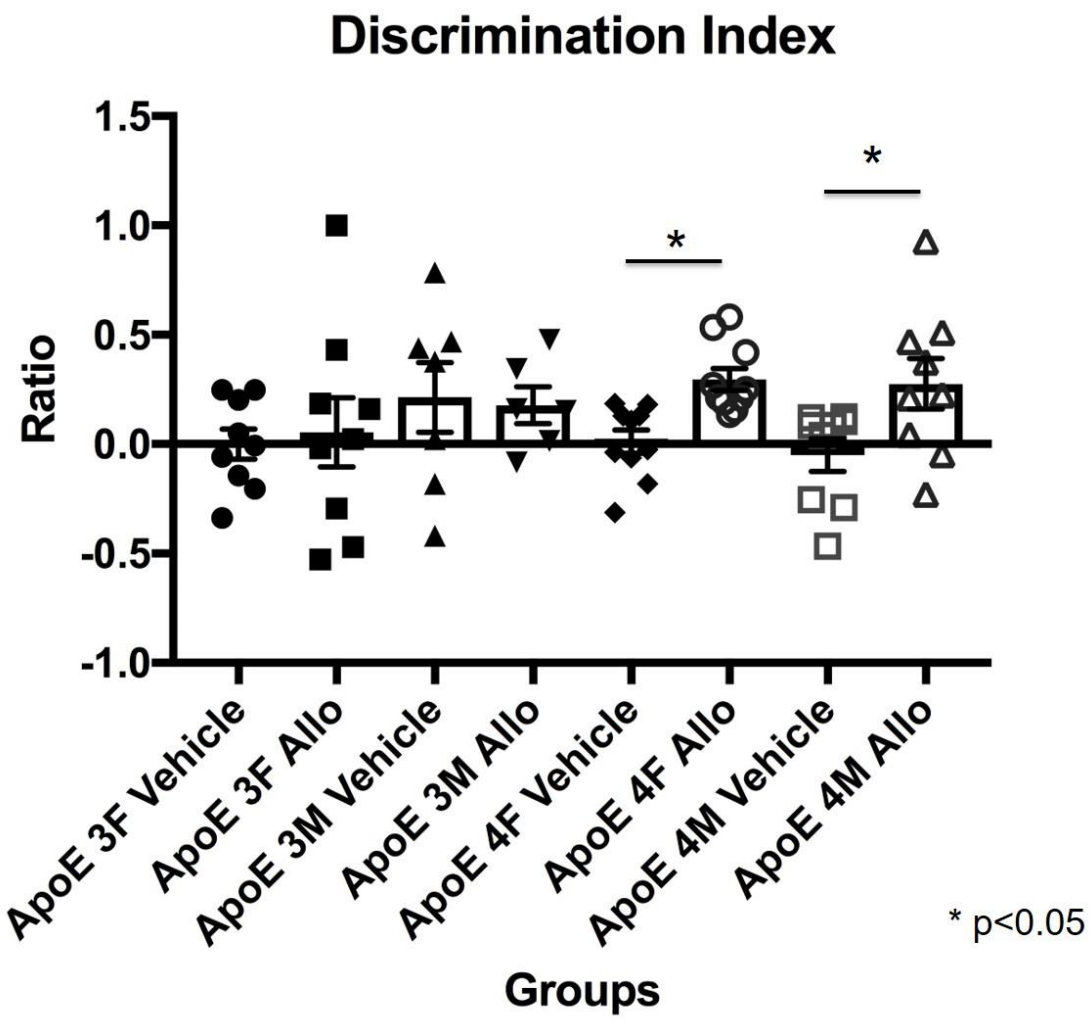

Figure 4.4 **Discrimination index in different groups**.
Both Allo-treated ApoE 4/4 males and females have statistcally significantly higher discrimination index compared to their saline-treated counterparts.

NOR test results indicate that ApoE 4/4 female mice spent significantly more time exploring the novel object compared to the object seen previously suggesting that ApoE 4/4 female mice benefit significantly from Allo treatment and Allo prevents decline in cognitive function in ApoE 4/4 female mice (Figure 4.1). ApoE 4/4 male mice spend more time exploring the novel object compared to the object seen previously, however, this difference in time does not reach the level of significance ($p = 0.08$). Discrimination Index

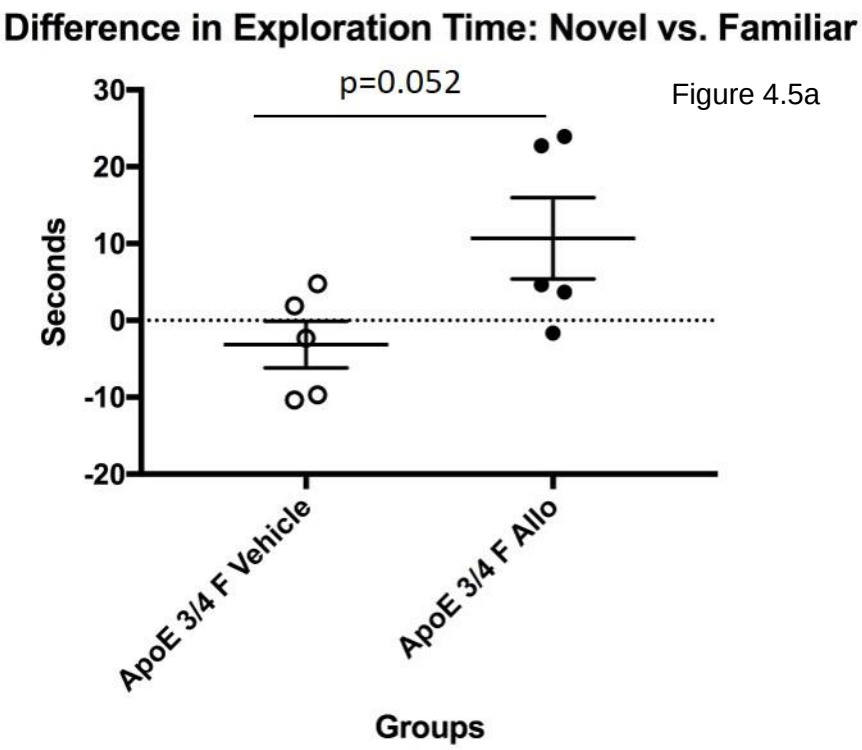

Figure 4.5a

(DI) is the ratio of the difference in exploration time to the total time spent exploring both objects and it controls for the variation in the amount of time mice spend exploring both objects. Both ApoE

Figure 4.5a-b **Difference in exploration time and discrimination index for Allo and saline treated ApoE 3/4 heterozygous female mice**.
Allo treated ApoE 3/4 mice showed considerable improvement in cognitive function but it did not reach statistical significance. I believe increasing the number of mice in each group could facilitate detection of statistically significant difference on Allo treatment, if present.

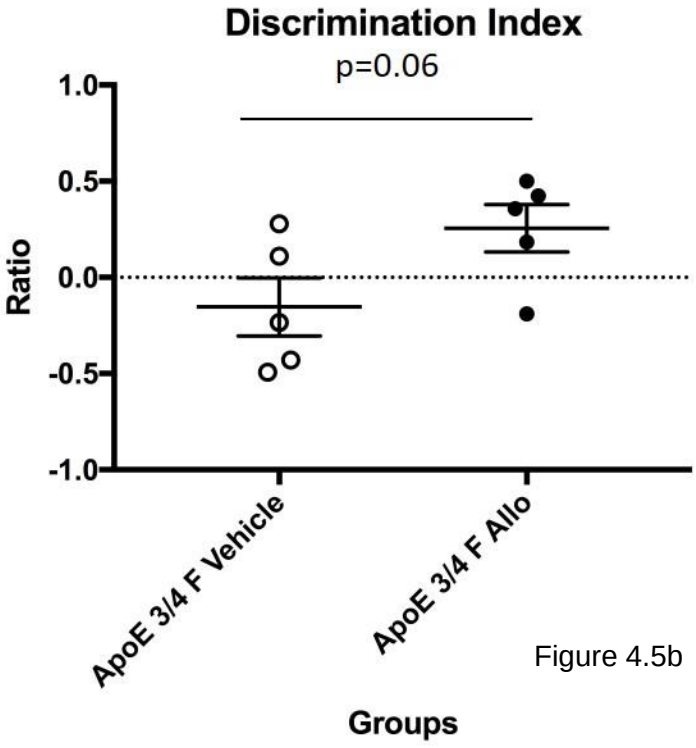

Figure 4.5b

4/4 female and male mice have a significantly higher DI than ApoE 3/3 female and male,

respectively (Figure 4.2). ApoE 3/3 female and male mice do not show cognitive benefit from Allo treatment.

In ApoE 3/4 female mice, Allo treatment improves cognitive function when tested by the novel object recognition test. However due to low number of animals in each group (n=5 per treatment group), the results are not statically significant (p-values are slightly higher than 0.05).

4.4.3 RNA-SEQ

Canonical pathways in ApoE 4/4 Allo treated females

In ApoE 4/4 Allo treated mice the canonical pathways found through the RNA-Seq are shown in Figure 4.6. Out of the 23 pathways shown almost half (11/23) are connected to the immune system and involve innate and adaptive immune system, Th1 and Th2 activation, cytokine production and antibody-mediated immunity. Other pathways of note include pathways related to estrogen, glucocorticoids and mineralocorticoids, pathways that suggest increased metabolism and energy utilization such as mannose degradation and acyl-CoA hydrolysis as well as pathways related to gene and transcription regulation. These pathways suggest that Allo plays a role in cell cycle regulation and signaling as well as repression of DNA transcription via methylation.

Comparison of Allo treated female mice of all three genotypes

Figure 4.7 shows the comparison of all canonical pathways up- or downregulated when all Allo treated female mice are compared to their vehicle treated counterparts. Interestingly the top pathways are consistently similar between ApoE 4/4 Allo vs. saline treated females, while ApoE 3/3 are different. Based on hippocampal transcriptome ApoE 3/3 Allo treated females are a distinct phenotype while ApoE 3/4 and ApoE 4/4 Allo treated

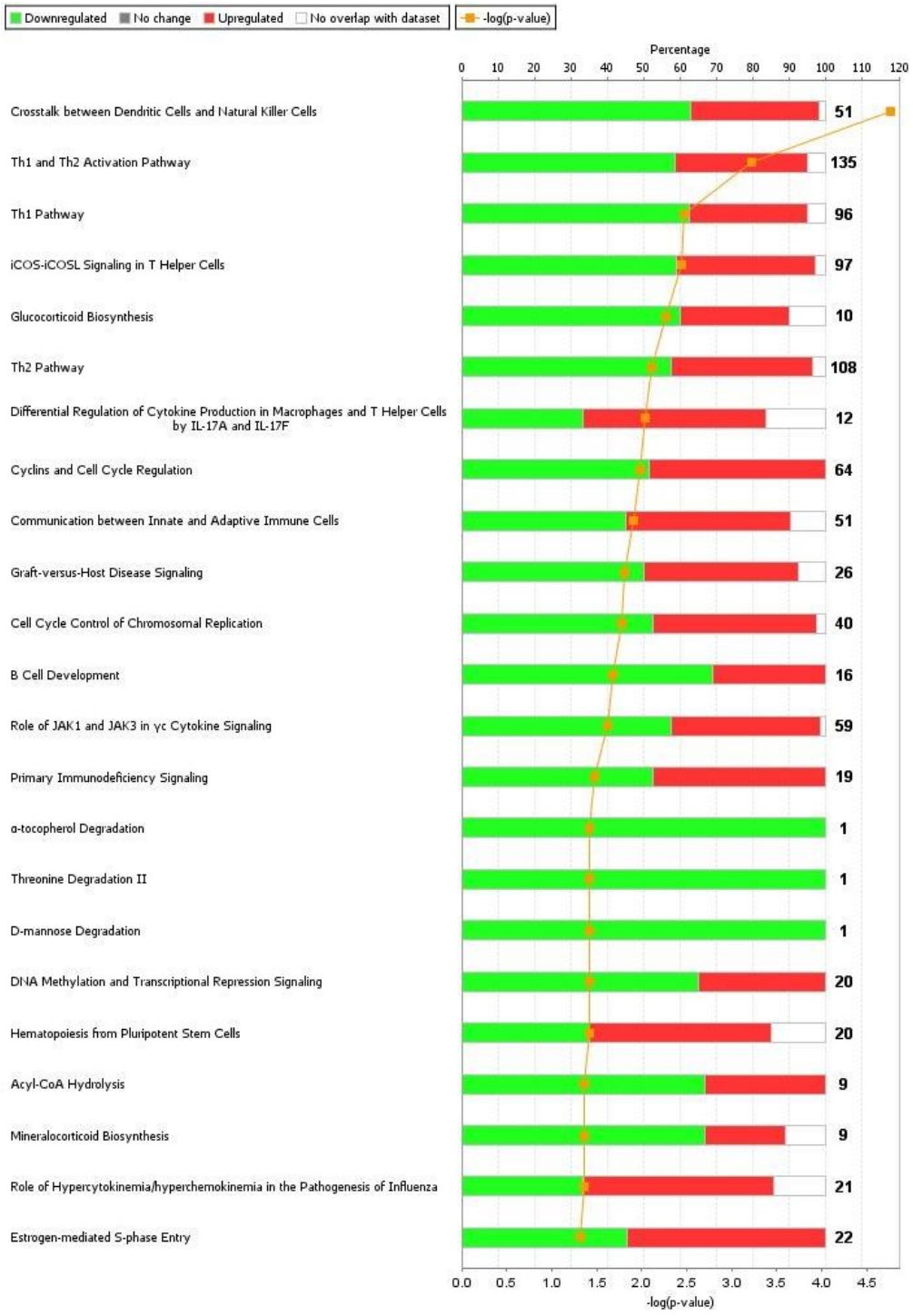

Figure 4.6 **Up- and down-regulated canonical pathways in ApoE 4/4 females in response to Allo**.
Canonical pathways up- and down-regulated when ApoE 4/4 Allo treated females are compared to saline treated females of identical genotype. A number of immune system related pathways, along with metabolomic and signaling pathways are seen.

females are similar. IL-3 and IL-7 signaling as well as leptin and prolactin pathways which

Figure 4.7 Canonical pathways up- and down-regulated by Allo treatment in all three female genotypes.
When all Allo treated female mice are compared to their saline treated counterparts, similar canonical pathways are seen up- and downregulated in female ApoE 4/4 and 3/4 mice, while ApoE 3/3 mice are different based on hippocampal gene expression.

are considered pro-inflammatory are seen upregulated in ApoE 3/3 Allo treated female mice while the same canonical pathways are downregulated in both ApoE 4/4 and ApoE 3/4 female mice due to Allo treatment suggesting Allo's effect on immune regulation. This corroborates the results of NOR in which both ApoE 3/4 and ApoE 4/4 females showed cognitive improvement while ApoE 3/3 females did not. The mechanism of Allo-induced amelioration of cognitive function in ApoE 4/4 and 3/4 females is likely due to differential hippocampal transcription.

<u>PDGF-BB upregulation by Allo</u>

In response to Allo treatment, I found that PDGF is upregulated. Specifically, PDGF-BB isoform was found to be upregulated in Allo treated ApoE 4/4 females when compared to saline treated ApoE 4/4 females (Fig. 4.8),

ApoE 4 Allo-treated females vs. ApoE 4 Saline-treated females

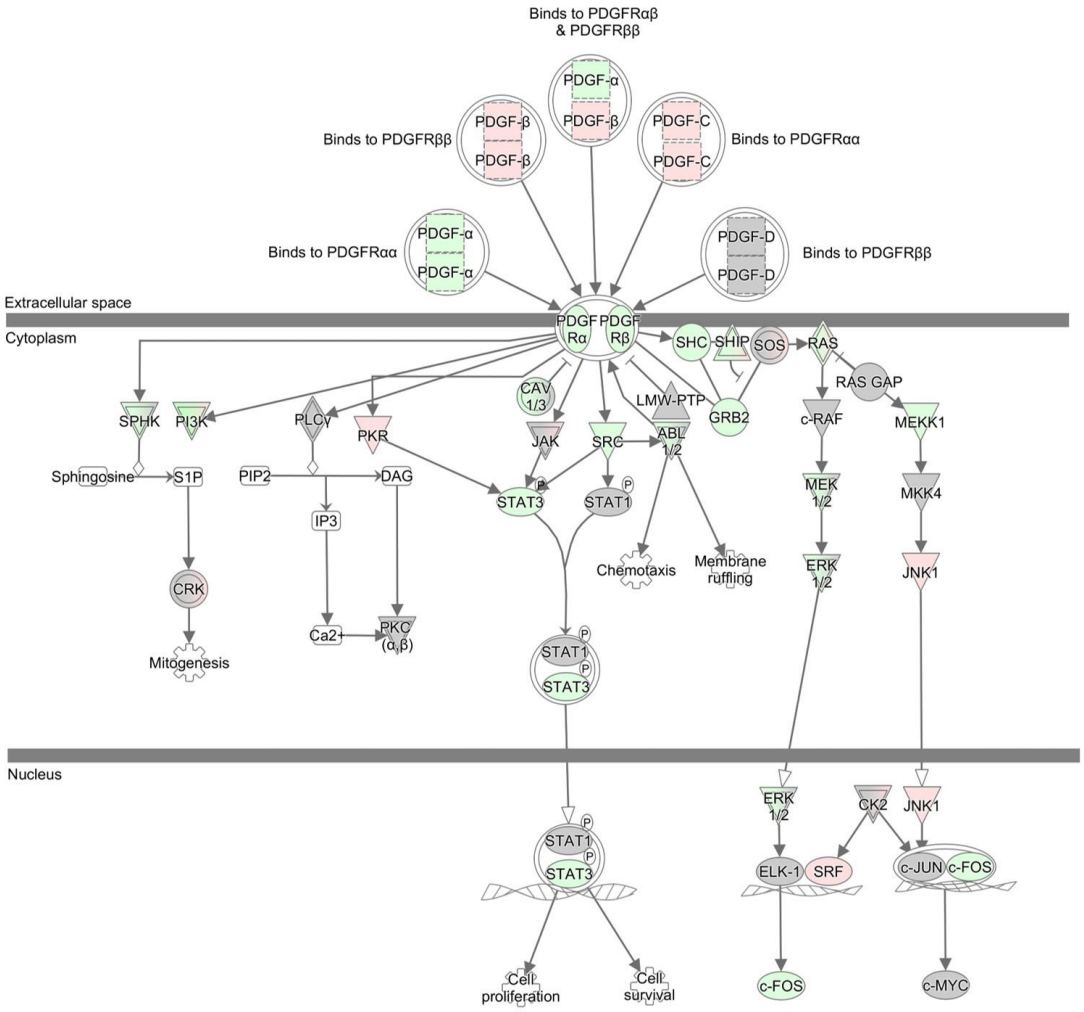

Figure 4.8 Upregulation of PDGF-BB in ApoE 4/4 Allo treated females compared to saline treated females of identical genotype.
PDGF signaling pathway in the hippocampal RNA-Seq data shows upregulation of PDGF-BB and downregulation of PDGFRα.

while -AA and -CC variants of PDGF were downregulated and the -DD variant remained unchanged. Also, PDGFRα is downregulated. Downstream, the data suggests that most molecules are downregulated except JNK1, SRF and PKR.

Genotype and gender differences in Allo treatment

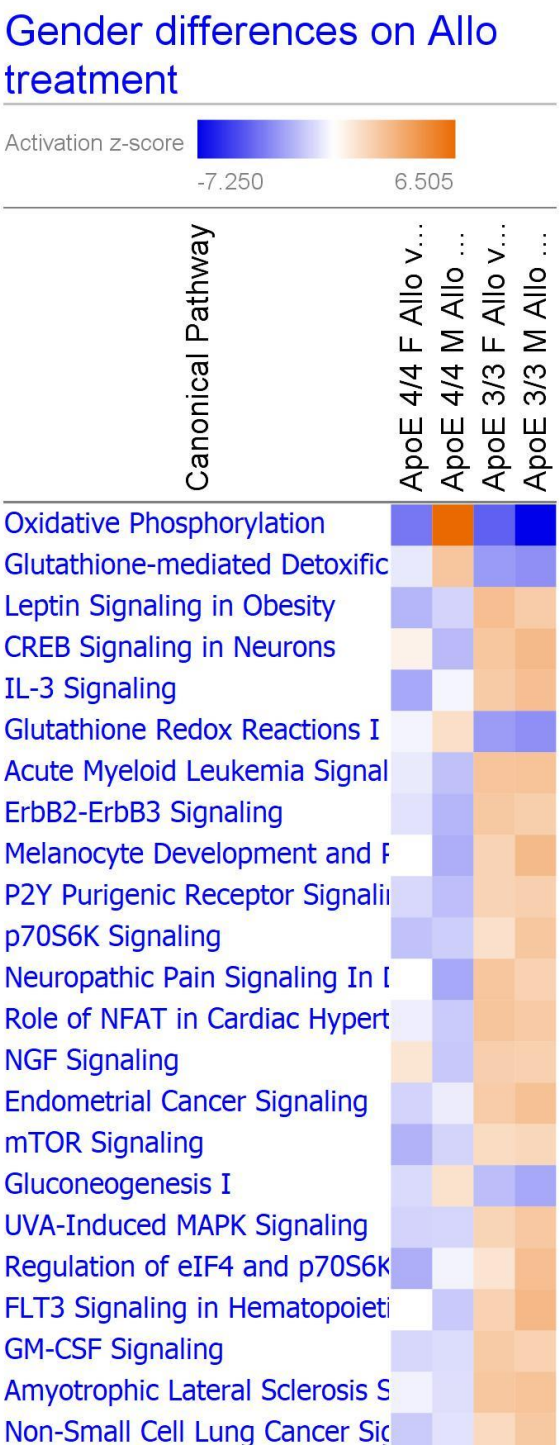

Figure 4.9 Genotype and gender differences in treatment effect of Allo on hippocampal transcriptome in ApoE mice.
Effects of Allo on the hippocampus are genotype specific, as evinced by the canonical pathways seen here. Majority of the pathways are downregulated in ApoE 4/4 mice, after Allo treatment while the same pathways are upregulated in ApoE 3/3 mice despite treatment with Allo.

Effects of Allo on the hippocampus are genotype specific, as evinced by the canonical pathways seen in Figure 4.9. ApoE 3/3 mice have a different transcriptomic phenotype from ApoE 4/4, both males and females. Majority of the pathways are downregulated in ApoE 4/4 mice, both males and females, after treatment with Allo, while the same pathways are upregulated in ApoE 3/3 male and female mice despite treatment with Allo. Inflammatory pathways like Leptin signaling and IL-3 signaling as well as GM-CSF signaling are upregulated in ApoE 3/3 but downregulated in ApoE 4/4. Surprisingly oxidative phosphorylation and gluconeogenesis are upregulated only in ApoE 4/4 males and downregulated in all other

groups. Allo induced downregulation of ALS signaling in ApoE 4/4 supports its neuroprotective credentials. This observation hints at genotype specific regulation of hippocampal transcriptome by Allopregnanolone and is similar to what I observed when only female groups treated with Allo were compared to saline groups. ApoE genotype is the primary variable that modifies Allo treatment rather than sex and this could justify phase IIb trial in ApoE 4/4 enriched cohort.

4.4.4 METABOLOMIC PANEL

The metabolomic panel was an extensive study of 185 metabolites in plasma and cortex of mice from all ten groups. I am discussing selected results from the metabolomic study below.

4.4.4.1 ApoE 4/4 Females Allo vs. Saline treated

Metabolites	Class	log2(FC) Allo vs Veh	p.value	p.adjusted
PC aa C42:0	Glycerophospholipid	-0.221	0.020	0.7963
PC ae C44:4	Glycerophospholipid	-0.136	0.020	0.7963
C12-DC	Acylcarnitine	0.104	0.031	0.7963
Nitro-Tyr	Biogenic amine	0.690	0.032	0.7963
PC aa C24:0	Glycerophospholipid	-0.222	0.032	0.7963
C12	Acylcarnitine	0.145	0.036	0.7963
PC aa C36:6	Glycerophospholipid	-0.207	0.043	0.7963
C16:2	Acylcarnitine	0.287	0.045	0.7963

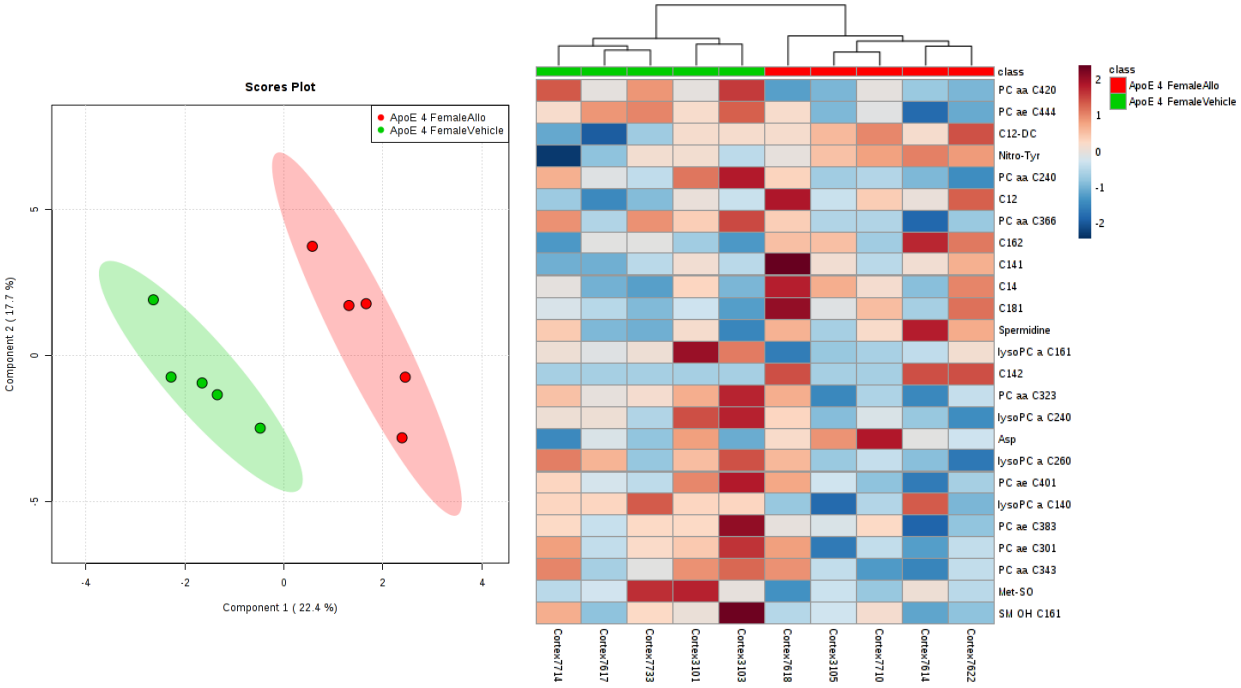

Figure 4.10 Differences in cortical metabolites in Allo vs. saline treated ApoE 4/4 females.
In cortex eight metabolites and four glycerophospholipids were slightly lower and acylcarnitines were higher upon allopregnanolone treatment. The Allo and saline treated groups showed clear separation on PCA plot. However, no single metabolite was significantly different in plasma.

Eight metabolites were significantly different in cortex of Allopregnanolone and vehicle treated Apo E4/4 females. Although the Allo and saline treated groups of ApoE 4/4 females showed a clear separation on PCA plot, no metabolites reached significance when p-value was corrected for multiple comparisons in either cortex or plasma.

4.4.4.2 Saline treated ApoE 3/3 vs. ApoE 3/4 females

Metabolite	Class	log2(FC) ApoE3/4 vs. ApoE3	p.value	p.Adjusted
lysoPC a C204	Glycerophospholipid	0.505	0.032	0.676
Non essential AA	Aminoacid	0.276	0.032	0.676
C18:1-OH	Acylcarnitine	0.305	0.043	0.676

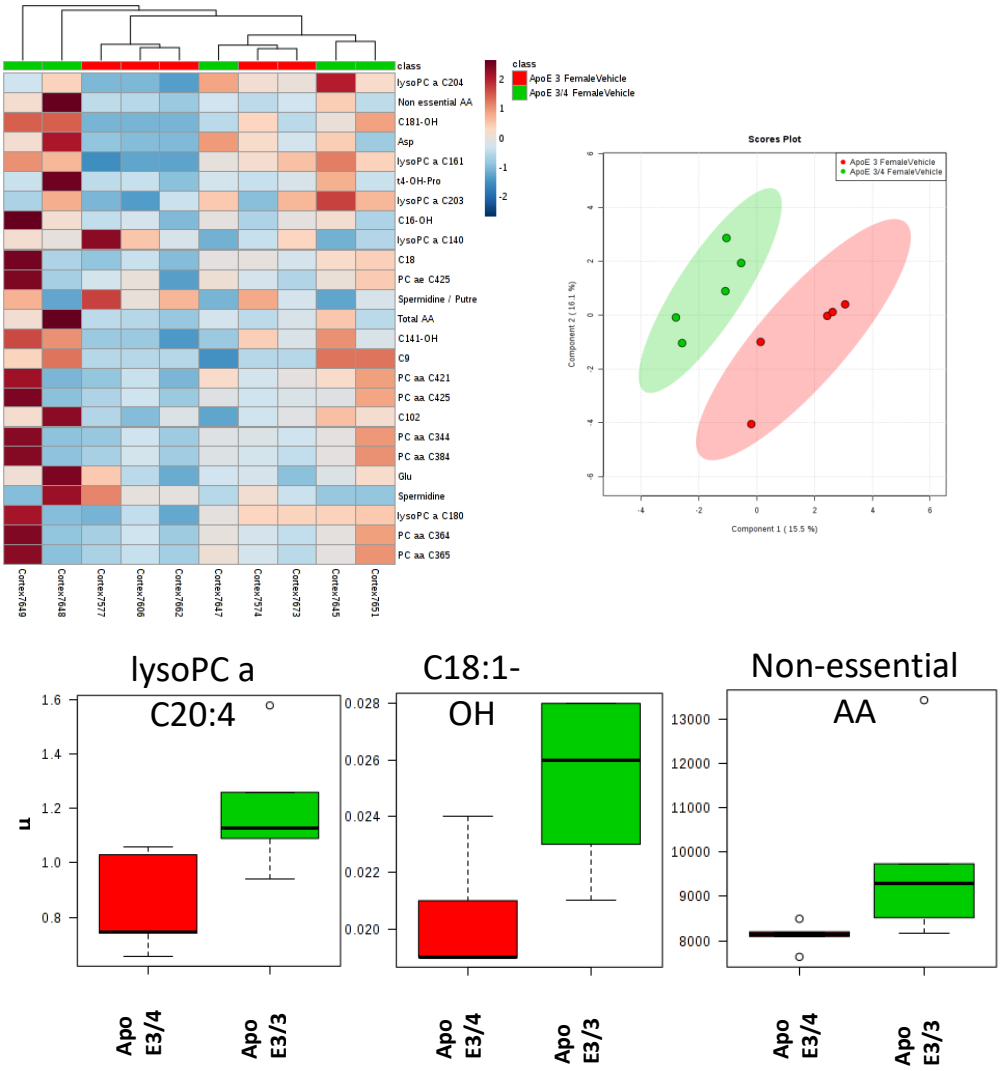

Figure 4.11 Cortical metabolite differences between saline treated ApoE 3/3 and 3/4 females.
Three metabolites were significantly different in cortex of saline treated ApoE 3/3 and ApoE 3/4 female mice. However, none reached a level of significance after adjusting the p-value.

Metabolites	Class	log2(FC) Apo E3/3 vsApo E3/4	p.value	p.adjusted
PC ae C444	Glycerophospholipid	-0.492	0.012	0.057
PC ae C302	Glycerophospholipid	-0.699	0.012	0.057
SFA PC	Glycerophospholipid	-0.376	0.012	0.057
C3-DC C4-OH	Acylcarnitine	-0.486	0.016	0.061
lysoPC a C281	Glycerophospholipid	-0.725	0.016	0.061
PC aa C240	Glycerophospholipid	-0.761	0.016	0.061
PC aa C362	Glycerophospholipid	-0.520	0.016	0.061
PC aa C405	Glycerophospholipid	-0.537	0.016	0.061
PC ae C300	Glycerophospholipid	-0.551	0.016	0.061
PC ae C343	Glycerophospholipid	-0.444	0.016	0.061
PC ae C362	Glycerophospholipid	-0.476	0.016	0.061
PC ae C421	Glycerophospholipid	-0.406	0.016	0.061
PC ae C443	Glycerophospholipid	-0.674	0.016	0.061
PC aa C300	Glycerophospholipid	-0.395	0.016	0.061
PC ae C446	Glycerophospholipid	-0.503	0.021	0.079
Total PC ae	Glycerophospholipid	-0.412	0.021	0.079
C5-OH C3-DC-M	Acylcarnitine	-0.374	0.027	0.097
PC aa C260	Glycerophospholipid	-0.722	0.028	0.097
PC ae C383	Glycerophospholipid	-0.364	0.028	0.097
Ac-Orn	Biogenic amine	-0.476	0.032	0.097
Kynurenine	Biogenic amine	-0.401	0.032	0.097
PC aa C383	Glycerophospholipid	-0.349	0.032	0.097
PC ae C401	Glycerophospholipid	-0.531	0.032	0.097
PC ae C402	Glycerophospholipid	-0.412	0.032	0.097
PC ae C404	Glycerophospholipid	-0.275	0.032	0.097
PC ae C420	Glycerophospholipid	-0.213	0.032	0.097
PC ae C445	Glycerophospholipid	-0.359	0.032	0.097
SM OH C161	Glycerophospholipid	-0.409	0.032	0.097
SM C161	Glycerophospholipid	-0.398	0.032	0.097
C141	Acylcarnitine	-0.292	0.034	0.103
PC aa C342	Glycerophospholipid	-0.383	0.036	0.107
C41	Acylcarnitine	-0.282	0.047	0.134
PC ae C342	Glycerophospholipid	-0.274	0.047	0.134

Metabolites	Class	log2(FC) Apo E3/3 vsApo E3/4	p.value	p.adjusted
C4	Acylcarnitine	-0.414	0.008	0.040
lysoPC a C160	Glycerophospholipid	-0.529	0.008	0.040
lysoPC a C161	Glycerophospholipid	-0.483	0.008	0.040
lysoPC a C170	Glycerophospholipid	-0.583	0.008	0.040
lysoPC a C180	Glycerophospholipid	-0.530	0.008	0.040
lysoPC a C181	Glycerophospholipid	-0.455	0.008	0.040
lysoPC a C182	Glycerophospholipid	-0.615	0.008	0.040
lysoPC a C203	Glycerophospholipid	-0.485	0.008	0.040
lysoPC a C240	Glycerophospholipid	-0.764	0.008	0.040
lysoPC a C260	Glycerophospholipid	-0.901	0.008	0.040
lysoPC a C261	Glycerophospholipid	-0.784	0.008	0.040
lysoPC a C280	Glycerophospholipid	-0.913	0.008	0.040
PC aa C323	Glycerophospholipid	-0.501	0.008	0.040
PC aa C360	Glycerophospholipid	-0.457	0.008	0.040
PC aa C386	Glycerophospholipid	-0.555	0.008	0.040
PC aa C402	Glycerophospholipid	-0.517	0.008	0.040
PC aa C403	Glycerophospholipid	-0.478	0.008	0.040
PC aa C404	Glycerophospholipid	-0.426	0.008	0.040
PC aa C406	Glycerophospholipid	-0.528	0.008	0.040
PC aa C420	Glycerophospholipid	-0.440	0.008	0.040
PC aa C421	Glycerophospholipid	-0.553	0.008	0.040
PC aa C422	Glycerophospholipid	-0.578	0.008	0.040
PC aa C424	Glycerophospholipid	-0.536	0.008	0.040
PC aa C425	Glycerophospholipid	-0.539	0.008	0.040
PC aa C426	Glycerophospholipid	-0.452	0.008	0.040
PC ae C301	Glycerophospholipid	-0.956	0.008	0.040
PC ae C321	Glycerophospholipid	-0.503	0.008	0.040
PC ae C322	Glycerophospholipid	-0.637	0.008	0.040
PC ae C340	Glycerophospholipid	-0.383	0.008	0.040
PC ae C360	Glycerophospholipid	-0.425	0.008	0.040
PC ae C361	Glycerophospholipid	-0.461	0.008	0.040
PC ae C381	Glycerophospholipid	-0.707	0.008	0.040
PC ae C382	Glycerophospholipid	-0.468	0.008	0.040
PC ae C403	Glycerophospholipid	-0.426	0.008	0.040
PC ae C405	Glycerophospholipid	-0.403	0.008	0.040
PC ae C406	Glycerophospholipid	-0.496	0.008	0.040
PC ae C422	Glycerophospholipid	-0.522	0.008	0.040
PC ae C423	Glycerophospholipid	-0.518	0.008	0.040
PC ae C424	Glycerophospholipid	-0.679	0.008	0.040
PC ae C425	Glycerophospholipid	-0.411	0.008	0.040
Fisher ratio	Amino acid	0.480	0.008	0.040
Total lysoPC	Glycerophospholipid	-0.541	0.008	0.040
Tyr / Phe	Amino acid	-0.448	0.008	0.040

Figure 4.12 Plasma metabolite differences between saline treated ApoE 3/3 vs 3/4 female mice.
Several glycerophospholipids, amino acids, biogenic amines and acylcarnitines were significantly different in plasma of saline treated ApoE 3/3 and ApoE 3/4 female mice. Majority of glycerophospholipids and two amino acids reached significance after adjusting for p-value. ApoE 3/4 had higher glycerophospholipids than ApoE 3/3, which can be used as metabolic phenotype.

When Saline treated ApoE 3/3 and ApoE 3/4 are compared, cortical metabolites show no statistically significant difference with corrected p-value, but in plasma several glycerophospholipids, amino acid, biogenic amines and acylcarnitines were significantly different between the two groups.

4.4.4.3 Saline treated ApoE 4/4 vs. ApoE 3/4 females

In both plasma and cortex, several glycerophospholipid were different between ApoE 3/4 and ApoE 4/4 female mice (uncorrected p-value <0.05). None reached significance with corrected p-value. All glycerophospholipids were higher in Apo E3/4, similar to comparison of saline treated ApoE 3/3 with ApoE 3/4.

Figure 4.13a: Plasma

Metabolites	Class	Log2(FC) ApoE3/4 vs ApoE4/4	p.value	p.adjusted
C6 C41-DC	Acylcarnitine	-0.546	0.008	0.158
lysoPC a C170	Glycerophospholipid	0.619	0.008	0.158
lysoPC a C240	Glycerophospholipid	0.549	0.008	0.158
lysoPC a C260	Glycerophospholipid	0.912	0.008	0.158
lysoPC a C261	Glycerophospholipid	0.778	0.008	0.158
lysoPC a C280	Glycerophospholipid	0.936	0.008	0.158
lysoPC a C281	Glycerophospholipid	0.824	0.008	0.158
PC aa C240	Glycerophospholipid	1.028	0.008	0.158
PC ae C322	Glycerophospholipid	0.507	0.008	0.158
PC ae C421	Glycerophospholipid	0.515	0.008	0.158
PC ae C443	Glycerophospholipid	0.771	0.008	0.158
PC ae C302	Glycerophospholipid	0.746	0.012	0.183
PC aa C281	Glycerophospholipid	0.752	0.016	0.183
PC aa C323	Glycerophospholipid	0.402	0.016	0.183
PC aa C403	Glycerophospholipid	0.436	0.016	0.183
PC aa C405	Glycerophospholipid	0.640	0.016	0.183
PC aa C426	Glycerophospholipid	0.315	0.016	0.183
PC ae C300	Glycerophospholipid	0.487	0.016	0.183
Fisher ratio	Amino acid	-0.497	0.016	0.183
PC ae C420	Glycerophospholipid	0.230	0.021	0.232
Ac-Orn	Biogenic amine	0.634	0.032	0.240
PC aa C260	Glycerophospholipid	0.727	0.032	0.240
PC aa C362	Glycerophospholipid	0.400	0.032	0.240
PC aa C402	Glycerophospholipid	0.413	0.032	0.240
PC ae C301	Glycerophospholipid	0.846	0.032	0.240
PC ae C321	Glycerophospholipid	0.294	0.032	0.240
H1	Sugar	0.210	0.032	0.240
Spermidine / Putrescine	Biogenic amine	-1.778	0.032	0.240

Figure 4.13a-c Plasma metabolite differences between saline treated ApoE 4/4 vs 3/4 female mice.
Several glycerophospholipid were signficantly different in plasma between saline treated ApoE 3/4 and ApoE 4/4 female mice based on p-value before correction for multiple comparisons. However, none reached significance with adjusted p-value. All glycerophospholipids were higher in ApoE 3/4, similar to the comparison between saline treated ApoE 3/3 and ApoE 3/4 females. Both groups showed clear separation on PCA plot. In the cortex only one glycerophospholipid was found to be different, lysoPC a C14:0.

Figure 4.13b: Plasma

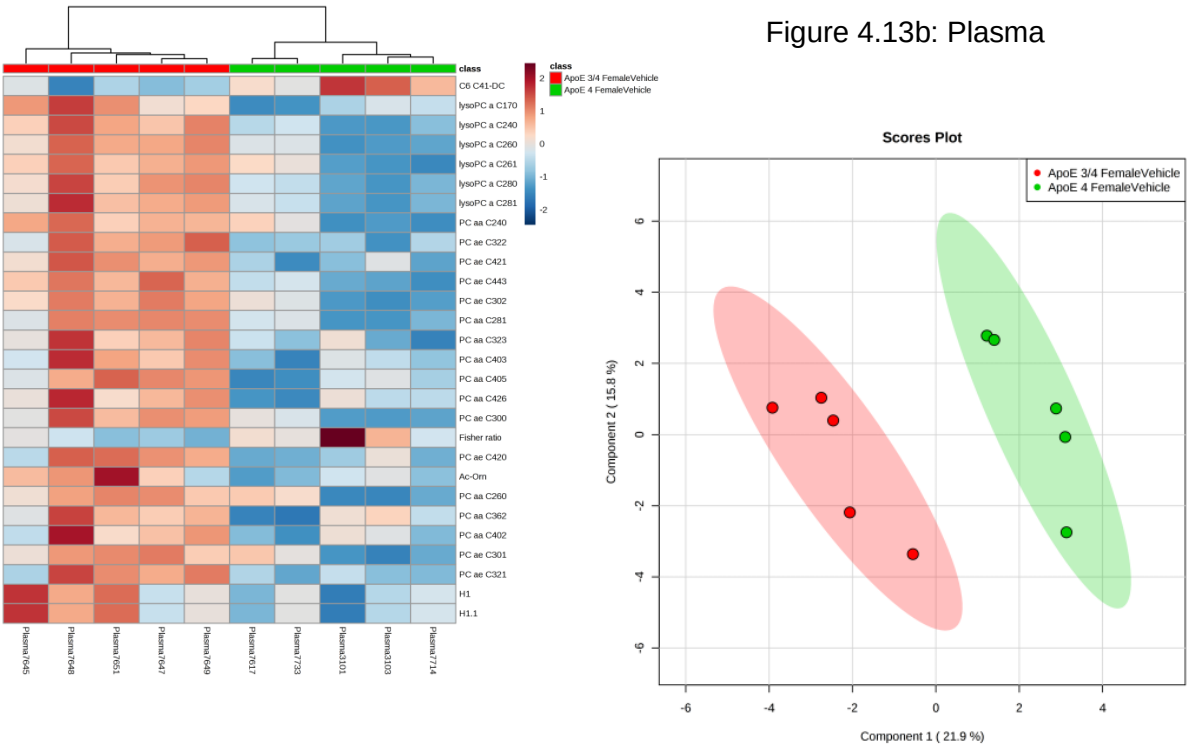

In the cortex only one glycerophospholipid, lysoPC a C14:0 was found to be different between the two groups but did not reach a level of significance.

Figure 4.13c: Cortex

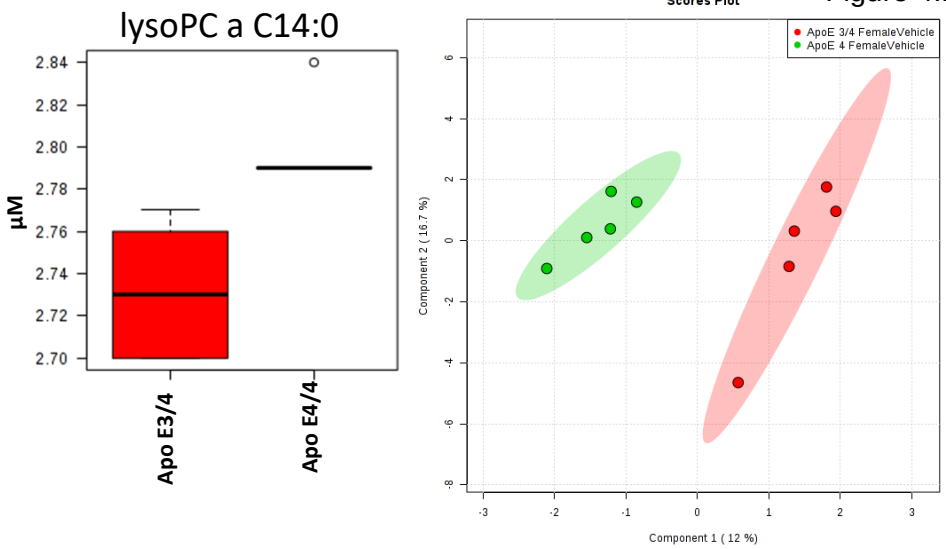

4.4.4.4 Saline treated ApoE 3/3 vs. ApoE 4/4 females

When saline treated ApoE 3/3 and ApoE 4/4 females were compared, 17 metabolites were significantly (uncorrected p-value) different in cortex and 26 metabolites were significantly (uncorrected p-value) different in plasma. Even though none reached significance with corrected p-value, PCA plot shows a clear separation between the two groups in both plasma and cortex and a much tighter clustering of saline treated ApoE 3/3 female mice in data obtained from plasma.

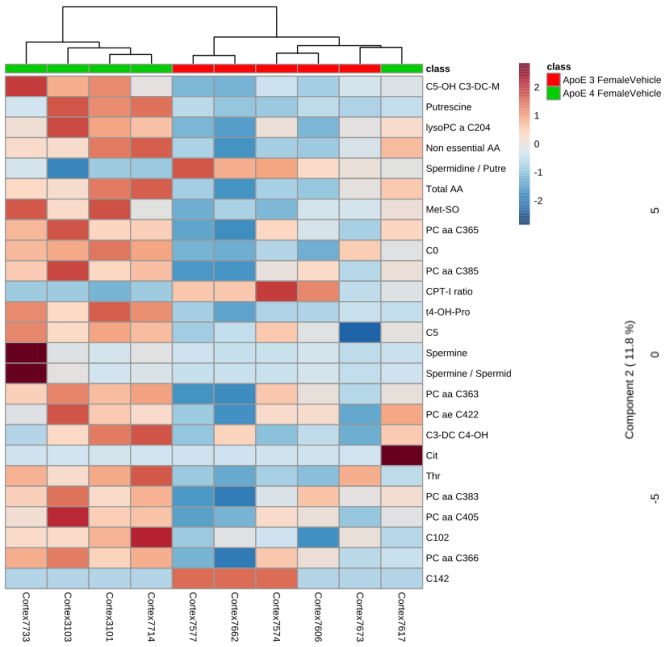

Figure 4.14a: Cortex

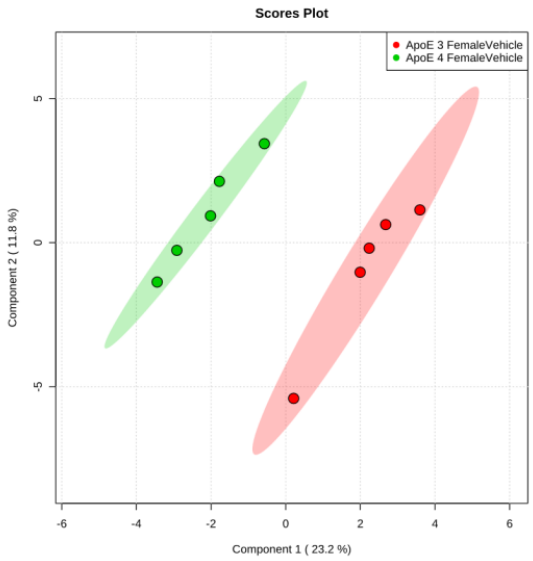

Figure 4.14a-b Cortical and plasma differences in metabolites between saline treated ApoE 3/3 and 4/4 female mice.
Saline treated ApoE 3/3 and ApoE 4/4 females show a clear separation on the PCA plot, both in cortex (4.10a) and plasma (4.10b). In plasma the ApoE 3/3 saline treated females cluster tighter together compared to cortex.

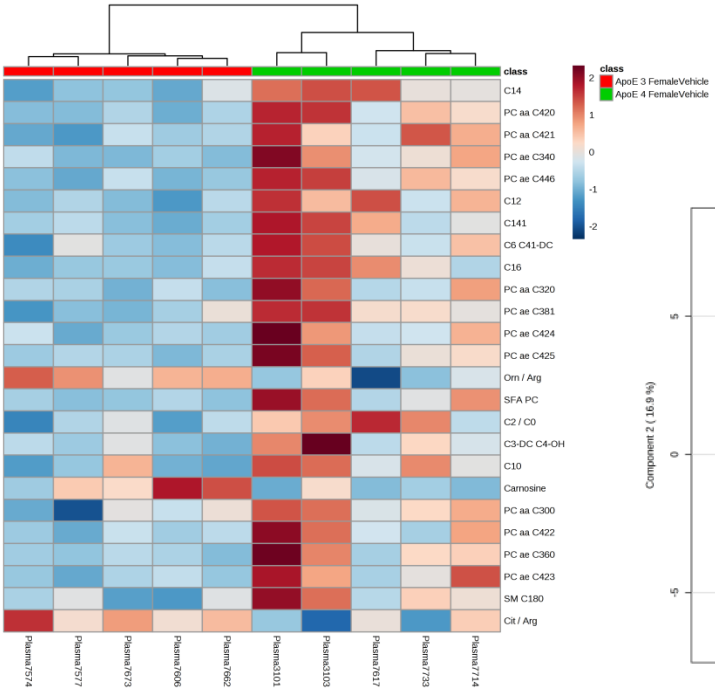

Figure 4.14b: Plasma

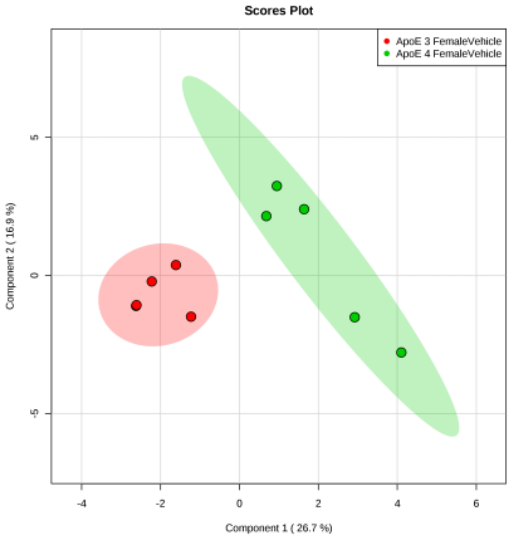

4.4.4.5 Saline treated ApoE 3/3 and ApoE 4/4 females and males

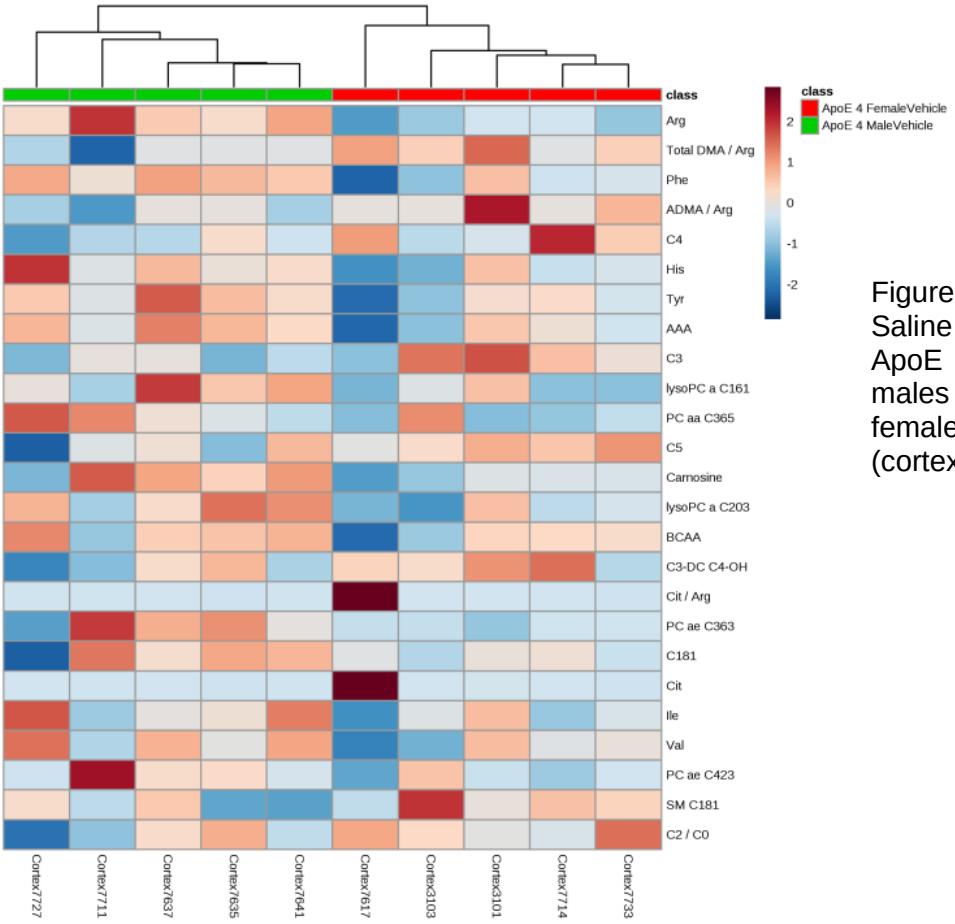

Figure 4.15a Saline treated ApoE 4/4 males and females (cortex).

In both ApoE 3/3 and ApoE 4/4 models, plasma glycerophospholipids were higher in males in comparison to females. In ApoE 4/4, in cortex arginine and phenylalanine were found to be higher in males, and polyamines (as a result of arginine catabolism) were lower in males compared to females. In ApoE 3/3 plasma, carnosine, acyl-ornithine (Ac-Orn) and asymmetric dimethylarginine (ADMA) were higher in females and alpha-aminoadipate (αAA) was lower, whereas in cortex, spermidine was high in females and putrescine and αAA were lower. Ac-Orn, ADMA and carnosine are the end products of arginine catabolism through urea cycle, polyamine biosynthesis-oxidative stress and carnosine anabolism, respectively.

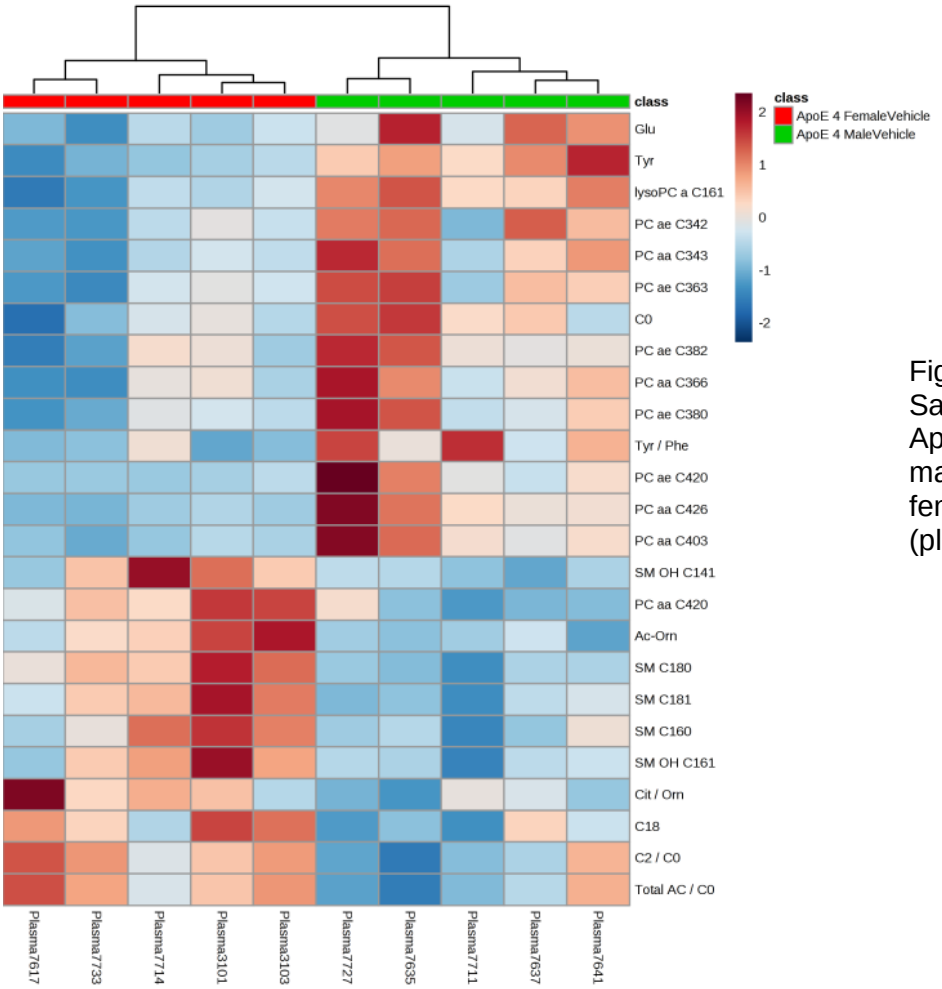

Figure 4.15b Saline treated ApoE 4/4 males and female (plasma).

Figure 4.15a-d Metabolite differences in cortex and plasma between saline treated ApoE 3/3 and 4/4 males and females.

Saline treated ApoE 3/3 and ApoE 4/4 males and females were compared to understand differences based on sex in plasma and cortex. In ApoE 4/4 genotype, males exhibit higher glycerophopholipids, arginine and phenylalanine, while in ApoE 3/3, carnosine, Ac-Orn and ADMA are higher in females and alpha-AA is lower.

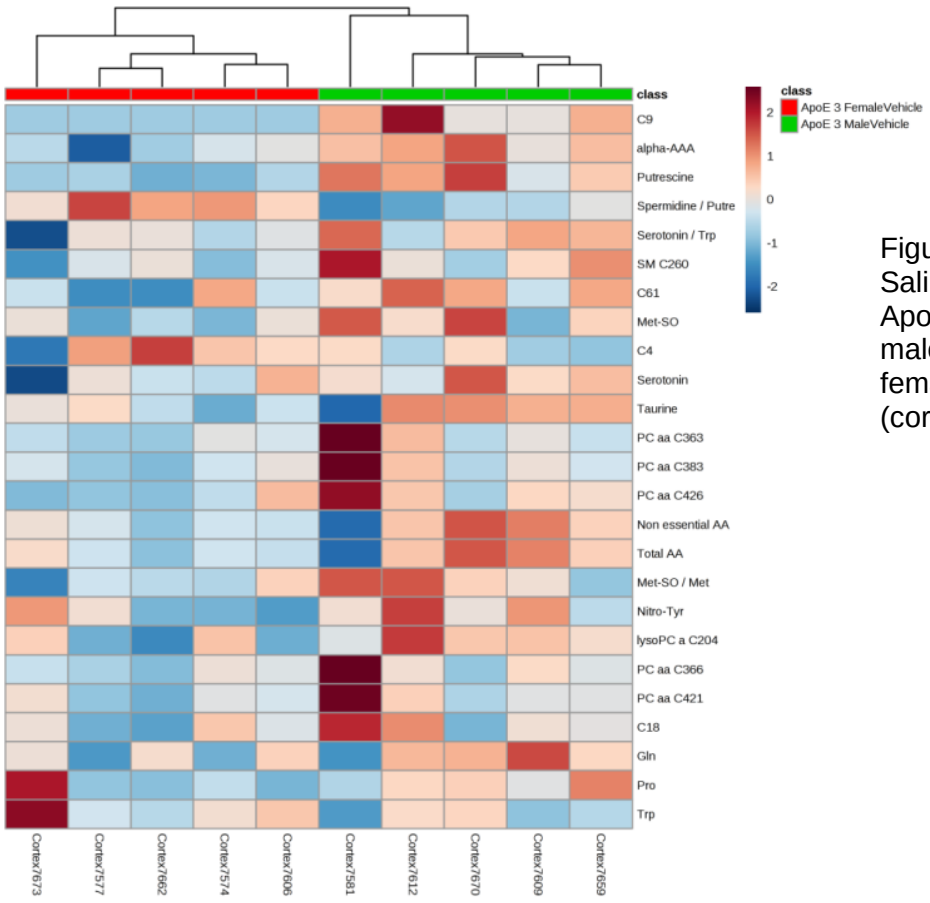

Figure 4.15c Saline treated ApoE 3/3 males and female (cortex).

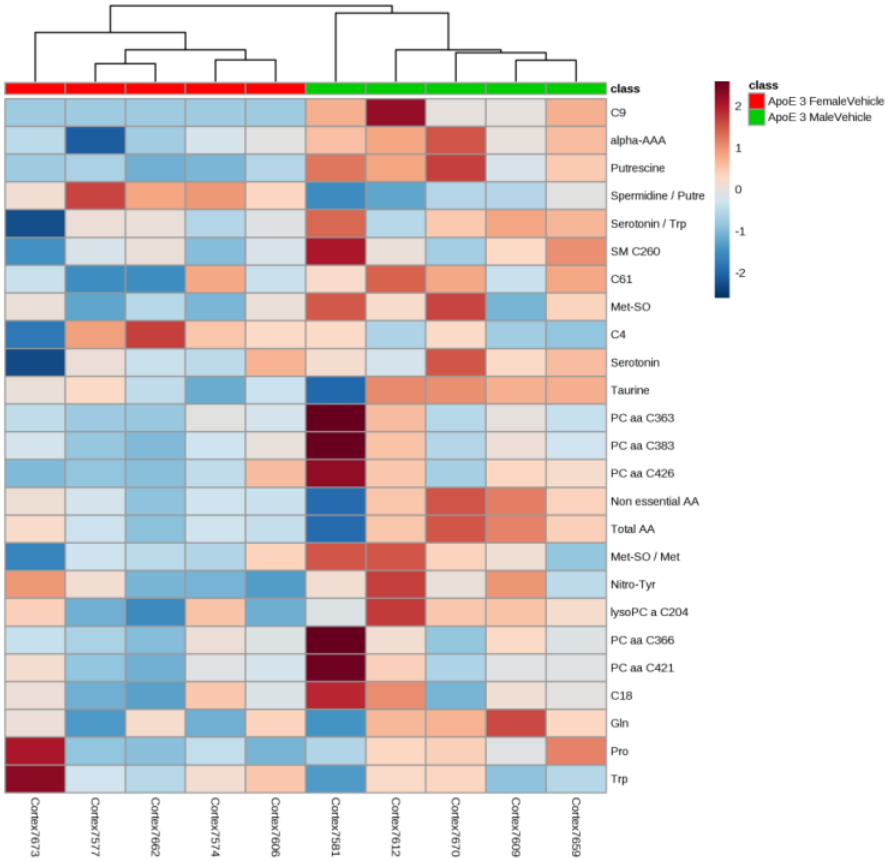

Figure 4.15d Saline treated ApoE 3/3 males and female (plasma).

4.4.5 MITOCHONDRIAL POTENTIATION OF HNSCS BY ALLO AND ALLO ANALOGUES

<u>Allo dose response curve</u>

Dose response study in hNSCs with respect to Allo treatment is shown in Figure 4.16. Allo at both doses (10nm and 100nM) potentiates mitochondrial function similarly, even though Allo 100nM seems to potentiate mitochondrial function more than Allo 10nM, these results are within margin of error. I chose the dose of 100nM for other experiments in order to be consistent with previous studies from our lab and also because dose response data from 100nM dose was less variable.

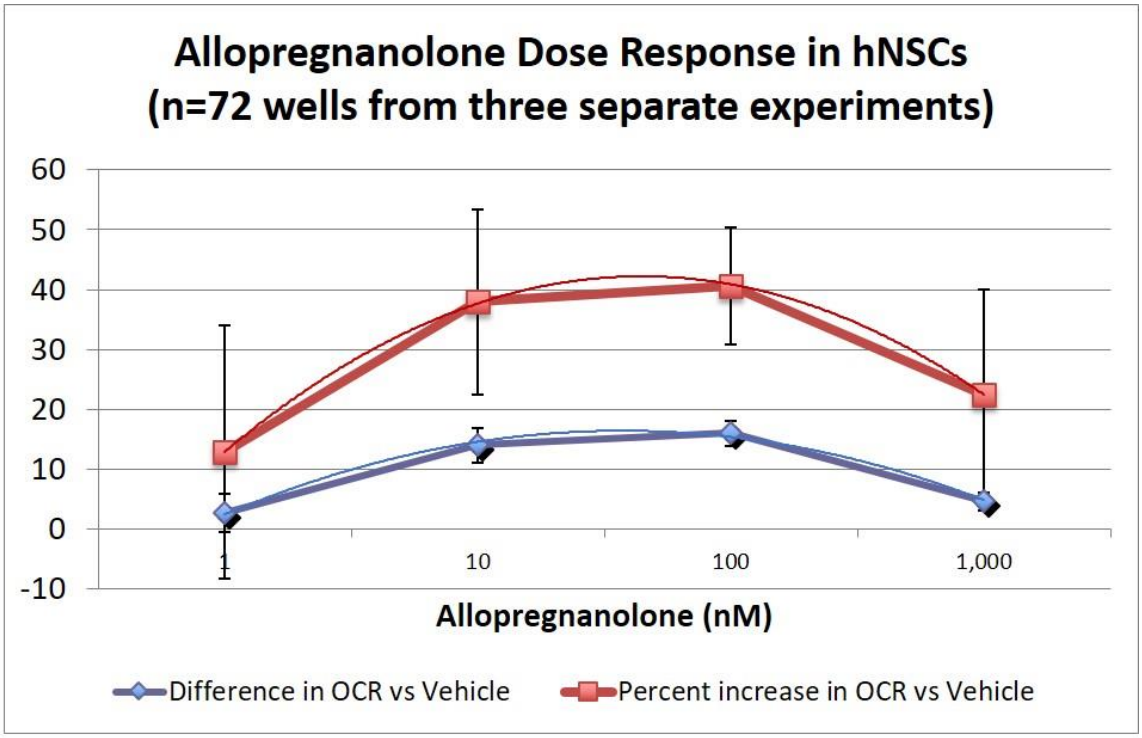

OCR: Oxygen Consumption Rate

Figure 4.16 **Allo dose response curve in hNSCs with respect to mitochondrial potentiation**.
The optimal dose of Allo for mitochondrial potentiation in hNSCs is 10-100nM. A dose of 100nM was chosen to maintain consistency with earlier experiments with rat NSCs.

Allopregnanolone and its analogues potentiate mitochondrial function

Figure 4.17 represents a graphical representation of data obtained from the extracellular flux analyzer. The data shows that while no treatment and vehicle treated hNSCs exhibit much lower level of mitochondrial potentiation compared to hNSCs treated with Allo and its analogues as measured OCR. Maximal respiration and spare respiratory capacity of hNSCs were increased by 39% and 53% respectively after treatment with Allo for 24h, compared to vehicle. It is also interesting to note that the analogues cluster into groups with UCI 2-261 100nM, 5β-pregnan-3α-ol-20-one 100nM and Progesterone 100nM highest potentiation followed by rest of the analogues including Allo. The chemical

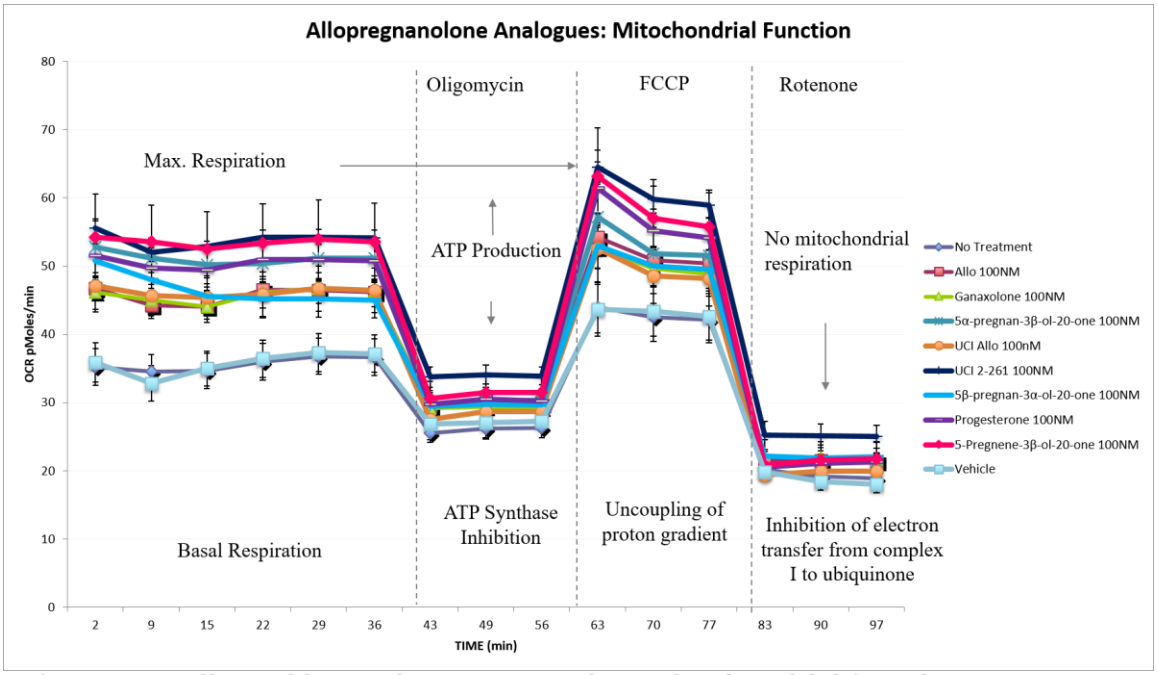

Figure 4.18 **Allo and its analogues potentiate mitochondrial function**.
Treating hNSCs in vitro with Allo and its analogues shows improved mitochondrial function when compared to vehicle treated controls, as measured by the extracellular flux analyzer.

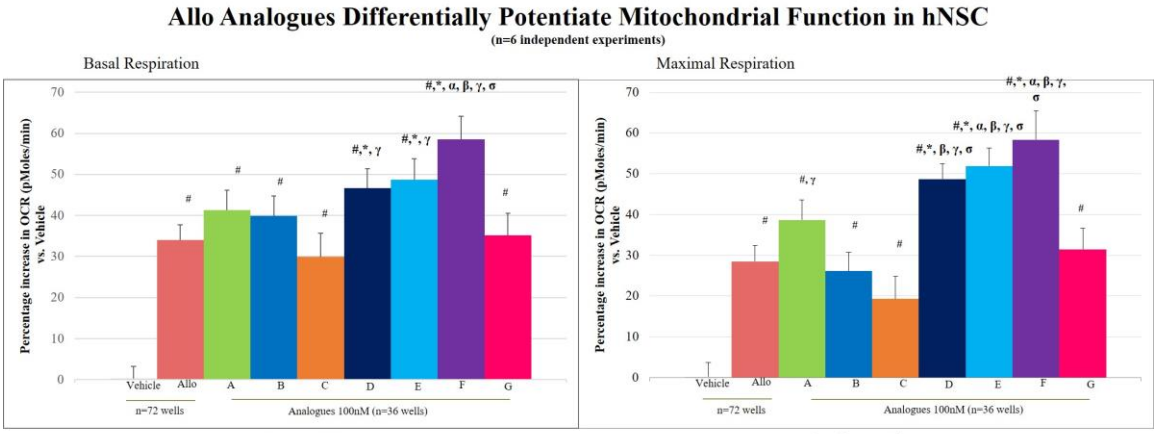

Figure 4.17a

# p< 0.05 vs Vehicle
* p< 0.05 vs Allo 100nM
α p< 0.05 vs Ganaxolone
β p< 0.05 vs 5α-pregnan-3β-ol-20-one
γ p< 0.05 vs UCI Allo
σ p< 0.05 vs 5-Pregnene-3β-ol-20-one

A = Ganaxolone
B = 5α-pregnan-3β-ol-20-one
C = UCI Allo (5α-pregnan-3α-ol-20-one)
D = UCI 2-261
E = 5β-pregnan-3α-ol-20-one (epi-Allo)
F = Progesterone
G = 5-Pregnene-3β-ol-20-one

Figure 4.17a-b **Allo and its analogues differentially potentiate mitochondrial function and increase spare respiratory capacity of hNSCs**.
Based on their potentiation of mitochondrial function Allo and its analogues can be divided into two groups that are statistically significantly different from each other.

structures and names of these analogues were originally not known to me and at the end

of the experiment I discovered that what I had labelled as Analogue C was Allo from the

Figure 4.17b

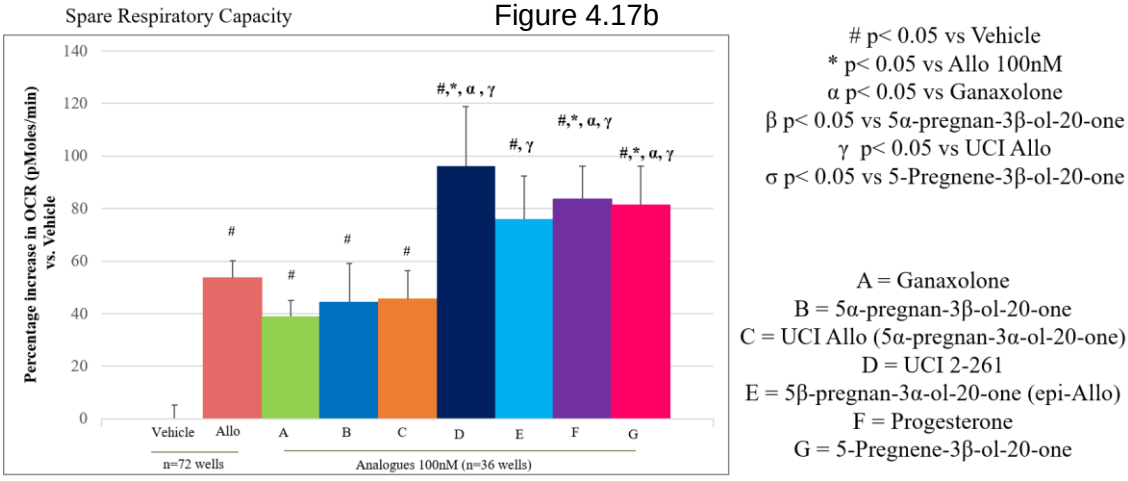

lab of Dr. Gee at University of Irvine, and therefore I labelled it as UCI Allo in the graphs. The aggregated differences in mitochondrial potentiation in response to Allo treatment of hNSCs is shown in Figure 4.18. I obtained these data from six different experiments. All the data were normalized to protein content as described earlier. From the graph it is evident that Allo and its analogues can be divided into two groups based on their potentiation of mitochondrial function in hNSCs. First group consists of Allo, Ganaxolone, 5a-pregnan-3ß-ol-20-one and 5-Pregnene-3ß-ol-20-one which are statistically not dissimilar in their effect on mitochondrial potentiation in hNSCs. The second group consists of UCI 2-261 (a proprietary compound whose chemical structure and name I am not aware of), 5ß-pregnan-3a-ol-20-one (epi-Allo) and Progesterone which potentiate mitochondrial function to a magnitude which is higher and statistically significantly different from the first group of compounds including Allo. Allo increased spare respiratory capacity (SRC) by 53% in hNSCs, while Allo's analogue, UCI 2-261, almost doubled (96%) SRC of hNSC mitochondria. Both our Allo and UCI Allo show little difference in increasing OCR in hNSCs and provide validation for this experiment. Another point of interest I noted was that the effect of Allo (and analogues) declined with increase in passage numbers of

hNSCs and the effect completely disappeared after passage number 21. The gradual decline started at either passage 15 or 16 in preliminary experiments (data not shown) and therefore I did not use any hNSCs beyond passage 14 for these experiments.

Allo 'pulse' treatment of hNSCs

The time period of the pulse was defined as the number of hours that elapsed after the completion of the 30-min. exposure of hNSCs to Allo and before measurement of mitochondrial function using extracellular flux analyzer. There were five such groups based on number of hours, 24h(100nM), 24h (1000nM), 8h, 4h and 2h. Additional groups were the positive control (24h continuous Allo treatment) and vehicle treatment. Treatment with a higher dose of Allo (1000nM) was carried out in order to evaluate whether a larger dose of Allo 24 hours before measurement had any beneficial effect on mitochondrial function in hNSCs compared to 100nM dose of Allo, everything else being the same.

Results (Fig. 4.19a-b) showed that while my positive control of 24h continues treatment

Figure 4.19a

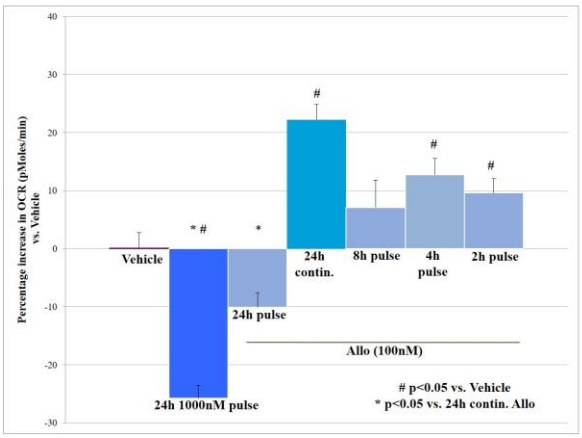

Figure 4.19b

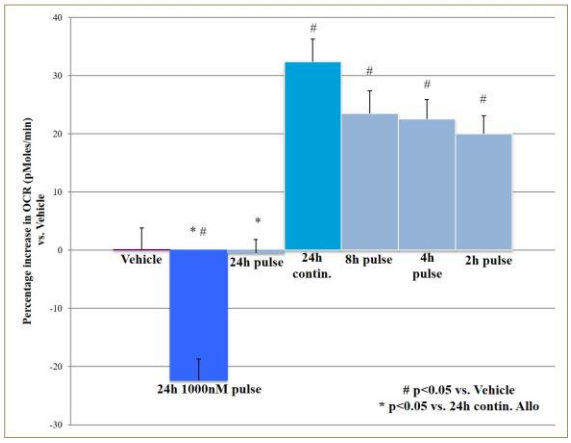

Figure 4.19a-b **Exposure of hNSCs to 30-min. pulse of Allo and its effects on mitochondrial function**.
The effect of the 30-min Allo exposure lasts at least up to 8 hours and the magnitude of this effect is not significantly different from a 24-hour Allo exposure. Higher dose of Allo (1000nM) for 30-min has significant deleterious effect on mitochondrial function in hNSCs that persists even after 24 hours.

appeared to be the best with respect to potentiation of mitochondrial function in hNSCs,

all three pulse treatments (8h, 4h and 2h) were statistically not significantly different from the positive control for maximal respiration and for basal respiration only 8h treatment was not dissimilar to vehicle treated cells, statistically speaking. A 30-min pulse exposure to Allo 8h before measurement of mitochondrial function is closest to a 24-hour continuous Allo exposure at maximal respiration but not statistically distinguishable (4.18a-b). Surprisingly 1000nM dose of Allo did more harm than good and it actually decreased the mitochondrial function of hNSCs and this effect was visible even 24h after exposure to a 30-min. 'pulse' of Allo. 24h 'pulse' of 100nM Allo did not fare well either but appeared to be less deleterious compared to 1000nM but was statistically not significantly different from the 24h 1000nM 'pulse'.

Evaluation of Allo as an agonist or antagonist of TSPO

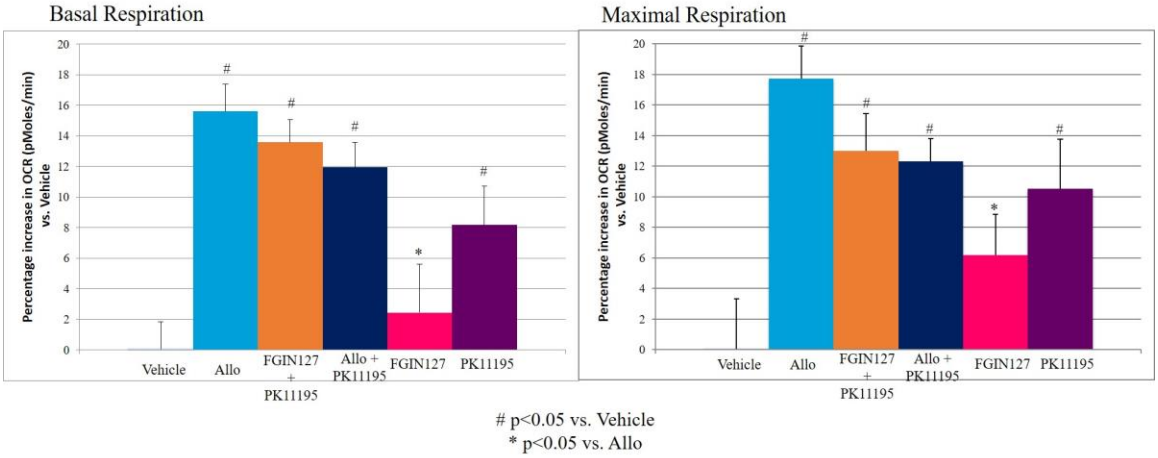

Figure 4.20 **Evaluation of Allo as an agonist or antagonist of TSPO in mitochondria**.
Based on data from measurement of mitochondrial function it was is not clear if Allo is an agonist or antagonist of TSPO even though Allo exhibits a more antagonistic picture when compared to known agonist and antagonist of TSPO.

Evaluation of Allo as a TSPO agonist or antagonist produced mixes results as shown in Figure 4.20. While Allo exhibited its characteristic potentiation of mitochondrial function, the results from agonist and antagonist were different from my expectations. TSPO

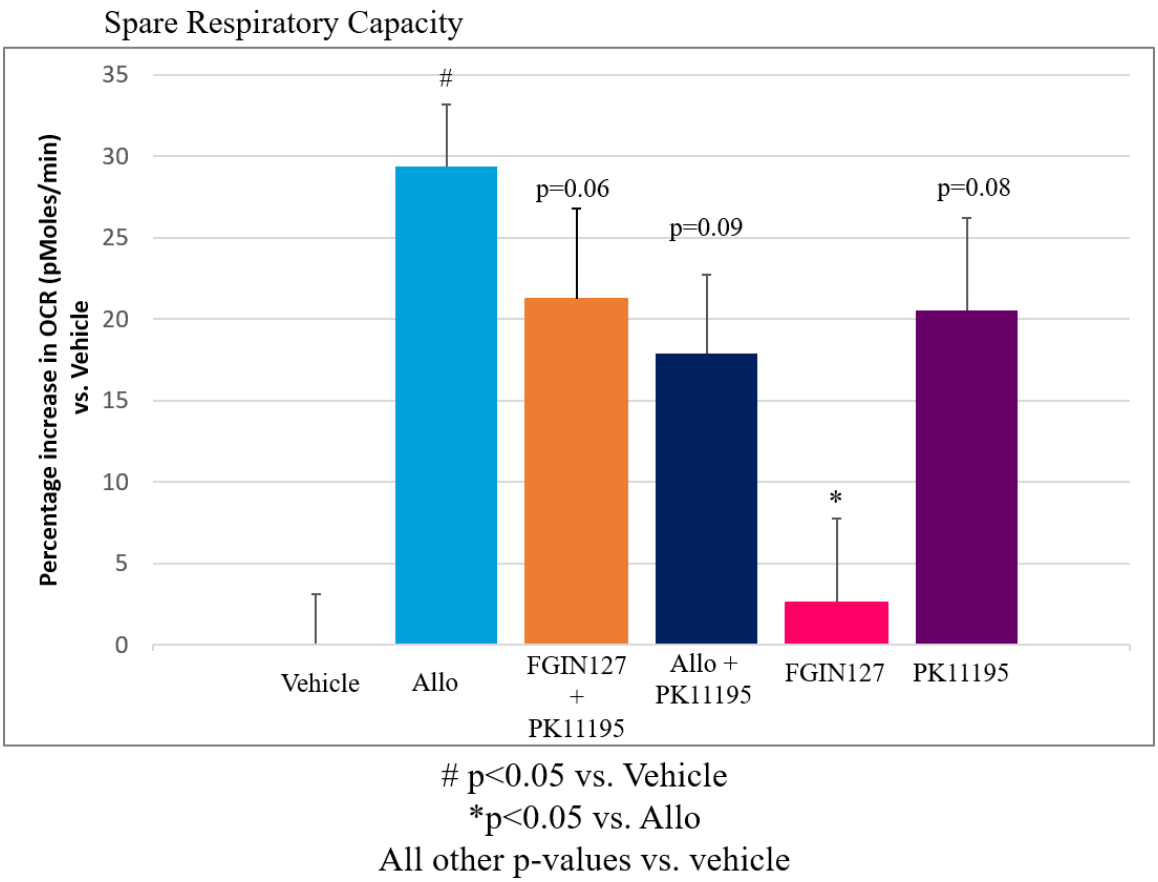

Figure 4.21 **Allo statistically significantly increased SRC of mitochondria in hNSC after 24-hour exposure compared to TSPO agonist and antagonist**.
However, neither TSPO agonist or antagonist increased SRC significantly although the antagonist, PK11195, exhibits a trend towards statistical significance, suggesting that Allo's action may be antagonistic-like at TSPO.

antagonist PK 11195 statistically significantly potentiated mitochondrial function compared to vehicle while TSPO agonist FGIN 1-27 was not statistically dissimilar from vehicle. A combination of the agonist and antagonist led to potentiation of mitochondrial function, not as much as the positive control (Allo 100nM) but statistically the difference was not significant. Allo and the antagonist (PK 11195) in combination too potentiated mitochondrial function but visibly less than Allo and the agonist + antagonist combination. However, these differences were not statistically significant. When I calculated Spare Respiratory Capacity, I found that Allo statistically significantly increased SRC compared

to vehicle (Fig. 4.21), but neither TSPO agonist nor TSPO antagonist nor a combination increased SRC in a statistically significant manner. TSPO agonist FGIN 1-27 was statistically not dissimilar from vehicle and significantly different from Allo treatment. These findings suggest Allo's mitochondrial potentiation in hNSCs to be a TSPO-antagonist-like action and not TSPO-agonist-like action.

4.4.6 IMAGING

MRI study was carried out on brains of certain Allo and saline treated mice that I shipped to University of Arizona. While the imaging process is complete, data analysis is underway and should be available soon.

4.5 Discussion

I discussed earlier that ApoE4 allele is strongly associated with the risk of developing AD and AD, as a disease, currently lacks any therapeutic intervention to thwart its march. Allo is a novel neuroregenerative that has shown promising effects in the 3xTg mouse model of AD and in this experiment was used to treat ApoE-TR mice in order to determine its effects on cognition, hippocampal transcriptome, brain imaging and metabolism. This extensive study was an attempt to apply a systems biology approach to translation research in AD and at the same time target a genotype that is clearly highly susceptible to development of AD. In fact, the Allo and saline I used in this experiment as well as the dose (extrapolated to mice) were identical to the clinical trial in human participants. The duration of the study was 6 months, double of the phase Ib/IIa trial but in line with our proposed phase IIb clinical trial in human participants.

The novel object recognition test used to measure cognitive function showed considerable improvement in both Allo treated males and females of ApoE 4/4 genotype while males

and females of ApoE 3/3 genotype failed to show any improvement compared to their saline treated counterparts. Interestingly, while all groups exhibited variability in measurement of cognitive function, Allo treated groups are more readily divisible into two subpopulations: responders and non-responders, which is similar to the results of our phase Ib/IIa clinical trial. While the difference in cognition between Allo treated ApoE 4/4 males was trending towards significance ($p=0.08$) when difference in exploration time was measured, statistical significance was achieved when discrimination index (DI) of both these groups were compared. DI is derived by normalizing the difference in exploration time to the total time spent exploring by the mouse and thus is a ratio. DI is a better measure of cognitive improvement since it takes into account the total time spent exploring.

The hippocampal RNA-Seq resulted in extensive amount of data from comparing ten separate groups. Allo treated ApoE 4/4 females were the only group that exhibited upregulation of PDGF-BB when compared to their saline treated counterparts. There are four known PDGF genes with broad expression patterns and except for PDGF-DD, all others are expressed in the brain in varying amounts (Fredriksson et al., 2004; LaRochelle et al., 2001). These literature findings agree with absence of PDGF-DD and the expression of the other three in hippocampus (Fredriksson et al., 2004) of ApoE 4/4 Allo treated female mice. While PDGF-BB is necessary for maintenance of healthy BBB, PDGFRα signaling may contribute to BBB disruption (Ma et al., 2011). Allo's downregulation of PDGFRα is therefore in agreement with its suggested action of protecting BBB integrity. However, further downstream regulation of the PDGF signaling pathway needs additional elucidation.

To reiterate, estrogens play a major role in maintaining BBB integrity via PDGF as described in Chapter 1. ApoE 4/4 genotype is also risk factor for increased blood brain barrier permeability and multiple studies have found that magnitude of BBB damage may be determined by which ApoE allele is present i.e. E2, E3 or E4 (Hultman et al., 2013; Salloway et al., 2002; Zipser et al., 2007; Zonneveld et al., 2014). ApoE4 carriers are vulnerable to BBB disruption in the prodromal phase of cognitive decline (Halliday et al., 2013). Mechanistically, ApoE4 appears to expedite death of pericytes which could contribute to BBB compromise (Halliday et al., 2016). Literature suggests that in a model of TBI, Allo inhibits proinflammatory pathways and reduces cerebral edema (Ishrat et al., 2010). Also, in a different study, Allo reduced the magnitude of BBB compromise as well as size of infarct in focal ischemia (He et al., 2004). Based on these findings it is likely that the predicted upregulation of PDGF-BB by Allo could ameliorate the increased blood brain barrier permeability and could potentially be one of the mechanisms by which Allo neutralizes the deleterious effects of ApoE 4/4 genotype on BBB.

The canonical pathways that I found when I compared the hippocampal transcriptome of Allo treated ApoE 4/4 females to their saline treated counterparts suggest that various immune system pathways along with metabolic and signaling cascade pathways are regulated by Allo. The presence of immune system markers in a perfused hippocampus strongly suggests immune system regulation of the brain parenchyma by Allo. Another pathway of interest is Acyl-CoA hydrolysis pathway which in conjunction with data from the metabolomic study suggests increase in energy metabolism utilizing lipids.

Effects of Allo on hippocampal transcriptome were found to be genotype specific. Allo downregulated a large number of pathways in ApoE 4/4 animals, both males and females while the same pathways were either upregulated or unchanged in ApoE 3/3 mice. This

suggests that Allo maybe useful only in certain genotypes of ApoE such as E4 and this is corroborated by our clinical trial data from phase Ib/IIa trial.

It was unfortunate that only a few metabolites were significantly different between most groups of the study, however, I had only five animals in each group for the metabolomic panel study and therefore increasing the number of animals in each group may result in larger number of metabolites that meet statistical significance after correction for multiple comparisons. Some effect of treatment, genotype and sex is observed in the data from the metabolomic panel since the results from the inter-group comparisons discussed above show clear separation of individual animals into groups on the PCA plot. Data comparing ApoE 4/4 Allo females to saline treated counterparts suggests that Allo increases glycerophospholipids and reduces acylcarnitines. While data from the cortex showed little difference between saline treated ApoE 3/3 females and ApoE 3/4 females, several glycerophospholipids, amino acids, biogenic amines and acylcarnitines were significantly different in plasma of saline treated ApoE 3/3 and ApoE 3/4 female mice and majority of glycerophospholipids and two amino acids reached significance after adjusting the p-value. ApoE 3/4 had higher glycerophospholipids than ApoE 3/3, which potentially can be utilized as a metabolic phenotype, if these findings are reproducible. In both plasma and cortex, several glycerophospholipid were different between ApoE 3/4 and ApoE 4/4 female mice, even though none are statistically significantly different. When saline treated ApoE 3/3 and ApoE 4/4 females were compared, 17 metabolites different in cortex and 26 metabolites were different in plasma. Even though none reached significance with corrected p-value, PCA plot shows a clear separation between the two groups in both plasma and cortex and a much tighter clustering of saline treated ApoE 3/3 female mice in data obtained from plasma. These results indicate that females of all three genotypes

exhibit a unique metabolomic signature and a metabolomic panel such as the one we have used can potentially be used to classify ApoE genotypes into metabolomic phenotypes, if this data can be verified in human participants. The presence of human ApoE genes in these mice suggest a strong possibility that humans too may exhibit a similar pattern.

In saline treated ApoE 3/3 and 4/4 mice, plasma glycerophospholipids were higher in males in comparison to females. Other findings suggested higher arginine catabolism in males compared to females. Also plasma αAA has been shown to be lower in APP/PS1 Alzheimer's model (Pan et al., 2016). Additionally, increase in spermidine, spermine, putrescine have been reported in Alzheimer disease pathology (Inoue et al., 2013). Thus, lower αAA in female mice may indicate greater susceptibility or likelihood of AD but higher spermidine and lower putrescine and αAA are inconclusive to evaluate risk of AD based on data from the metabolomic panel alone. Both the metabolomic panel and RNA-Seq are expensive studies and therefore five animals per group for ten groups was considered cost-effective. However, the effects of Allo treatment may be too subtle and much larger number of animals (n=9 to 12) per group may be necessary for the metabolomic study to resolve any statistically significant differences, if truly present. Also, a cell-type specific RNA-Seq of hippocampal neurons may reveal greater details regarding the transcriptomic regulation of observed effects of Allo.

Mechanistically, Allo potentiated mitochondrial function in hNSCs in a dose dependent manner: 100nM was optimal dose of whereas 1mM suppressed mitochondrial function. Epi-Allo, UCI 2-261 and progesterone significantly increased mitochondrial respiration to a greater magnitude than Allo. 30-min of exposure to Allo up to 8 hours before measurement was as effective as 24h of continuous Allo exposure. Allo 30-min. pulse

resulted in maximal mitochondrial respiration 2-8h post-treatment and this further supports the 30-min. infusion protocol of Allo phase Ib/IIa clinical trial for mild cognitive impairment (MCI) or early AD (ClinicalTrials.gov Identifier: NCT02221622).

Published studies have assigned a central role to mitochondrial dysfunction in pathogenesis of neurodegenerative disorders, including AD (Beal, 2002; Blass et al., 2000; Brinton, 2008), corroborated by a shift in cerebral glucose utilization observed in AD patients compared to controls (Hoyer, 1991; Ishii et al., 1997), which lead to oxidative stress and eventual cognitive decline (Atamna and Frey, 2007; Reddy and Beal, 2008). Aβ binding alcohol dehydrogenase (ABAD) is a mitochondrial Aβ binding enzyme suspected as a cause of mitochondrial dysfunction (Lustbader et al., 2004). In both AD patients and the 3xTgAD mouse model of AD, ABAD expression has been found to be correlated with the magnitude of Aβ load and it has been demonstrated that Allo inhibits ABAD (Yao et al., 2009).

Based on these results and findings in published literature it is evident that Allo significantly potentiates mitochondrial function and Allo, either alone or with analogues could be used to improve mitochondrial function in neurodegenerative diseases. Mitochondrial spare respiratory capacity (SRC) is considered a crucial measure of mitochondrial function and is defined as the difference between basal ATP production and its maximal activity, and higher SRC is believed to assist cells in countering oxidative stress (Hill et al., 2009). Therefore, Allo induced 53% increase in SRC of hNSCs suggests a strong neuroprotective effect. Allo's analogue, UCI 2-261 almost doubled SRC and deserves evaluation as a novel therapeutic. Potentiation of mitochondrial function of human neural stem cells by Allo and its analogues is in support of its potential to be the first-of-its-kind neuroregenerative therapeutic. It was also observed that some analogues

of Allo such as epi-Allo, UCI 2-261 and progesterone may be better candidates for improving mitochondrial function *in vivo* if they possess favorable safety and toxicity profiles and satisfactory pharmacokinetic characteristics. The results obtained by 'pulse' treatment of hNSCs with Allo strengthens our rational for infusing Allo in human participants over a 30-min period in phase Ib/IIa clinical trial and suggests that effects of Allo on neural stem cells in humans likely persist at least up to 8 hours after exposure. This long-term effect of Allo could be attributable to protein changes triggered by Allo's allosteric activation of $GABA_A$ receptor channels. Detailed elucidation of the exact mechanism is warranted.

Evaluation of Allo as a TSPO agonist or antagonist produced unexpected results which suggests Allo's mitochondrial potentiation action is not due to agonism of TSPO since TSPO agonist FGIN 1-27 produced an action not statistically dissimilar to vehicle treatment. In fact, antagonism of TSPO (PK 11195) results in potentiation of mitochondrial function of a magnitude less than that produced by Allo, although this difference in magnitude is not statistically significant. This suggests that TSPO antagonism could potentially be one of the mechanism of action through which Allo potentiates mitochondrial function, and Allo likely acts through other mechanisms and signaling pathways as well. The hypothesis that Allo's agonistic action on TSPO is responsible for mitochondrial potentiation in hNSCs was rejected.

4.6 Conclusion

Collectively, the data indicate that Allo improves cognitive function in both female and male ApoE 4/4 mice with females exhibiting a greater response to Allo treatment. Metabolomic data are suggestive of an effect that Allo to increases protein metabolism,

as well as lipid metabolism to generate acetyl-CoA to feed into the TCA cycle to generate ATP in the mitochondria. Further, Allo treatment increased indicators of protein metabolism. Allo treatment was evident in both females and males and modified by ApoE genotype. Hippocampal RNA-Seq suggested Allo's action as an anti-inflammatory agent, and protective of BBB integrity as well as Allo's role in cell cycle regulation and metabolic pathways based on observed changes in hippocampal transcriptome. Allo's regulation of the hippocampal transcriptome was found to be genotype specific rather than gender specific. Further therapeutic development of Allo is underway and a repeat of the metabolomic and RNA-Seq study with larger number of animals may help confirm the underlying mechanisms that are responsible for improved cognitive function. While its neuroregenerative therapeutic potential has been repeatedly demonstrated *in vivo*, this is the first time Allo is being tested in a targeted genotype, as an ongoing effort to promote precision medicine. Allo's action on mitochondrial function of hNSCs *in vitro* strongly supports its credentials as a potential neuroregenerative therapeutic. Allo's mitochondrial potentiation action is not due to agonism of TSPO and in fact, antagonism of TSPO could potentially be one of the mechanisms of action through which Allo potentiates mitochondrial function in hNSCs. In addition, Allo likely acts through other mechanisms and signaling pathways as well since it seems to produce higher magnitude of mitochondrial potentiation than attributable to TSPO antagonism alone. Exact mechanisms of Allo's actions remain to be explored.

5 Conclusion

The findings presented herein describe a systems biology approach to a critical period during chronological and endocrinological aging in women. Menopause obviously is not a new phenomenon, but its current definitions are relatively novel. Since the 1970s, menopause has received increased attention in medical, academic, social and popular spheres (Bell, 1987; Chornesky, 1998; Utian, 2004). In 1938, the first synthetic replacement hormone was developed which resulted in menopause being characterized simply as a 'hormone deficiency disease' (Ballard et al., 2001; Bell, 1987; Meyer, 2003). Even though menopause is a near universal endocrine transition state in women affecting their holistic health, most research studies in menopausal aged women neglect to include control for menopausal status (Newhart, 2013). The physiological processes that end in menopause i.e. cessation of menses, take many years to complete and 'perimenopause' is used to denote this period in women's life leading to menopause (Utian, 2004).

Perimenopause has been demonstrated to be a neurological transition state (Brinton et al., 2015) with far reaching effects on glucose metabolism, mitochondrial bioenergetics and immune system (Yin et al., 2015) *in vivo* in the perimenopausal rat model of natural reproductive senescence described in Chapter 1. In order to better understand the complex hippocampal biological processes that occur during perimenopause in the hippocampus, transcriptomic analysis was carried out by sequencing the RNA obtained from hippocampi of female SD rats.

5.1 Transcriptomic and bioinformatic approach to the systems biology of endocrine aging

The transcriptomic analysis described in Chapter 2 verify some of the earlier published findings (Yin et al., 2015) and demonstrated that perimenopausal transition in female rats significantly changes the expression of certain genes in the hippocampus. The hippocampal RNA-Seq also resulted in an unexpected discovery; it predicted upregulation of functions such as T cell development and development of lymphocytes, and downregulation of apoptosis of lymphocytes and leukocytes. Coupled with prediction of increased BBB permeability by IPA based on the RNA-Seq data and support of published findings in literature, resulted in a systems biology hypothesis of increased BBB permeability in female rats during endocrine aging and a potential amelioration of this phenomenon by Allo.

RNA-Seq demonstrated that both age and endocrine changes influence hippocampal gene expression in female SD rats and that Regular to Irregular transition at 9-10 months had higher number of genes that were significantly differentially expressed compared to the Irregular to Acyclic transition at the same age of 9-10 months in female SD rats. The surgical menopausal group of Regular OVX 10-10.5 months had the largest number of significantly differentially expressed genes when compared to Regular cyclers 9m group, making it evident that natural reproductive senescence model described in Chapter 1 is more representative of the perimenopausal transition experienced by women.

Analysis of the functions of significantly differentially expressed genes during the Regular to Irregular transition at 9-10 months as well as pathway analysis using IPA and PANTHER illustrated the menopausal BBB transition where reduction in sex hormones, mainly estrogen, that regulates blood brain barrier permeability via PDGF, results in a

compromised BBB, making it easier for peripheral blood components, both cellular and non-cellular, to cross into the brain parenchyma and potentially cause toxicity, sensitization to previously unfamiliar antigens and immune response. Additionally, downregulated mitochondrial bioenergetics and insulin signaling pathway were also observed along with statistically significantly reduced expression of neuroprotective UCP2. It is possible that aging, coupled with genetic susceptibility and environmental injury leads to perimenopause, senescence of immune system (Giménez-Llort et al., 2008; Michaud et al., 2013) and abnormal T cell reactivity to external and self-antigens (Prelog, 2006). Perimenopausal reduction in circulating sex steroids could result in a compromised blood-brain barrier as evinced in Chapter 3. A dysregulated immune system, age-related low-grade inflammation and risk factors such as ApoE ε4 too contribute to a more permeable BBB and neuroinflammation (Dorey et al., 2017; Maftei et al., 2013; Newcombe et al., 2018). A neuroinflammatory milieu and a leaky blood brain barrier can potentially trigger cognitive dysfunction (Esteras et al., 2012; Masdeu et al., 2012). BBB itself has been implicated as a source of this inflammation (Festoff et al., 2016; Grammas et al., 2011; Liu et al., 2012; Rochfort and Cummins, 2015).

C-Reactive protein (CRP), a measure of peripheral systemic inflammation (Felger et al., 2018) was found to be higher in AD patients (Gong et al., 2016). CRP is known to have a negative effect on BBB permeability leading to a compromised barrier (Hsuchou et al., 2012). In a 9 year long longitudinal study, Corlier *et al* found that those individuals who at baseline had higher serum CRP were more likely to have thinner cortex after 9 years (Corlier et al., 2018).

AD and associated neuropathology does not manifest in the form of clinical symptoms for many years which implies a long prodromal or preclinical phase of pathogenesis (Sperling

et al., 2013). Hormonal changes in women i.e. perimenopausal transition may therefore contribute to the elevated risk of AD in women (Mosconi et al., 2017).

Based on the perimenopausal hippocampal transcriptome that shows elevated inflammatory markers, increased leukocytes and lymphocytes infiltration in the brain coupled with immune system dysregulation, downregulated mitochondrial bioenergetics and insulin signaling pathway, reduced expression of neuroprotective UCP2 and downregulated PDGF signaling pathway, and corroborative evidence from literature, it is likely that a neuroinflammatory axis emerges during perimenopause with the BBB and its integrity or lack thereof, playing a central role in pathologic processes.

It must be taken into account that this transcriptomic study was carried out only on homogenized hippocampal tissue and not on other brain regions of the female rats, and the transcriptome represents the messenger RNA from protein-coding regions of DNA of all cell types that are found in the hippocampus. Therefore, the pathways and functions detected by IPA and PANTHER based on this data are limited in their ability to pinpoint cell-specific pathways or functions. Additionally, RNA species that do not code for proteins such as microRNA, small nucleolar RNA, small interfering RNA, are known to play crucial roles in brain evolution, development, plasticity and neurodegenerative diseases (Fatica and Bozzoni, 2014; Qureshi and Mehler, 2012; Salta and De Strooper, 2012) but are not covered in this study, and their role in perimenopausal hippocampal transition remains to be elicited.

5.2 Functional confirmation

In my study I used sodium fluorescein dye to confirm the predicted increase in BBB permeability in perimenopausal SD rats. An OVX group was added in order to delineate

the effect of age and endocrine status on permeability of BBB in aging perimenopausal female rats. It was notable that 6-month-old regularly cycling female rats had the lowest BBB permeability in all three tissues analyzed, whereas Regular OVX 7m group of female rats that belonged to the same group as the Regular cyclers 6m, but which underwent ovariectomy at 6 months of age had significantly more permeable BBB. The Sham OVX group at 7m had BBB permeability only slightly elevated compared to Regular cyclers 6m group and was statistically not significantly different suggesting a stronger role for endocrine aging in BBB compromise. Both Regular and Irregular cyclers at 9-10 months had significantly higher BBB permeability compared to the 6-month Regular cycler group indicating that processes that compromise BBB are initiated much before the stage of actual reproductive senescence is reached (Acyclic 9-10m). In fact, only hypothalamus showed BBB permeability significantly different between Regular and Irregular 9-10-month-old female rats whereas BBB permeability in hippocampus and cortex was statistically not dissimilar between these two groups, which indicates increase in BBB permeability precedes the perimenopausal transition as confirmed by vaginal cytology, which is corroborated in literature (Bacon et al., 2018) where neuroendocrine aging has been shown to precede perimenopause via analysis of RNA-Seq data based on identical bioinformatics pipeline discussed in section 2.4.1.

Another point of interest was the increased variability (Figure 3.7) seen between animals of the same group in Regular, Irregular, Acyclic 9-10m, whereas Regular 6m, Regular OVX 7m and Regular Sham OVX 7m display lower variability (comparatively lower values of standard deviation). This variability suggests that not all female SD rats undergo perimenopause and emerge from this endocrine transition in an identical manner, resulting in differences in BBB permeability index. This, if found extrapolatable to humans, supports

the assertion that not all women will be at increased risk of developing AD or neurodegenerative diseases during or after endocrinological transition but, for some women endocrine transition induced hormonal flux portends much greater probability of severely compromised BBB, a potentially dysfunctional immune system, defective bioenergetic regulation, cognitive decline and reduced quality of life. Alternatively, this variability among the female rats could simply be due to differences in exposure to light in the vivarium, differences in microbiota acquired due to difference in location of each cage of female rats in the room or due to, unexplained as yet, epigenetic causes. However, if external factors were affecting the variability, then it is more likely that the variability would be uniformly distributed across the six different groups.

The transcriptomic study of the hippocampus during perimenopausal transition, the discovery of a compromised BBB and its functional proof furthers our knowledge of the complex interaction between cerebrovasculature and the HPA. However, the exact mechanisms of these interactions are currently unknown and need further elucidation. The exact role of estrogens, as well as the chemical nature of the specific estrogen metabolite(s) involved, its interaction with PDGF-BB during perimenopause and the involvement of endothelial cells, astrocyte foot processes and basement membrane in a compromised BBB are all potential areas of research that could elicit further evidence in support of the functional BBB compromise during perimenopause in female rats outlined herein.

5.3 Role of Allopregnanolone

Multiple studies have shown that ApoE isoforms have differential effects on Aβ aggregation, degradation and clearance and may affect synaptic function (Bu, 2009;

Castellano et al., 2011; Chalmers et al., 2003; Dorey et al., 2014; Nwabuisi-Heath et al., 2013) and a recent study demonstrated that ApoE4 promotes AD/Aβ-induced inflammation while ApoE2 inhibits it (Dorey et al., 2017).

Allopregnanolone (Allo), a novel neuroregenerative therapeutic which is structurally an endogenous neurosteroid, has been in pre-clinical and clinical development (Singh et al., 2012; Wang and Brinton, 2008; Wang et al., 2005; Wang et al., 2010) and I conducted a systems biology study to understand the effect of Allo in a targeted genotype (ApoE4), findings from which could be extrapolated to the clinic since the mice under study have human ApoE gene. I confirmed Allo's potential in improvement of cognitive function but surprisingly Allo's effect was genotype dependent but sex independent and only males and females of ApoE4 genotype showed improvement. These results make a strong case for a phase IIb study in an enriched cohort of ApoE4 carriers, both males and females to verify Allo's efficacy in a human population susceptible to AD. Also, based on NOR study each Allo and saline treated group indicate the existence of sub-populations, such that some mice respond better to Allo treatment compared to others. This reinforces our human data from the phase Ib/IIa clinical trial (not enriched for any particular genotype) that exhibited human responders and non-responders to Allo treatment.

Transcriptomic data from the hippocampus of saline and Allo treated mice supported by findings in published literature suggest that Allo may be able to ameliorate the increased BBB permeability observed during endocrine and chronological aging by upregulating PDGF-BB and downregulating PDGFRα. If this is verified in future studies, an intact BBB due to Allo treatment could reduce the risk of AD and other diseases such as multiple sclerosis, where Allo shows promise (Noorbakhsh et al., 2014).

In vitro studies in hNSCs showed that Allo and its analogues increase mitochondrial function and this effect is likely due to downstream changes in transcription and proteins since the changes are measurable and statistically significant up to 8 hours after Allo treatment. Allo is dose dependent effect on hNSCs with optimal dose being 10-100nM; a dose of 1000nM (=1μM) has deleterious effect measurable even 24 hours after Allo removal. Allo's potentiation of mitochondrial function is not due to TSPO agonism but possibly due to antagonism of TSPO as well as due to other signaling pathways.

Some of the factors affecting women's risk of developing a dysfunctional immune system, defective bioenergetic regulation and cognitive decline were analyzed in a healthy cohort of post-menopausal women at risk for cognitive decline using a panel of clinical metabolic indicators (Rettberg et al., 2016). Further studies of women in perimenopausal transition are required to confirm findings presented here in humans and explore potential of Allo as a preventive therapeutic in at-risk populations.

Bibliography

Abdullah, M., Chai, P.-S., Chong, M.-Y., Tohit, E.R.M., Ramasamy, R., Pei, C.P., and Vidyadaran, S. (2012). Gender effect on in vitro lymphocyte subset levels of healthy individuals. Cellular Immunology *272*, 214-219.

Acosta, J.I., Mayer, L., Talboom, J.S., Tsang, C.W., Smith, C.J., Enders, C.K., and Bimonte-Nelson, H.A. (2009). Transitional versus surgical menopause in a rodent model: etiology of ovarian hormone loss impacts memory and the acetylcholine system. Endocrinology *150*, 4248-4259.

Acosta, J.I., Mayer, L.P., Braden, B.B., Nonnenmacher, S., Mennenga, S.E., and Bimonte-Nelson, H.A. (2010). The cognitive effects of conjugated equine estrogens depend on whether menopause etiology is transitional or surgical. Endocrinology *151*, 3795-3804.

Afshan, G., Afzal, N., and Qureshi, S. (2012). CD4+CD25(hi) regulatory T cells in healthy males and females mediate gender difference in the prevalence of autoimmune diseases. Clin Lab *58*, 567-571.

Alterovitz, G., Xiang, M., Mohan, M., and Ramoni, M.F. (2006). GO PaD: the gene ontology partition database. Nucleic acids research *35*, D322-D327.

Altmann, A., Tian, L., Henderson, V.W., and Greicius, M.D. (2014). Sex modifies the APOE-related risk of developing Alzheimer disease. Annals of Neurology *75*, 563-573.

Amor, S., Puentes, F., Baker, D., and Van Der Valk, P. (2010). Inflammation in neurodegenerative diseases. Immunology *129*, 154-169.

Andorn, A.C., Britton, R.S., Bacon, B.R., and Kalaria, R.N. (1998). Ascorbate-stimulated lipid peroxidation and non-heme iron concentrations in Alzheimer disease. Molecular and chemical neuropathology *33*, 15-26.

Andrews-Zwilling, Y., Bien-Ly, N., Xu, Q., Li, G., Bernardo, A., Yoon, S.Y., Zwilling, D., Yan, T.X., Chen, L., and Huang, Y. (2010). Apolipoprotein E4 causes age- and Tau-dependent impairment of GABAergic interneurons, leading to learning and memory deficits in mice. J Neurosci *30*, 13707-13717.

Andrews, Z.B., and Horvath, T.L. (2009). Uncoupling protein-2 regulates lifespan in mice. American Journal of Physiology-Endocrinology and Metabolism *296*, E621-E627.

Antunes, M., and Biala, G. (2012). The novel object recognition memory: neurobiology, test procedure, and its modifications. Cognitive processing *13*, 93-110.

Aomatsu, M., Kato, T., Kasahara, E., and Kitagawa, S. (2013). Gender difference in tumor necrosis factor-α production in human neutrophils stimulated by lipopolysaccharide and interferon-γ. Biochemical and biophysical research communications *441*, 220-225.

Arimoto, J.M., Wong, A., Rozovsky, I., Lin, S.W., Morgan, T.E., and Finch, C.E. (2013). Age increase of estrogen receptor-α (ERα) in cortical astrocytes impairs neurotrophic support in male and female rats. Endocrinology *154*, 2101-2113.

Armulik, A., Genové, G., Mäe, M., Nisancioglu, M.H., Wallgard, E., Niaudet, C., He, L., Norlin, J., Lindblom, P., and Strittmatter, K. (2010). Pericytes regulate the blood–brain barrier. Nature *468*, 557.

Ashburner, M., Ball, C.A., Blake, J.A., Botstein, D., Butler, H., Cherry, J.M., Davis, A.P., Dolinski, K., Dwight, S.S., and Eppig, J.T. (2000). Gene Ontology: tool for the unification of biology. Nature genetics *25*, 25.

Association, A.s. (2014). 2014 Alzheimer's disease facts and figures. Alzheimer's & Dementia *10*, e47-e92.

Association, A.s. (2018). 2018 Alzheimer's disease facts and figures. Alzheimer's & Dementia *14*, 367-429.
Atallah, A., Mhaouty-Kodja, S., and Grange-Messent, V. (2017). Chronic depletion of gonadal testosterone leads to blood–brain barrier dysfunction and inflammation in male mice. Journal of Cerebral Blood Flow & Metabolism *37*, 3161-3175.
Atamna, H., and Frey, W.H. (2007). Mechanisms of mitochondrial dysfunction and energy deficiency in Alzheimer's disease. Mitochondrion *7*, 297-310.
Attems, J., and Jellinger, K.A. (2004). Only cerebral capillary amyloid angiopathy correlates with Alzheimer pathology—a pilot study. Acta neuropathologica *107*, 83-90.
Bacon, E.R., Mishra, A., Wang, Y., Desai, M.k., Yin, F., and Brinton, R.D. (2018). Neuroendocrine Aging Precedes Perimenopause and is Regulated by DNA Methylation. Neurobiology of Aging.
Bake, S., and Sohrabji, F. (2004). 17β-Estradiol differentially regulates blood-brain barrier permeability in young and aging female rats. Endocrinology *145*, 5471-5475.
Ballard, K.D., Kuh, D.J., and Wadsworth, M.E. (2001). The role of the menopause in women's experiences of the 'change of life'. Sociology of Health & Illness *23*, 397-424.
Baumgartner Jr, W.A., Cohen, K.B., Fox, L.M., Acquaah-Mensah, G., and Hunter, L. (2007). Manual curation is not sufficient for annotation of genomic databases. Bioinformatics *23*, i41-i48.
Beal, M.F. (2002). Mitochondria in neurodegeneration. In Mitochondrial Disorders (Springer), pp. 17-35.
Bell, M., and Ball, M. (1986). The correlation of vascular capacity with the parenchymal lesions of Alzheimer's disease. Canadian Journal of Neurological Sciences *13*, 456-461.
Bell, S.E. (1987). Changing ideas: The medicalization of menopause. Social science & medicine *24*, 535-542.
Bellino, F.L. (2000). Nonprimate animal models of menopause: workshop report. Menopause *7*, 14-24.
Bellino, F.L., and Wise, P.M. (2003). Nonhuman primate models of menopause workshop. Biol Reprod *68*, 10-18.
Bentley, D.R., Balasubramanian, S., Swerdlow, H.P., Smith, G.P., Milton, J., Brown, C.G., Hall, K.P., Evers, D.J., Barnes, C.L., Bignell, H.R*., et al.* (2008). Accurate whole human genome sequencing using reversible terminator chemistry. Nature *456*, 53-59.
Berchtold, N.C., Cribbs, D.H., Coleman, P.D., Rogers, J., Head, E., Kim, R., Beach, T., Miller, C., Troncoso, J., and Trojanowski, J.Q. (2008). Gene expression changes in the course of normal brain aging are sexually dimorphic. Proceedings of the National Academy of Sciences.
Berent-Spillson, A., Persad, C.C., Love, T., Sowers, M., Randolph, J.F., Zubieta, J.-K., and Smith, Y.R. (2012). Hormonal Environment Affects Cognition Independent of Age during the Menopause Transition. The Journal of Clinical Endocrinology & Metabolism *97*, E1686-E1694.
Bethea, C.L., Mirkes, S.J., Shively, C.A., and Adams, M.R. (2000). Steroid regulation of tryptophan hydroxylase protein in the dorsal raphe of macaques. Biol Psychiatry *47*, 562-576.
Beydoun, H.A., el-Amin, R., McNeal, M., Perry, C., and Archer, D.F. (2013). Reproductive history and postmenopausal rheumatoid arthritis among women 60 years or older: Third National Health and Nutrition Examination Survey. Menopause *20*, 930-935.

Bitran, D., Foley, M., Audette, D., Leslie, N., and Frye, C.A. (2000). Activation of peripheral mitochondrial benzodiazepine receptors in the hippocampus stimulates allopregnanolone synthesis and produces anxiolytic-like effects in the rat. Psychopharmacology *151*, 64-71.
Blass, J.P., SHEU, R.K.F., and Gibson, G.E. (2000). Inherent abnormalities in energy metabolism in Alzheimer disease: interaction with cerebrovascular compromise. Annals of the New York Academy of Sciences *903*, 204-221.
Boguski, M.S., Tolstoshev, C.M., and Bassett, D.E., Jr. (1994). Gene discovery in dbEST. Science *265*, 1993-1994.
Borman, S.M., VanDePol, B.J., Kao, S., Thompson, K.E., Sipes, I.G., and Hoyer, P.B. (1999). A single dose of the ovotoxicant 4-vinylcyclohexene diepoxide is protective in rat primary ovarian follicles. Toxicol Appl Pharmacol *158*, 244-252.
Brinton, R.D. (2008). The healthy cell bias of estrogen action: mitochondrial bioenergetics and neurological implications. Trends in neurosciences *31*, 529-537.
Brinton, R.D., Yao, J., Yin, F., Mack, W.J., and Cadenas, E. (2015). Perimenopause as a neurological transition state. Nature Reviews Endocrinology *11*, 393-405.
Brown, R.E. (2012). Improving animal models for nervous system disorders. Genes Brain Behav *11*, 753-756.
Bu, G. (2009). Apolipoprotein E and its receptors in Alzheimer's disease: pathways, pathogenesis and therapy. Nature Reviews Neuroscience *10*, 333.
Burger, Cahir, Robertson, Groome, Dudley, Green, and Dennerstein (1998). Serum Inhibins A and B fall differentially as FSH rises in perimenopausal women. Clinical Endocrinology *48*, 809-813.
Burger, H.G. (2006). Physiology and endocrinology of the menopause. Medicine *34*, 27-30.
Carcaillon, L., Brailly-Tabard, S., Ancelin, M.L., Rouaud, O., Dartigues, J.F., Guiochon-Mantel, A., and Scarabin, P.Y. (2014). High plasma estradiol interacts with diabetes on risk of dementia in older postmenopausal women. Neurology *82*, 504-511.
Castellano, J.M., Kim, J., Stewart, F.R., Jiang, H., DeMattos, R.B., Patterson, B.W., Fagan, A.M., Morris, J.C., Mawuenyega, K.G., and Cruchaga, C. (2011). Human apoE isoforms differentially regulate brain amyloid-β peptide clearance. Science translational medicine *3*, 89ra57-89ra57.
Chakraborty, T.R., and Gore, A.C. (2004). Aging-related changes in ovarian hormones, their receptors, and neuroendocrine function. Exp Biol Med (Maywood) *229*, 977-987.
Chalmers, K., Wilcock, G., and Love, S. (2003). APOEε4 influences the pathological phenotype of Alzheimer's disease by favouring cerebrovascular over parenchymal accumulation of Aβ protein. Neuropathology and applied neurobiology *29*, 231-238.
Chi, O., Barsoum, S., Wen, Y., Liu, X., and Weiss, H. (2004). 17β-estradiol prevents blood-brain barrier disruption induced by VEGF. Hormone and metabolic research *36*, 272-276.
Chi, O., Hunter, C., Liu, X., and Weiss, H. (2005). Effects of 17β-Estradiol on Blood-brain Barrier Disruption in Focal Ischemia during GABAA Receptor Inhibition. Hormone and metabolic research *37*, 209-213.
Chi, O., Liu, X., and Weiss, H. (2002). Effects of 17β-estradiol on blood-brain barrier disruption during focal ischemia in rats. Hormone and metabolic research *34*, 530-534.
Choi, J.M., Romeo, R.D., Brake, W.G., Bethea, C.L., Rosenwaks, Z., and McEwen, B.S. (2003). Estradiol increases pre- and post-synaptic proteins in the CA1 region of the hippocampus in female rhesus macaques (Macaca mulatta). Endocrinology *144*, 4734-4738.

Chornesky, A. (1998). Multicultural perspectives on menopause and the climacteric. Affilia *13*, 31-46.
Christensen, A., and Pike, C.J. (2015). Menopause, obesity and inflammation: interactive risk factors for Alzheimer's disease. Frontiers in Aging Neuroscience *7*.
Clarke, G., Grenham, S., Scully, P., Fitzgerald, P., Moloney, R., Shanahan, F., Dinan, T., and Cryan, J. (2013). The microbiome-gut-brain axis during early life regulates the hippocampal serotonergic system in a sex-dependent manner. Molecular psychiatry *18*, 666.
Cloonan, N., Forrest, A.R., Kolle, G., Gardiner, B.B., Faulkner, G.J., Brown, M.K., Taylor, D.F., Steptoe, A.L., Wani, S., Bethel, G.*, et al.* (2008). Stem cell transcriptome profiling via massive-scale mRNA sequencing. Nat Methods *5*, 613-619.
Colangelo, V., Schurr, J., Ball, M.J., Pelaez, R.P., Bazan, N.G., and Lukiw, W.J. (2002). Gene expression profiling of 12633 genes in Alzheimer hippocampal CA1: transcription and neurotrophic factor down-regulation and up-regulation of apoptotic and pro-inflammatory signaling. Journal of neuroscience research *70*, 462-473.
Colquhoun, D. (2014). An investigation of the false discovery rate and the misinterpretation of p-values. R Soc Open Sci *1*, 140216.
Corder, E.H., Saunders, A.M., Strittmatter, W.J., Schmechel, D.E., Gaskell, P.C., Small, G.W., Roses, A.D., Haines, J.L., and Pericak-Vance, M.A. (1993). Gene dose of apolipoprotein E type 4 allele and the risk of Alzheimer's disease in late onset families. Science *261*, 921-923.
Corlier, F., Hafzalla, G., Faskowitz, J., Kuller, L.H., Becker, J.T., Lopez, O.L., Thompson, P.M., and Braskie, M.N. (2018). Systemic inflammation as a predictor of brain aging: Contributions of physical activity, metabolic risk, and genetic risk. NeuroImage *172*, 118-129.
Cotran, R.S., and Karnovsky, M.J. (1967). Vascular leakage induced by horseradish peroxidase in the rat. Proceedings of the Society for Experimental Biology and Medicine *126*, 557-561.
COTRAN, R.S., KARNOVSKY, M.J., and GOTH, A. (1968). Resistance of Wistar/Furth rats to the mast cell-damaging effect of horseradish peroxidase. Journal of Histochemistry & Cytochemistry *16*, 382-383.
Cramer, S.P., Modvig, S., Simonsen, H.J., Frederiksen, J.L., and Larsson, H.B. (2015). Permeability of the blood–brain barrier predicts conversion from optic neuritis to multiple sclerosis. Brain *138*, 2571-2583.
Crosby, J.R., Seifert, R.A., Soriano, P., and Bowen-Pope, D.F. (1998). Chimaeric analysis reveals role of Pdgf receptors in all muscle lineages. Nature genetics *18*, 385.
Curtis, R.K., Orešič, M., and Vidal-Puig, A. (2005). Pathways to the analysis of microarray data. TRENDS in Biotechnology *23*, 429-435.
D'Andrea, M.R. (2003). Evidence linking neuronal cell death to autoimmunity in Alzheimer's disease. Brain research *982*, 19-30.
D'Andrea, M.R. (2005). Add Alzheimer's disease to the list of autoimmune diseases. Medical hypotheses *64*, 458-463.
Damoiseaux, J.S., Seeley, W.W., Zhou, J., Shirer, W.R., Coppola, G., Karydas, A., Rosen, H.J., Miller, B.L., Kramer, J.H., Greicius, M.D.*, et al.* (2012). Gender modulates the APOE ε4 effect in healthy older adults: convergent evidence from functional brain connectivity and spinal fluid tau levels. J Neurosci *32*, 8254-8262.

Darland, D., and D'amore, P. (2001). TGFβ is required for the formation of capillary-like structures in three-dimensional cocultures of 10T1/2 and endothelial cells. Angiogenesis *4*, 11-20.
Daugherty, D.J., Selvaraj, V., Chechneva, O.V., Liu, X.-B., Pleasure, D.E., and Deng, W. (2013). A TSPO ligand is protective in a mouse model of multiple sclerosis. EMBO Molecular Medicine *5*, 891-903.
Deleidi, M., Jäggle, M., and Rubino, G. (2015). Immune aging, dysmetabolism, and inflammation in neurological diseases. Frontiers in neuroscience *9*, 172.
Dennis, G., Sherman, B.T., Hosack, D.A., Yang, J., Gao, W., Lane, H.C., and Lempicki, R.A. (2003). DAVID: database for annotation, visualization, and integrated discovery. Genome biology *4*, R60.
Diano, S., and Horvath, T.L. (2012). Mitochondrial uncoupling protein 2 (UCP2) in glucose and lipid metabolism. Trends in Molecular Medicine *18*, 52-58.
Diaz Brinton, R. (2012). Minireview: translational animal models of human menopause: challenges and emerging opportunities. Endocrinology *153*, 3571-3578.
Diz-Chaves, Y., Kwiatkowska-Naqvi, A., Von Hulst, H., Pernia, O., Carrero, P., and Garcia-Segura, L.M. (2012). Behavioral effects of estradiol therapy in ovariectomized rats depend on the age when the treatment is initiated. Exp Gerontol *47*, 93-99.
Dohgu, S., Takata, F., Yamauchi, A., Nakagawa, S., Egawa, T., Naito, M., Tsuruo, T., Sawada, Y., Niwa, M., and Kataoka, Y. (2005). Brain pericytes contribute to the induction and up-regulation of blood–brain barrier functions through transforming growth factor-β production. Brain research *1038*, 208-215.
Dohm, J.C., Lottaz, C., Borodina, T., and Himmelbauer, H. (2008). Substantial biases in ultra-short read data sets from high-throughput DNA sequencing. Nucleic Acids Res *36*, e105.
Dorey, E., Bamji-Mirza, M., Najem, D., Li, Y., Liu, H., Callaghan, D., Walker, D., Lue, L.-F., Stanimirovic, D., and Zhang, W. (2017). Apolipoprotein E isoforms differentially regulate Alzheimer's disease and amyloid-β-induced inflammatory response in vivo and in vitro. Journal of Alzheimer's Disease *57*, 1265-1279.
Dorey, E., Chang, N., Liu, Q.Y., Yang, Z., and Zhang, W. (2014). Apolipoprotein E, amyloid-beta, and neuroinflammation in Alzheimer's disease. Neuroscience bulletin *30*, 317-330.
Dorheim, M.-A., Tracey, W.R., Pollock, J.S., and Grammas, P. (1994). Nitric oxide synthase activity is elevated in brain microvessels in Alzheimer′ s disease. Biochemical and biophysical research communications *205*, 659-665.
Downs, J.L., and Wise, P.M. (2009). The role of the brain in female reproductive aging. Mol Cell Endocrinol *299*, 32-38.
Dubal, D.B., Broestl, L., and Worden, K. (2012). Sex and gonadal hormones in mouse models of Alzheimer's disease: what is relevant to the human condition? Biol Sex Differ *3*, 24.
Edelman, D.A., Jiang, Y., Tyburski, J.G., Wilson, R.F., and Steffes, C.P. (2007a). Cytokine production in lipopolysaccharide-exposed rat lung pericytes. Journal of Trauma and Acute Care Surgery *62*, 89-93.
Edelman, D.A., Jiang, Y., Tyburski, J.G., Wilson, R.F., and Steffes, C.P. (2007b). Lipopolysaccharide activation of pericyte's Toll-like receptor-4 regulates co-culture permeability. The American journal of surgery *193*, 730-735.

Emmer, K.M., Russart, K.L., Walker, I., William, H., Nelson, R.J., and DeVries, A.C. (2018). Effects of light at night on laboratory animals and research outcomes. Behavioral neuroscience *132*, 302.
Ennaceur, A. (2010). One-trial object recognition in rats and mice: methodological and theoretical issues. Behavioural brain research *215*, 244-254.
Enninga, E.A.L., Nevala, W.K., Creedon, D.J., Markovic, S.N., and Holtan, S.G. (2015). Fetal Sex-Based Differences in Maternal Hormones, Angiogenic Factors, and Immune Mediators During Pregnancy and the Postpartum Period. Am J Reprod Immunol *73*, 251-262.
Espeland, M.A., Rapp, S.R., Shumaker, S.A., Brunner, R., Manson, J.E., Sherwin, B.B., Hsia, J., Margolis, K.L., Hogan, P.E., Wallace, R.*, et al.* (2004). Conjugated equine estrogens and global cognitive funtion in postmenopausal women: Women's Health Initiative Memory Study. Journal of the American Medical Association *291*, 2959-2968.
Esteras, N., Alquézar, C., Bartolomé, F., Antequera, D., Barrios, L., Carro, E., Cerdán, S., and Martín-Requero, Á. (2012). Systematic evaluation of magnetic resonance imaging and spectroscopy techniques for imaging a transgenic model of Alzheimer's disease (AβPP/PS1). Journal of Alzheimer's Disease *30*, 337-353.
Fairweather, D., Frisancho-Kiss, S., and Rose, N.R. (2008). Sex Differences in Autoimmune Disease from a Pathological Perspective. The American Journal of Pathology *173*, 600-609.
Fan, H., Dong, G., Zhao, G., Liu, F., Yao, G., Zhu, Y., and Hou, Y. (2014). Gender Differences of B Cell Signature in Healthy Subjects Underlie Disparities in Incidence and Course of SLE Related to Estrogen. Journal of Immunology Research *2014*, 1-17.
Farrer, L.A., Cupples, L.A., Haines, J.L., Hyman, B., Kukull, W.A., Mayeux, R., Myers, R.H., Pericak-Vance, M.A., Risch, N., and van Duijn, C.M. (1997a). Effects of age, sex, and ethnicity on the association between apolipoprotein E genotype and Alzheimer disease. A meta-analysis. APOE and Alzheimer Disease Meta Analysis Consortium. JAMA *278*, 1349-1356.
Farrer, L.A., Cupples, L.A., Haines, J.L., Hyman, B., Kukull, W.A., Mayeux, R., Myers, R.H., Pericak-Vance, M.A., Risch, N., and Van Duijn, C.M. (1997b). Effects of age, sex, and ethnicity on the association between apolipoprotein E genotype and Alzheimer disease: A meta-analysis. Journal of the American Medical Association *278*, 1349-1356.
Fatica, A., and Bozzoni, I. (2014). Long non-coding RNAs: new players in cell differentiation and development. Nature Reviews Genetics *15*, 7.
Felger, J.C., Haroon, E., Patel, T.A., Goldsmith, D.R., Wommack, E.C., Woolwine, B.J., Le, N.A., Feinberg, R., Tansey, M.G., and Miller, A.H. (2018). What does plasma CRP tell us about peripheral and central inflammation in depression? Mol Psychiatry.
Festoff, B.W., Sajja, R.K., van Dreden, P., and Cucullo, L. (2016). HMGB1 and thrombin mediate the blood-brain barrier dysfunction acting as biomarkers of neuroinflammation and progression to neurodegeneration in Alzheimer's disease. Journal of Neuroinflammation *13*, 194.
Fiala, M., Liu, Q., Sayre, J., Pop, V., Brahmandam, V., Graves, M., and Vinters, H. (2002). Cyclooxygenase-2-positive macrophages infiltrate the Alzheimer's disease brain and damage the blood–brain barrier. European journal of clinical investigation *32*, 360-371.
Finch, C.E. (2014). The menopause and aging, a comparative perspective. The Journal of Steroid Biochemistry and Molecular Biology *142*, 132-141.
Finch, C.E., Felicio, L.S., Mobbs, C.V., and Nelson, J.F. (1984). Ovarian and steroidal influences on neuroendocrine aging processes in female rodents. Endocr Rev *5*, 467-497.

Fischer, V., Siddiqi, A., and Yusufaly, Y. (1990). Altered angioarchitecture in selected areas of brains with Alzheimer's disease. Acta neuropathologica *79*, 672-679.
Flaws, J.A., Doerr, J.K., Sipes, I.G., and Hoyer, P.B. (1994). Destruction of preantral follicles in adult rats by 4-vinyl-1-cyclohexene diepoxide. Reprod Toxicol *8*, 509-514.
Fleisher, A.S., Sun, S., Taylor, C., Ward, C.P., Gamst, A.C., Petersen, R.C., Jack, C.R., Aisen, P.S., and Thal, L.J. (2008). Volumetric MRI vs clinical predictors of Alzheimer disease in mild cognitive impairment. Neurology *70*, 191-199.
Foster, T.C., Sharrow, K.M., Kumar, A., and Masse, J. (2003). Interaction of age and chronic estradiol replacement on memory and markers of brain aging. Neurobiol Aging *24*, 839-852.
Fredriksson, L., Li, H., and Eriksson, U. (2004). The PDGF family: four gene products form five dimeric isoforms. Cytokine & Growth Factor Reviews *15*, 197-204.
Fung, A., Vizcaychipi, M., Lloyd, D., Wan, Y., and Ma, D. (2012). Central nervous system inflammation in disease related conditions: mechanistic prospects. Brain research *1446*, 144-155.
Gaceb, A., Özen, I., Padel, T., Barbariga, M., and Paul, G. (2018). Pericytes secrete pro-regenerative molecules in response to platelet-derived growth factor-BB. Journal of Cerebral Blood Flow & Metabolism *38*, 45-57.
Gammal, E., and Zuk, A. (1980). Effect of ethinyl estradiol on endothelial permeability to 125I-labeled albumin in female rats. Experimental and molecular pathology *32*, 91-101.
Genazzani, A.R., Bernardi, F., Pluchino, N., Begliuomini, S., Lenzi, E., Casarosa, E., and Luisi, M. (2005). Endocrinology of menopausal transition and its brain implications. CNS spectrums *10*, 449-457.
Genin, E., Hannequin, D., Wallon, D., Sleegers, K., Hiltunen, M., Combarros, O., Bullido, M.J., Engelborghs, S., De Deyn, P., Berr, C*., et al.* (2011). APOE and Alzheimer disease: a major gene with semi-dominant inheritance. Mol Psychiatry *16*, 903-907.
Gerhard, D.S., Wagner, L., Feingold, E.A., Shenmen, C.M., Grouse, L.H., Schuler, G., Klein, S.L., Old, S., Rasooly, R., Good, P*., et al.* (2004). The status, quality, and expansion of the NIH full-length cDNA project: the Mammalian Gene Collection (MGC). Genome Res *14*, 2121-2127.
Giménez-Llort, L., Arranz, L., Maté, I., and De la Fuente, M. (2008). Gender-specific neuroimmunoendocrine aging in a triple-transgenic 3× Tg-AD mouse model for Alzheimer's disease and its relation with longevity. Neuroimmunomodulation *15*, 331-343.
Giron-Gonzalez, J., Moral, F., Elvira, J., Garcia-Gil, D., Guerrero, F., Gavilan, I., and Escobar, L. (2000). Consistent production of a higher TH1:TH2 cytokine ratio by stimulated T cells in men compared with women. European Journal of Endocrinology *143*, 31-36.
Gleason, C.E., Dowling, N.M., Wharton, W., Manson, J.E., Miller, V.M., Atwood, C.S., Brinton, E.A., Cedars, M.I., Lobo, R.A., Merriam, G.R*., et al.* (2015). Effects of Hormone Therapy on Cognition and Mood in Recently Postmenopausal Women: Findings from the Randomized, Controlled KEEPS–Cognitive and Affective Study. PLOS Medicine *12*, e1001833.
Gong, C., Wei, D., Wang, Y., Ma, J., Yuan, C., Zhang, W., Yu, G., and Zhao, Y. (2016). A meta-analysis of C-reactive protein in patients with Alzheimer's disease. American Journal of Alzheimer's Disease & Other Dementias® *31*, 194-200.
Grammas, P., Martinez, J., and Miller, B. (2011). Cerebral microvascular endothelium and the pathogenesis of neurodegenerative diseases. Expert reviews in molecular medicine *13*.

Greendale, G.A., Wight, R.G., Huang, M.-H., Avis, N., Gold, E.B., Joffe, H., Seeman, T., Vuge, M., and Karlamangla, A.S. (2010). Menopause-associated symptoms and cognitive performance: results from the study of women's health across the nation. American journal of epidemiology *171*, 1214-1224.
Griesbeck, M., Ziegler, S., Laffont, S., Smith, N., Chauveau, L., Tomezsko, P., Sharei, A., Kourjian, G., Porichis, F., and Hart, M. (2015). Sex differences in plasmacytoid dendritic cell levels of IRF5 drive higher IFN-α production in women. The Journal of Immunology, 1501684.
Grytten, N., Aarseth, J.H., Lunde, H.M.B., and Myhr, K.M. (2015). A 60-year follow-up of the incidence and prevalence of multiple sclerosis in Hordaland County, Western Norway. Journal of Neurology, Neurosurgery & Psychiatry, jnnp-2014-309906.
Gulinello, M., and Etgen, A.M. (2005). Sexually dimorphic hormonal regulation of the gap junction protein, CX43, in rats and altered female reproductive function in CX43+/− mice. Brain research *1045*, 107-115.
Guo, J., Xu, N., Li, Z., Zhang, S., Wu, J., Kim, D.H., Sano Marma, M., Meng, Q., Cao, H., Li, X.*, et al.* (2008). Four-color DNA sequencing with 3'-O-modified nucleotide reversible terminators and chemically cleavable fluorescent dideoxynucleotides. Proc Natl Acad Sci U S A *105*, 9145-9150.
Haines, B.A., Mehta, S.L., Pratt, S.M., Warden, C.H., and Li, P.A. (2010). Deletion of mitochondrial uncoupling protein-2 increases ischemic brain damage after transient focal ischemia by altering gene expression patterns and enhancing inflammatory cytokines. Journal of Cerebral Blood Flow & Metabolism *30*, 1825-1833.
Hall, A.O.H., Beiting, D.P., Tato, C., John, B., Oldenhove, G., Lombana, C.G., Pritchard, G.H., Silver, J.S., Bouladoux, N., and Stumhofer, J.S. (2012). The cytokines interleukin 27 and interferon-γ promote distinct Treg cell populations required to limit infection-induced pathology. immunity *37*, 511-523.
Halliday, M.R., Pomara, N., Sagare, A.P., Mack, W.J., Frangione, B., and Zlokovic, B.V. (2013). Relationship between cyclophilin a levels and matrix metalloproteinase 9 activity in cerebrospinal fluid of cognitively normal apolipoprotein e4 carriers and blood-brain barrier breakdown. JAMA Neurology *70*, 1198-1200.
Halliday, M.R., Rege, S.V., Ma, Q., Zhao, Z., Miller, C.A., Winkler, E.A., and Zlokovic, B.V. (2016). Accelerated pericyte degeneration and blood–brain barrier breakdown in apolipoprotein E4 carriers with Alzheimer's disease. Journal of Cerebral Blood Flow & Metabolism *36*, 216-227.
Hannah, M.F., Bajic, V.B., and Klein, S.L. (2008). Sex differences in the recognition of and innate antiviral responses to Seoul virus in Norway rats. Brain, behavior, and immunity *22*, 503-516.
Hass, D.T., and Barnstable, C.J. (2016). Uncoupling protein 2 in the glial response to stress: implications for neuroprotection. Neural regeneration research *11*, 1197.
Hawkins, B.T., and Davis, T.P. (2005). The blood-brain barrier/neurovascular unit in health and disease. Pharmacological reviews *57*, 173-185.
He, J., Evans, C.-O., Hoffman, S.W., Oyesiku, N.M., and Stein, D.G. (2004). Progesterone and allopregnanolone reduce inflammatory cytokines after traumatic brain injury. Experimental neurology *189*, 404-412.
Hellström, M., Gerhardt, H., Kalén, M., Li, X., Eriksson, U., Wolburg, H., and Betsholtz, C. (2001). Lack of pericytes leads to endothelial hyperplasia and abnormal vascular morphogenesis. The Journal of cell biology *153*, 543-554.

Henderson, V.W., and Brinton, R.D. (2010). Menopause and mitochondria: windows into estrogen effects on Alzheimer's disease risk and therapy. Prog Brain Res *182*, 77-96.
Henderson, V.W., St John, J.A., Hodis, H.N., McCleary, C.A., Stanczyk, F.Z., Shoupe, D., Kono, N., Dustin, L., Allayee, H., and Mack, W.J. (2016). Cognitive effects of estradiol after menopause. Neurology *87*, 699-708.
Hermes, G., Nagy, D., Waterson, M., Zsarnovszky, A., Varela, L., Hajos, M., and Horvath, T.L. (2016). Role of mitochondrial uncoupling protein-2 (UCP2) in higher brain functions, neuronal plasticity and network oscillation. Molecular Metabolism *5*, 415-421.
Hewagama, A., Patel, D., Yarlagadda, S., Strickland, F.M., and Richardson, B.C. (2009). Stronger inflammatory/cytotoxic T-cell response in women identified by microarray analysis. Genes & Immunity *10*, 509-516.
Heywood, L. (1980). Testosterone levels in the male laboratory rat: variation under experimental conditions. International journal of Andrology *3*, 519-529.
Hill, B.G., Dranka, B.P., Zou, L., Chatham, J.C., and Darley-Usmar, V.M. (2009). Importance of the bioenergetic reserve capacity in response to cardiomyocyte stress induced by 4-hydroxynonenal. Biochemical Journal *424*, 99-107.
Hirshfield, A.N. (1991). Development of follicles in the mammalian ovary. Int Rev Cytol *124*, 43-101.
Holtzman, D.M., Herz, J., and Bu, G. (2012). Apolipoprotein E and apolipoprotein E receptors: normal biology and roles in Alzheimer disease. Cold Spring Harbor perspectives in medicine, a006312.
Hoyer, P.B., Devine, P.J., Hu, X., Thompson, K.E., and Sipes, I.G. (2001). Ovarian toxicity of 4-vinylcyclohexene diepoxide: a mechanistic model. Toxicol Pathol *29*, 91-99.
Hoyer, S. (1991). Abnormalities of glucose metabolism in Alzheimer's disease. Annals of the New York Academy of Sciences *640*, 53-58.
Hsuchou, H., Kastin, A.J., Mishra, P.K., and Pan, W. (2012). C-reactive protein increases BBB permeability: implications for obesity and neuroinflammation. Cellular physiology and biochemistry *30*, 1109-1119.
Hu, X., Christian, P., Sipes, I.G., and Hoyer, P.B. (2001a). Expression and redistribution of cellular Bad, Bax, and Bcl-X(L) protein is associated with VCD-induced ovotoxicity in rats. Biol Reprod *65*, 1489-1495.
Hu, X., Christian, P.J., Thompson, K.E., Sipes, I.G., and Hoyer, P.B. (2001b). Apoptosis induced in rats by 4-vinylcyclohexene diepoxide is associated with activation of the caspase cascades. Biol Reprod *65*, 87-93.
Huang, D.W., Sherman, B.T., and Lempicki, R.A. (2008a). Bioinformatics enrichment tools: paths toward the comprehensive functional analysis of large gene lists. Nucleic acids research *37*, 1-13.
Huang, D.W., Sherman, B.T., and Lempicki, R.A. (2008b). Systematic and integrative analysis of large gene lists using DAVID bioinformatics resources. Nature protocols *4*, 44.
Huang, Y., and Mucke, L. (2012). Alzheimer mechanisms and therapeutic strategies. Cell *148*, 1204-1222.
Huber, M., Steinwald, V., Guralnik, A., Brüstle, A., Kleemann, P., Rosenplänter, C., Decker, T., and Lohoff, M. (2007). IL-27 inhibits the development of regulatory T cells via STAT3. International immunology *20*, 223-234.
Hultman, K., Strickland, S., and Norris, E.H. (2013). The APOE ε4/ε4 genotype potentiates vascular fibrin (ogen) deposition in amyloid-laden vessels in the brains of Alzheimer's disease patients. Journal of Cerebral Blood Flow & Metabolism *33*, 1251-1258.

Humphreys, G.I., Ziegler, Y.S., and Nardulli, A.M. (2014). 17β-estradiol modulates gene expression in the female mouse cerebral cortex. PloS one *9*, e111975.
Hunter, C., and Kastelein, R. (2012a). Fifteen years of interleukin-27-discovery, advances and translation. Immunity *37*, 960.
Hunter, C.A., and Kastelein, R. (2012b). Interleukin-27: balancing protective and pathological immunity. Immunity *37*, 960-969.
Iadecola, C. (2004). Neurovascular regulation in the normal brain and in Alzheimer's disease. Nature Reviews Neuroscience *5*, 347.
Inoue, K., Tsutsui, H., Akatsu, H., Hashizume, Y., Matsukawa, N., Yamamoto, T., and Toyo'Oka, T. (2013). Metabolic profiling of Alzheimer's disease brains. Scientific reports *3*, 2364.
Irwin, R.W., and Brinton, R.D. (2014). Allopregnanolone as regenerative therapeutic for Alzheimer's disease: translational development and clinical promise. Prog Neurobiol *113*, 40-55.
Ishii, K., Sasaki, M., Kitagaki, H., Yamaji, S., Sakamoto, S., Matsuda, K., and Mori, E. (1997). Reduction of cerebellar glucose metabolism in advanced Alzheimer's disease. Journal of Nuclear Medicine *38*, 925-928.
Ishrat, T., Sayeed, I., Atif, F., Hua, F., and Stein, D.G. (2010). Progesterone and allopregnanolone attenuate blood–brain barrier dysfunction following permanent focal ischemia by regulating the expression of matrix metalloproteinases. Experimental neurology *226*, 183-190.
Jellinger, K. (2002). Alzheimer disease and cerebrovascular pathology: an update. Journal of neural transmission *109*, 813-836.
Jiang, X., Andjelkovic, A.V., Zhu, L., Yang, T., Bennett, M.V.L., Chen, J., Keep, R.F., and Shi, Y. (2018). Blood-brain barrier dysfunction and recovery after ischemic stroke. Progress in Neurobiology *163-164*, 144-171.
Jucker, M. (2010). The benefits and limitations of animal models for translational research in neurodegenerative diseases. Nat Med *16*, 1210-1214.
Kao, S.W., Sipes, I.G., and Hoyer, P.B. (1999). Early effects of ovotoxicity induced by 4-vinylcyclohexene diepoxide in rats and mice. Reprod Toxicol *13*, 67-75.
Kaplan, J.R., Chen, H., Appt, S.E., Lees, C.J., Franke, A.A., Berga, S.L., Wilson, M.E., Manuck, S.B., and Clarkson, T.B. (2010). Impairment of ovarian function and associated health-related abnormalities are attributable to low social status in premenopausal monkeys and not mitigated by a high-isoflavone soy diet. Hum Reprod *25*, 3083-3094.
Kappos, L., Hardmeier, M., Gugleta, K., Ecsedi, M., Kappos, L., and Disanto, G. (2015). A 10-year follow-up of the European multicenter trial of interferon β-1b in secondary-progressive multiple sclerosis.
Kaya, M., and Ahishali, B. (2011). Assessment of permeability in barrier type of endothelium in brain using tracers: Evans blue, sodium fluorescein, and horseradish peroxidase. In Permeability Barrier (Springer), pp. 369-382.
Kermath, B.A., and Gore, A.C. (2012). Neuroendocrine control of the transition to reproductive senescence: lessons learned from the female rodent model. Neuroendocrinology *96*, 1-12.
Khan-Dawood, F., Yang, J., and Dawood, M. (1996). Localization and expression of zonula occludens-1 tight junction-associated protein in baboon (Papio anubis) corpora lutea. Human reproduction *11*, 1262-1267.
Khatri, P., and Drăghici, S. (2005). Ontological analysis of gene expression data: current tools, limitations, and open problems. Bioinformatics *21*, 3587-3595.

Kim, D., Pertea, G., Trapnell, C., Pimentel, H., Kelley, R., and Salzberg, S.L. (2013a). TopHat2: accurate alignment of transcriptomes in the presence of insertions, deletions and gene fusions. Genome Biol *14*, R36.
Kim, G., Shinnakasu, R., Saris, C.J., Cheroutre, H., and Kronenberg, M. (2013b). A novel role for IL-27 in mediating the survival of activated mouse CD4 T lymphocytes. The Journal of Immunology, 1201017.
Klein, S.L., and Flanagan, K.L. (2016). Sex differences in immune responses. Nature Reviews Immunology *16*, 626.
Kodzius, R., Kojima, M., Nishiyori, H., Nakamura, M., Fukuda, S., Tagami, M., Sasaki, D., Imamura, K., Kai, C., Harbers, M*., et al.* (2006). CAGE: cap analysis of gene expression. Nat Methods *3*, 211-222.
Koebele, S.V., and Bimonte-Nelson, H.A. (2016). Modeling menopause: The utility of rodents in translational behavioral endocrinology research. Maturitas *87*, 5-17.
Kozler, P., and Pokorny, J. (2003). Altered blood-brain barrier permeability and its effect on the distribution of Evans blue and sodium fluorescein in the rat brain applied by intracarotid injection. Physiol Res *52*, 607-614.
Krämer, A., Green, J., Pollard Jr, J., and Tugendreich, S. (2013). Causal analysis approaches in ingenuity pathway analysis. Bioinformatics *30*, 523-530.
LaRochelle, W.J., Jeffers, M., McDonald, W.F., Chillakuru, R.A., Giese, N.A., Lokker, N.A., Sullivan, C., Boldog, F.L., Yang, M., and Vernet, C. (2001). PDGF-D, a new protease-activated growth factor. Nature cell biology *3*, 517.
Laughlin, G.A., Kritz-Silverstein, D., and Barrett-Connor, E. (2010). Endogenous oestrogens predict 4-year decline in verbal fluency in postmenopausal women: The Rancho Bernardo Study. Clinical Endocrinology *72*, 99-106.
Lee, B.W., Yap, H.K., Chew, F.T., Quah, T.C., Prabhakaran, K., Chan, G.S., Wong, S.C., and Seah, C.C. (1996). Age- and sex-related changes in lymphocyte subpopulations of healthy Asian subjects: from birth to adulthood. Cytometry *26*, 8-15.
Lee, C.-K., Weindruch, R., and Prolla, T.A. (2000). Gene-expression profile of the ageing brain in mice. Nature genetics *25*, 294.
Leger, M., Quiedeville, A., Bouet, V., Haelewyn, B., Boulouard, M., Schumann-Bard, P., and Freret, T. (2013). Object recognition test in mice. Nat Protoc *8*, 2531-2537.
Leung, L., Andrews-Zwilling, Y., Yoon, S.Y., Jain, S., Ring, K., Dai, J., Wang, M.M., Tong, L., Walker, D., and Huang, Y. (2012). Apolipoprotein E4 causes age- and sex-dependent impairments of hilar GABAergic interneurons and learning and memory deficits in mice. PLoS One *7*, e53569.
Lewis, S.E. (2017). The vision and challenges of the gene ontology. In The Gene Ontology Handbook (Springer), pp. 291-302.
Li, F., Wang, Y., Yu, L., Cao, S., Wang, K., Yuan, J., Wang, C., Wang, K., Cui, M., and Fu, Z.F. (2015). Viral infection of the Central Nervous System and neuroinflammation precede Blood Brain Barrier disruption during Japanese Encephalitis. Journal of virology, JVI. 00143-00115.
Li, G., Bien-Ly, N., Andrews-Zwilling, Y., Xu, Q., Bernardo, A., Ring, K., Halabisky, B., Deng, C., Mahley, R.W., and Huang, Y. (2009). GABAergic interneuron dysfunction impairs hippocampal neurogenesis in adult apolipoprotein E4 knockin mice. Cell Stem Cell *5*, 634-645.
Lindahl, P., Johansson, B.R., Levéen, P., and Betsholtz, C. (1997). Pericyte loss and microaneurysm formation in PDGF-B-deficient mice. Science *277*, 242-245.

Lisse, I.M., Aaby, P., Whittle, H., Jensen, H., Engelmann, M., and Christensen, L.B. (1997). T-lymphocyte subsets in West African children: impact of age, sex, and season. The Journal of Pediatrics *130*, 77-85.
Liu, C.C., Kanekiyo, T., Xu, H., and Bu, G. (2013). Apolipoprotein e and Alzheimer disease: Risk, mechanisms and therapy. Nature Reviews Neurology *9*, 106-118.
Liu, S., Liu, Y., Hao, W., Wolf, L., Kiliaan, A.J., Penke, B., Rübe, C.E., Walter, J., Heneka, M.T., and Hartmann, T. (2012). TLR2 is a primary receptor for Alzheimer's amyloid β peptide to trigger neuroinflammatory activation. The Journal of Immunology *188*, 1098-1107.
Louveau, A., Smirnov, I., Keyes, T.J., Eccles, J.D., Rouhani, S.J., Peske, J.D., Derecki, N.C., Castle, D., Mandell, J.W., and Lee, K.S. (2015). Structural and functional features of central nervous system lymphatic vessels. Nature *523*, 337.
Loy, C.T., Schofield, P.R., Turner, A.M., and Kwok, J.B. (2014). Genetics of dementia. The Lancet *383*, 828-840.
Lu, K.H., Hopper, B.R., Vargo, T.M., and Yen, S.S. (1979). Chronological changes in sex steroid, gonadotropin and prolactin secretions in aging female rats displaying different reproductive states. Biol Reprod *21*, 193-203.
Lustbader, J.W., Cirilli, M., Lin, C., Xu, H.W., Takuma, K., Wang, N., Caspersen, C., Chen, X., Pollak, S., and Chaney, M. (2004). ABAD directly links Aß to mitochondrial toxicity in Alzheimer's Disease. Science *304*, 448-452.
Ma, Q., Huang, B., Khatibi, N., Rolland, W., Suzuki, H., Zhang, J.H., and Tang, J. (2011). PDGFR-α Inhibition Preserves Blood-Brain Barrier after Intracerebral Hemorrhage. Annals of neurology *70*, 920-931.
Ma, S., Ma, L., Yang, D., Luo, Z., Hao, X., Liu, D., and Zhu, Z. (2010). Uncoupling protein 2 ablation exacerbates high-salt intake-induced vascular dysfunction. American journal of hypertension *23*, 822-828.
Ma, S., Wang, Q., Zhang, Y., Yang, D., Li, D., Tang, B., and Yang, Y. (2013). Transgenic overexpression of uncoupling protein 2 attenuates salt-induced vascular dysfunction by inhibition of oxidative stress. American journal of hypertension *27*, 345-354.
Ma, S., Zhang, Y., Wang, Q., Yang, D., Tang, B., and Yang, Y. (2014). Ablation of uncoupling protein 2 exacerbates salt-induced cardiovascular and renal remodeling associated with enhanced oxidative stress. International journal of cardiology *175*, 206-210.
Maddaluno, L., Rudini, N., Cuttano, R., Bravi, L., Giampietro, C., Corada, M., Ferrarini, L., Orsenigo, F., Papa, E., and Boulday, G. (2013). EndMT contributes to the onset and progression of cerebral cavernous malformations. Nature *498*, 492.
Maftei, M., Thurm, F., Schnack, C., Tumani, H., Otto, M., Elbert, T., Kolassa, I.-T., Przybylski, M., Manea, M., and von Arnim, C.A. (2013). Increased levels of antigen-bound β-amyloid autoantibodies in serum and cerebrospinal fluid of Alzheimer's disease patients. PLoS One *8*, e68996.
Maggioli, E., McArthur, S., Mauro, C., Kieswich, J., Kusters, D., Reutelingsperger, C., Yaqoob, M., and Solito, E. (2016). Estrogen protects the blood–brain barrier from inflammation-induced disruption and increased lymphocyte trafficking. Brain, behavior, and immunity *51*, 212-222.
Majno, G., Palade, G., and Schoefl, G.I. (1961). Studies on inflammation: II. The site of action of histamine and serotonin along the vascular tree: A topographic study. The Journal of Cell Biology *11*, 607-626.

Maki, P.M., Drogos, L.L., Rubin, L.H., Banuvar, S., Shulman, L.P., and Geller, S.E. (2008). Objective hot flashes are negatively related to verbal memory performance in midlife women. Menopause (New York, NY) *15*, 848.
Maki, P.M., and Henderson, V.W. (2016). Cognition and the menopause transition. Menopause *23*, 803-805.
Malutan, A.M., Dan, M., Nicolae, C., and Carmen, M. (2014). Proinflammatory and anti-inflammatory cytokine changes related to menopause. Przegląd Menopauzalny = Menopause Review *13*, 162-168.
Masdeu, J.C., Kreisl, W.C., and Berman, K.F. (2012). The neurobiology of Alzheimer disease defined by neuroimaging. Current opinion in neurology *25*, 410-420.
Mattiasson, G., Shamloo, M., Gido, G., Mathi, K., Tomasevic, G., Yi, S., Warden, C.H., Castilho, R.F., Melcher, T., and Gonzalez-Zulueta, M. (2003). Uncoupling protein-2 prevents neuronal death and diminishes brain dysfunction after stroke and brain trauma. Nature medicine *9*, 1062.
Mayer, L.P., Devine, P.J., Dyer, C.A., and Hoyer, P.B. (2004). The follicle-deplete mouse ovary produces androgen. Biol Reprod *71*, 130-138.
Mayer, L.P., Dyer, C.A., Eastgard, R.L., Hoyer, P.B., and Banka, C.L. (2005). Atherosclerotic lesion development in a novel ovary-intact mouse model of perimenopause. Arterioscler Thromb Vasc Biol *25*, 1910-1916.
Mayer, L.P., Pearsall, N.A., Christian, P.J., Devine, P.J., Payne, C.M., McCuskey, M.K., Marion, S.L., Sipes, I.G., and Hoyer, P.B. (2002). Long-term effects of ovarian follicular depletion in rats by 4-vinylcyclohexene diepoxide. Reprod Toxicol *16*, 775-781.
Mazariegos, M.R., Tice, L.W., and Hand, A.R. (1984). Alteration of tight junctional permeability in the rat parotid gland after isoproterenol stimulation. The Journal of cell biology *98*, 1865-1877.
McCombe, P.A., Greer, J.M., and Mackay, I.R. (2009). Sexual dimorphism in autoimmune disease. Current molecular medicine *9*, 1058-1079.
McKinlay, S.M., Brambilla, D.J., and Posner, J.G. (1992). The normal menopause transition. Maturitas *14*, 103-115.
Meyer, V. (2003). Medicalized menopause, US style. Health care for women international *24*, 822-830.
Mi, H., Muruganujan, A., Casagrande, J.T., and Thomas, P.D. (2013). Large-scale gene function analysis with the PANTHER classification system. Nature protocols *8*, 1551.
Michaud, M., Balardy, L., Moulis, G., Gaudin, C., Peyrot, C., Vellas, B., Cesari, M., and Nourhashemi, F. (2013). Proinflammatory cytokines, aging, and age-related diseases. Journal of the American Medical Directors Association *14*, 877-882.
Minami, T., Sakita, Y., Ichida, S., and Dohi, Y. (2002). Gender difference regarding selenium penetration into the mouse brain. Biological trace element research *89*, 85-93.
Moon, S.-J., Park, J.-S., Heo, Y.-J., Kang, C.-M., Kim, E.-K., Lim, M.-A., Ryu, J.-G., Park, S.J., Park, K.S., and Sung, Y.-C. (2013). In vivo action of IL-27: reciprocal regulation of Th17 and Treg cells in collagen-induced arthritis. Experimental & molecular medicine *45*, e46.
Morin, R., Bainbridge, M., Fejes, A., Hirst, M., Krzywinski, M., Pugh, T., McDonald, H., Varhol, R., Jones, S., and Marra, M. (2008). Profiling the HeLa S3 transcriptome using randomly primed cDNA and massively parallel short-read sequencing. Biotechniques *45*, 81-94.
Morrison, J.H., and Baxter, M.G. (2012). The ageing cortical synapse: hallmarks and implications for cognitive decline. Nat Rev Neurosci *13*, 240-250.

Mortazavi, A., Williams, B.A., McCue, K., Schaeffer, L., and Wold, B. (2008). Mapping and quantifying mammalian transcriptomes by RNA-Seq. Nature methods *5*, 621.
Mosconi, L., Berti, V., Guyara-Quinn, C., McHugh, P., Petrongolo, G., Osorio, R.S., Connaughty, C., Pupi, A., Vallabhajosula, S., Isaacson, R.S.*, et al.* (2017). Perimenopause and emergence of an Alzheimer's bioenergetic phenotype in brain and periphery. PLOS ONE *12*, e0185926.
Moukdar, F., Robidoux, J., Lyght, O., Pi, J., Daniel, K.W., and Collins, S. (2009). Reduced antioxidant capacity and diet-induced atherosclerosis in uncoupling protein-2-deficient mice. Journal of lipid research *50*, 59-70.
Naderi, V., Khaksari, M., Abbasi, R., and Maghool, F. (2015). Estrogen provides neuroprotection against brain edema and blood brain barrier disruption through both estrogen receptors α and β following traumatic brain injury. Iranian Journal of Basic Medical Sciences *18*, 138-144.
Nagalakshmi, U., Wang, Z., Waern, K., Shou, C., Raha, D., Gerstein, M., and Snyder, M. (2008). The transcriptional landscape of the yeast genome defined by RNA sequencing. Science *320*, 1344-1349.
Nakao, K., Yasoda, A., Ebihara, K., Hosoda, K., and Mukoyama, M. (2009). Translational research of novel hormones: lessons from animal models and rare human diseases for common human diseases. J Mol Med (Berl) *87*, 1029-1039.
National Toxicology, P. (1989). Toxicology and Carcinogenesis Studies of 4-Vinyl-1-cyclohexene Diepoxide (CAS No. 106-87-6) in F344/N Rats and B6C3F1 Mice (Dermal Studies). Natl Toxicol Program Tech Rep Ser *362*, 1-249.
Nelson, H.D. (2008). Menopause. Lancet *371*, 760-770.
Neufert, C., Becker, C., Wirtz, S., Fantini, M.C., Weigmann, B., Galle, P.R., and Neurath, M.F. (2007). IL-27 controls the development of inducible regulatory T cells and Th17 cells via differential effects on STAT1. European journal of immunology *37*, 1809-1816.
Newcombe, E.A., Camats-Perna, J., Silva, M.L., Valmas, N., Huat, T.J., and Medeiros, R. (2018). Inflammation: the link between comorbidities, genetics, and Alzheimer's disease. Journal of Neuroinflammation *15*, 276.
Newhart, M.R. (2013). Menopause matters: The implications of menopause research for studies of midlife health. Health Sociology Review *22*, 365-376.
Nishino, H., Nakajima, K., Kumazaki, M., Fukuda, A., Muramatsu, K., Deshpande, S.B., Inubushi, T., Morikawa, S., Borlongan, C.V., and Sanberg, P.R. (1998). Estrogen protects against while testosterone exacerbates vulnerability of the lateral striatal artery to chemical hypoxia by 3-nitropropionic acid. Neuroscience research *30*, 303-312.
Nishioku, T., Dohgu, S., Takata, F., Eto, T., Ishikawa, N., Kodama, K.B., Nakagawa, S., Yamauchi, A., and Kataoka, Y. (2009). Detachment of brain pericytes from the basal lamina is involved in disruption of the blood–brain barrier caused by lipopolysaccharide-induced sepsis in mice. Cellular and molecular neurobiology *29*, 309-316.
Noorbakhsh, F., Baker, G.B., and Power, C. (2014). Allopregnanolone and neuroinflammation: a focus on multiple sclerosis. Frontiers in cellular neuroscience *8*, 134.
Normoyle, K.P., Kim, M., Farahvar, A., Llano, D., Jackson, K., and Wang, H. (2015). The emerging neuroprotective role of mitochondrial uncoupling protein-2 in traumatic brain injury. Translational neuroscience *6*.
Nwabuisi-Heath, E., Rebeck, G.W., LaDu, M.J., and Yu, C. (2013). ApoE4 delays dendritic spine formation during neuron development and accelerates loss of mature spines in vitro. ASN neuro *6*, AN20130043.

Okoniewski, M.J., and Miller, C.J. (2006). Hybridization interactions between probesets in short oligo microarrays lead to spurious correlations. BMC Bioinformatics *7*, 276.
Olson, M.E., and Bruce, J. (1986). Ovariectomy, ovariohysterectomy and orchidectomy in rodents and rabbits. Can Vet J *27*, 523-527.
Oztaş, B., Kocak, H., Oner, P., and Küçük, M. (2000). Sex-dependent changes in blood-brain barrier permeability and brain NA (+), K (+) ATPase activity in rats following acute water intoxication. Journal of neuroscience research *62*, 750-753.
Pakulski, C., Drobnik, L., and Millo, B. (2000). Age and sex as factors modifying the function of the blood-cerebrospinal fluid barrier. Medical Science Monitor *6*, 314-318.
Pan, X., Nasaruddin, M.B., Elliott, C.T., McGuinness, B., Passmore, A.P., Kehoe, P.G., Hölscher, C., McClean, P.L., Graham, S.F., and Green, B.D. (2016). Alzheimer's disease–like pathology has transient effects on the brain and blood metabolome. Neurobiology of Aging *38*, 151-163.
Paris, J.J., Walf, A.A., and Frye, C.A. (2011). II. Cognitive performance of middle-aged female rats is influenced by capacity to metabolize progesterone in the prefrontal cortex and hippocampus. Brain research *1379*, 149-163.
Peppercorn, M.A. (2014). Definition, Epidemiology, and Risk Factors in Inflammatory Bowel Disease (UpToDate [Internet].).
Pfefferbaum, A., Rohlfing, T., Rosenbloom, M.J., Chu, W., Colrain, I.M., and Sullivan, E.V. (2013). Variation in longitudinal trajectories of regional brain volumes of healthy men and women (ages 10 to 85years) measured with atlas-based parcellation of MRI. NeuroImage *65*, 176-193.
Pisitkun, P., Deane, J.A., Difilippantonio, M.J., Tarasenko, T., Satterthwaite, A.B., and Bolland, S. (2006). Autoreactive B cell responses to RNA-related antigens due to TLR7 gene duplication. Science *312*, 1669-1672.
Piterkin, P., Cole, E., Cossette, M.-P., Gaskin, S., and Mumby, D.G. (2008). A limited role for the hippocampus in the modulation of novel-object preference by contextual cues. Learning & Memory *15*, 785-791.
Prelog, M. (2006). Aging of the immune system: a risk factor for autoimmunity? Autoimmunity reviews *5*, 136-139.
Qureshi, I.A., and Mehler, M.F. (2012). Emerging roles of non-coding RNAs in brain evolution, development, plasticity and disease. Nature Reviews Neuroscience *13*, 528.
Ramanan, V.K., Shen, L., Moore, J.H., and Saykin, A.J. (2012). Pathway analysis of genomic data: concepts, methods, and prospects for future development. TRENDS in Genetics *28*, 323-332.
Raub, T.J., Kuentzel, S.L., and Sawada, G.A. (1992). Permeability of bovine brain microvessel endothelial cells in vitro: barrier tightening by a factor released from astroglioma cells. Experimental cell research *199*, 330-340.
Reddy, P.H., and Beal, M.F. (2008). Amyloid beta, mitochondrial dysfunction and synaptic damage: implications for cognitive decline in aging and Alzheimer's disease. Trends in molecular medicine *14*, 45-53.
Reid, A., Teasdale, G., and McCulloch, J. (1983). Hormonal influence on water permeability across the blood-brain barrier. Clinical and experimental neurology *19*, 50-53.
Rettberg, J.R., Dang, H., Hodis, H.N., Henderson, V.W., St. John, J.A., Mack, W.J., and Brinton, R.D. (2016). Identifying postmenopausal women at risk for cognitive decline within a healthy cohort using a panel of clinical metabolic indicators: Potential for detecting an at-Alzheimer’s risk metabolic phenotype. Neurobiology of aging *40*, 155-163.

Rettew, J.A., Huet-Hudson, Y.M., and Marriott, I. (2008). Testosterone reduces macrophage expression in the mouse of toll-like receptor 4, a trigger for inflammation and innate immunity. Biology of reproduction *78*, 432-437.
Reyahi, A., Nik, A.M., Ghiami, M., Gritli-Linde, A., Pontén, F., Johansson, B.R., and Carlsson, P. (2015). Foxf2 is required for brain pericyte differentiation and development and maintenance of the blood-brain barrier. Developmental cell *34*, 19-32.
Roberts, C.W., Walker, W., and Alexander, J. (2001). Sex-Associated Hormones and Immunity to Protozoan Parasites. Clinical Microbiology Reviews *14*, 476-488.
Rochfort, K.D., and Cummins, P.M. (2015). The blood–brain barrier endothelium: a target for pro-inflammatory cytokines. Biochemical Society Transactions *43*, 702-706.
Royce, T.E., Rozowsky, J.S., and Gerstein, M.B. (2007). Toward a universal microarray: prediction of gene expression through nearest-neighbor probe sequence identification. Nucleic Acids Res *35*, e99.
Rubattu, S., Stanzione, R., Bianchi, F., Cotugno, M., Forte, M., Della Ragione, F., Fioriniello, S., D'Esposito, M., Marchitti, S., Madonna, M.*, et al.* (2017). Reduced brain UCP2 expression mediated by microRNA-503 contributes to increased stroke susceptibility in the high-salt fed stroke-prone spontaneously hypertensive rat. Cell Death &Amp; Disease *8*, e2891.
Russu, M.C., and Antonescu, A.C. (2018). Neuroprotection in Perimenopausal Women.
Ryu, J.K., and McLarnon, J.G. (2009). A leaky blood–brain barrier, fibrinogen infiltration and microglial reactivity in inflamed Alzheimer's disease brain. Journal of cellular and molecular medicine *13*, 2911-2925.
Salloway, S., Gur, T., Berzin, T., Zipser, B., Correia, S., Hovanesian, V., Fallon, J., Kuo-Leblanc, V., Glass, D., and Hulette, C. (2002). Effect of APOE genotype on microvascular basement membrane in Alzheimer's disease. Journal of the neurological sciences *203*, 183-187.
Salta, E., and De Strooper, B. (2012). Non-coding RNAs with essential roles in neurodegenerative disorders. The Lancet Neurology *11*, 189-200.
Sampedro, F., Vilaplana, E., de Leon, M.J., Alcolea, D., Pegueroles, J., Montal, V., Carmona-Iragui, M., Sala, I., Sánchez-Saudinos, M.B., Antón-Aguirre, S.*, et al.* (2015). APOE-by-sex interactions on brain structure and metabolism in healthy elderly controls. Oncotarget *6*, 26663-26674.
Sankaran-Walters, S., Macal, M., Grishina, I., Nagy, L., Goulart, L., Coolidge, K., Li, J., Fenton, A., Williams, T., Miller, M.K.*, et al.* (2013). Sex differences matter in the gut: effect on mucosal immune activation and inflammation. Biol Sex Differ *4*, 10.
Sans, N., Petralia, R.S., Wang, Y.X., Blahos Ii, J., Hell, J.W., and Wenthold, R.J. (2000). A developmental change in NMDA receptor-associated proteins at hippocampal synapses. Journal of Neuroscience *20*, 1260-1271.
Sárvári, M., Hrabovszky, E., Kalló, I., Solymosi, N., Likó, I., Berchtold, N., Cotman, C., and Liposits, Z. (2012). Menopause leads to elevated expression of macrophage-associated genes in the aging frontal cortex: rat and human studies identify strikingly similar changes. Journal of neuroinflammation *9*, 264.
Sárvári, M., Kalló, I., Hrabovszky, E., Solymosi, N., and Liposits, Z. (2014). Ovariectomy and subsequent treatment with estrogen receptor agonists tune the innate immune system of the hippocampus in middle-aged female rats. PloS one *9*, e88540.
Saunders, N.R., Dziegielewska, K.M., Møllgård, K., and Habgood, M.D. (2015). Markers for blood-brain barrier integrity: how appropriate is Evans blue in the twenty-first century and what are the alternatives? Frontiers in neuroscience *9*, 385.

Scheibel, A.B., and Duong, T. (1988). On the possible relationship of cortical microvascular pathology to blood brain barrier changes in Alzheimer's disease. Neurobiology of aging *9*, 41-42.
Setoyama, D., Fujimura, Y., and Miura, D. (2013). Metabolomics reveals that carnitine palmitoyltransferase-1 is a novel target for oxidative inactivation in human cells. Genes to Cells *18*, 1107-1119.
Sherman, B.M., WEST, J.H., and KORENMAN, S.G. (1976). The menopausal transition: analysis of LH, FSH, estradiol, and progesterone concentrations during menstrual cycles of older women. The Journal of Clinical Endocrinology & Metabolism *42*, 629-636.
Sherwin, B.B. (1994). Estrogenic Effects on Memory in Women. Annals of the New York Academy of Sciences *743*, 213-230.
Sherwin, B.B. (2003). Estrogen and Cognitive Functioning in Women. Endocrine Reviews *24*, 133-151.
Shifren, J.L., Gass, M.L., and Group, N.R.f.C.C.o.M.W.W. (2014). The North American Menopause Society recommendations for clinical care of midlife women. Menopause *21*, 1038-1062.
Shineman, D.W., Basi, G.S., Bizon, J.L., Colton, C.A., Greenberg, B.D., Hollister, B.A., Lincecum, J., Leblanc, G.G., Lee, L.B., Luo, F*., et al.* (2011). Accelerating drug discovery for Alzheimer's disease: best practices for preclinical animal studies. Alzheimers Res Ther *3*, 28.
Shmelkov, E., Tang, Z., Aifantis, I., and Statnikov, A. (2011). Assessing quality and completeness of human transcriptional regulatory pathways on a genome-wide scale. Biology direct *6*, 15.
Singh, C., Liu, L., Wang, J.M., Irwin, R.W., Yao, J., Chen, S., Henry, S., Thompson, R.F., and Brinton, R.D. (2012). Allopregnanolone restores hippocampal-dependent learning and memory and neural progenitor survival in aging 3xTgAD and nonTg mice. Neurobiol Aging *33*, 1493-1506.
Skup, M., Zhu, H., Wang, Y., Giovanello, K.S., Lin, J.A., Shen, D., Shi, F., Gao, W., Lin, W., Fan, Y*., et al.* (2011). Sex differences in grey matter atrophy patterns among AD and aMCI patients: Results from ADNI. NeuroImage *56*, 890-906.
Snyder, H.M., Asthana, S., Bain, L., Brinton, R., Craft, S., Dubal, D.B., Espeland, M.A., Gatz, M., Mielke, M.M., and Raber, J. (2016). Sex biology contributions to vulnerability to Alzheimer's disease: A think tank convened by the Women's Alzheimer's Research Initiative. Alzheimer's & Dementia *12*, 1186-1196.
Soares, C.N., and Maki, P.M. (2010). Introducing a special section on menopause, cognition, and mental health. Menopause *17*, 811.
Soules, M.R., Sherman, S., Parrott, E., Rebar, R., Santoro, N., Utian, W., and Woods, N. (2001). Stages of Reproductive Aging Workshop (STRAW). J Womens Health Gend Based Med *10*, 843-848.
Sperling, R.A., Karlawish, J., and Johnson, K.A. (2013). Preclinical Alzheimer disease—the challenges ahead. Nature Reviews Neurology *9*, 54.
Spinney, L. (2014). The forgetting gene. Nature *510*, 26.
Springer, L.N., Flaws, J.A., Sipes, I.G., and Hoyer, P.B. (1996a). Follicular mechanisms associated with 4-vinylcyclohexene diepoxide-induced ovotoxicity in rats. Reprod Toxicol *10*, 137-143.
Springer, L.N., McAsey, M.E., Flaws, J.A., Tilly, J.L., Sipes, I.G., and Hoyer, P.B. (1996b). Involvement of apoptosis in 4-vinylcyclohexene diepoxide-induced ovotoxicity in rats. Toxicol Appl Pharmacol *139*, 394-401.

Springer, L.N., Tilly, J.L., Sipes, I.G., and Hoyer, P.B. (1996c). Enhanced expression of bax in small preantral follicles during 4-vinylcyclohexene diepoxide-induced ovotoxicity in the rat. Toxicol Appl Pharmacol *139*, 402-410.
Straub, R.H., and Schradin, C. (2016). Chronic inflammatory systemic diseases – an evolutionary trade-off between acutely beneficial but chronically harmful programs. Evolution, Medicine, and Public Health, eow001.
Stumhofer, J.S., Silver, J.S., Laurence, A., Porrett, P.M., Harris, T.H., Turka, L.A., Ernst, M., Saris, C.J., O'Shea, J.J., and Hunter, C.A. (2007). Interleukins 27 and 6 induce STAT3-mediated T cell production of interleukin 10. Nature immunology *8*, 1363.
Taglialatela, G., Hogan, D., Zhang, W.-R., and Dineley, K.T. (2009). Intermediate-and long-term recognition memory deficits in Tg2576 mice are reversed with acute calcineurin inhibition. Behavioural brain research *200*, 95-99.
Teixeira, D., Longo-Maugeri, I.M., Santos, J.L.F., Duarte, Y.A.O., Lebrão, M.L., and Bueno, V. (2011). Evaluation of lymphocyte levels in a random sample of 218 elderly individuals from São Paulo city. Revista Brasileira de Hematologia e Hemoterapia *33*, 367-371.
Terao, A., Apte-Deshpande, A., Dousman, L., Morairty, S., Eynon, B.P., Kilduff, T.S., and Freund, Y.R. (2002). Immune response gene expression increases in the aging murine hippocampus. Journal of neuroimmunology *132*, 99-112.
Thomas, S., and Bonchev, D. (2010). A survey of current software for network analysis in molecular biology. Human genomics *4*, 353.
Tian, X.Y., Wong, W.T., Xu, A., Lu, Y., Zhang, Y., Wang, L., Cheang, W.S., Wang, Y., Yao, X., and Huang, Y. (2012). Uncoupling protein-2 protects endothelial function in diet-induced obese mice. Circulation research *110*, 1211-1216.
Timiras, P.S., Quay, W.B., and Vernadakis, A. (1995). Hormones and aging (CRC Press).
Timmons, J.A., Szkop, K.J., and Gallagher, I.J. (2015). Multiple sources of bias confound functional enrichment analysis of global-omics data. Genome biology *16*, 186.
Tomás-Camardiel, M., Venero, J., Herrera, A., De Pablos, R., Pintor-Toro, J.A., Machado, A., and Cano, J. (2005). Blood–brain barrier disruption highly induces aquaporin-4 mRNA and protein in perivascular and parenchymal astrocytes: protective effect by estradiol treatment in ovariectomized animals. Journal of neuroscience research *80*, 235-246.
Tong, L.M., Yoon, S.Y., Andrews-Zwilling, Y., Yang, A., Lin, V., Lei, H., and Huang, Y. (2016). Enhancing GABA Signaling during Middle Adulthood Prevents Age-Dependent GABAergic Interneuron Decline and Learning and Memory Deficits in ApoE4 Mice. J Neurosci *36*, 2316-2322.
Torcia, M.G., Nencioni, L., Clemente, A.M., Civitelli, L., Celestino, I., Limongi, D., Fadigati, G., Perissi, E., Cozzolino, F., and Garaci, E. (2012). Sex differences in the response to viral infections: TLR8 and TLR9 ligand stimulation induce higher IL10 production in males. PloS one *7*, e39853.
Trabzuni, D., Ramasamy, A., Imran, S., Walker, R., Smith, C., Weale, M.E., Hardy, J., Ryten, M., and Consortium, N.A.B.E. (2013). Widespread sex differences in gene expression and splicing in the adult human brain. Nature communications *4*, 2771.
Trapnell, C., Hendrickson, D.G., Sauvageau, M., Goff, L., Rinn, J.L., and Pachter, L. (2012). Differential analysis of gene regulation at transcript resolution with RNA-seq. Nature Biotechnology *31*, 46.
Trapnell, C., Hendrickson, D.G., Sauvageau, M., Goff, L., Rinn, J.L., and Pachter, L. (2013). Differential analysis of gene regulation at transcript resolution with RNA-seq. Nature biotechnology *31*, 46.

Trapnell, C., Williams, B.A., Pertea, G., Mortazavi, A., Kwan, G., van Baren, M.J., Salzberg, S.L., Wold, B.J., and Pachter, L. (2010). Transcript assembly and quantification by RNA-Seq reveals unannotated transcripts and isoform switching during cell differentiation. Nat Biotechnol *28*, 511-515.
Ujiie, M., Dickstein, D.L., Carlow, D.A., and Jefferies, W.A. (2003). Blood–brain barrier permeability precedes senile plaque formation in an Alzheimer disease model. Microcirculation *10*, 463-470.
Uppal, S.S., Verma, S., and Dhot, P.S. (2003). Normal values of CD4 and CD8 lymphocyte subsets in healthy indian adults and the effects of sex, age, ethnicity, and smoking. Cytometry B Clin Cytom *52*, 32-36.
Utian, W.H. (2004). Menopause-related definitions. Paper presented at: International Congress Series (Elsevier).
Van Geest, R.J., Klaassen, I., Vogels, I.M., Van Noorden, C.J., and Schlingemann, R.O. (2010). Differential TGF-β signaling in retinal vascular cells: a role in diabetic retinopathy? Investigative ophthalmology & visual science *51*, 1857-1865.
Van Kempen, T.A., Milner, T.A., and Waters, E.M. (2011). Accelerated ovarian failure: a novel, chemically induced animal model of menopause. Brain Res *1379*, 176-187.
Vera, J.C., Wheat, C.W., Fescemyer, H.W., Frilander, M.J., Crawford, D.L., Hanski, I., and Marden, J.H. (2008). Rapid transcriptome characterization for a nonmodel organism using 454 pyrosequencing. Mol Ecol *17*, 1636-1647.
von Tell, D., Armulik, A., and Betsholtz, C. (2006). Pericytes and vascular stability. Experimental cell research *312*, 623-629.
Walker, D.M., and Gore, A.C. (2011). Transgenerational neuroendocrine disruption of reproduction. Nat Rev Endocrinol *7*, 197-207.
Walker, M.L., and Herndon, J.G. (2008). Menopause in nonhuman primates? Biol Reprod *79*, 398-406.
Wang, J.M., and Brinton, R.D. (2008). Allopregnanolone-induced rise in intracellular calcium in embryonic hippocampal neurons parallels their proliferative potential. BMC Neurosci *9 Suppl 2*, S11.
Wang, J.M., Johnston, P.B., Ball, B.G., and Brinton, R.D. (2005). The neurosteroid allopregnanolone promotes proliferation of rodent and human neural progenitor cells and regulates cell-cycle gene and protein expression. J Neurosci *25*, 4706-4718.
Wang, J.M., Singh, C., Liu, L., Irwin, R.W., Chen, S., Chung, E.J., Thompson, R.F., and Brinton, R.D. (2010). Allopregnanolone reverses neurogenic and cognitive deficits in mouse model of Alzheimer's disease. Proc Natl Acad Sci U S A *107*, 6498-6503.
Wang, Z., Gerstein, M., and Snyder, M. (2009). RNA-Seq: a revolutionary tool for transcriptomics. Nature reviews Genetics *10*, 57-63.
Weber, M.T., Maki, P.M., and McDermott, M.P. (2014). Cognition and mood in perimenopause: A systematic review and meta-analysis. The Journal of Steroid Biochemistry and Molecular Biology *142*, 90-98.
Wise, P.M., Smith, M.J., Dubal, D.B., Wilson, M.E., Rau, S.W., Cashion, A.B., Bottner, M., and Rosewell, K.L. (2002). Neuroendocrine modulation and repercussions of female reproductive aging. Recent Prog Horm Res *57*, 235-256.
Wolburg, H., and Lippoldt, A. (2002). Tight junctions of the blood–brain barrier: development, composition and regulation. Vascular pharmacology *38*, 323-337.
Wolman, M., Klatzo, I., Chui, E., Wilmes, F., Nishimoto, K., Fujiwara, K., and Spatz, M. (1981). Evaluation of the dye-protein tracers in pathophysiology of the blood-brain barrier. Acta neuropathologica *54*, 55-61.

Woods, N.F., Mitchell, E.S., and Adams, C. (2000). Memory Functioning Among Midlife Women: Observations From the Seattle Midlife Women's Health Study. Menopause *7*, 257-265.
Wyss-Coray, T. (2006). Inflammation in Alzheimer disease: driving force, bystander or beneficial response? Nature medicine *12*, 1005.
Yao, J., Irwin, R.W., Zhao, L., Nilsen, J., Hamilton, R.T., and Brinton, R.D. (2009). Mitochondrial bioenergetic deficit precedes Alzheimer's pathology in female mouse model of Alzheimer's disease. Proceedings of the National Academy of Sciences *106*, 14670-14675.
Ye, L., Martin, T.A., Parr, C., Harrison, G.M., Mansel, R.E., and Jiang, W.G. (2003). Biphasic effects of 17-β-estradiol on expression of occludin and transendothelial resistance and paracellular permeability in human vascular endothelial cells. Journal of cellular physiology *196*, 362-369.
Yen, L.F., Wei, V.C., Kuo, E.Y., and Lai, T.W. (2013). Distinct Patterns of Cerebral Extravasation by Evans Blue and Sodium Fluorescein in Rats. PLOS ONE *8*, e68595.
Yin, F., Yao, J., Sancheti, H., Feng, T., Melcangi, R.C., Morgan, T.E., Finch, C.E., Pike, C.J., Mack, W.J., Cadenas, E.*, et al.* (2015). The perimenopausal aging transition in the female rat brain: decline in bioenergetic systems and synaptic plasticity. Neurobiology of Aging *36*, 2282-2295.
Yoshida, H., and Hunter, C.A. (2015). The Immunobiology of Interleukin-27. Annual review of immunology *33*, 417-443.
Young, M.D., Wakefield, M.J., Smyth, G.K., and Oshlack, A. (2010). Gene ontology analysis for RNA-seq: accounting for selection bias. Genome biology *11*, R14.
Zhang, M.A., Rego, D., Moshkova, M., Kebir, H., Chruscinski, A., Nguyen, H., Akkermann, R., Stanczyk, F.Z., Prat, A., Steinman, L.*, et al.* (2012). Peroxisome proliferator-activated receptor (PPAR) and - regulate IFN and IL-17A production by human T cells in a sex-specific way. Proceedings of the National Academy of Sciences *109*, 9505-9510.
Zhao, S., and Zhang, B. (2015). A comprehensive evaluation of ensembl, RefSeq, and UCSC annotations in the context of RNA-seq read mapping and gene quantification. BMC Genomics *16*, 97.
Zhao, Z., Nelson, A.R., Betsholtz, C., and Zlokovic, B.V. (2015). Establishment and Dysfunction of the Blood-Brain Barrier. Cell *163*, 1064-1078.
Zipser, B., Johanson, C., Gonzalez, L., Berzin, T., Tavares, R., Hulette, C., Vitek, M., Hovanesian, V., and Stopa, E. (2007). Microvascular injury and blood–brain barrier leakage in Alzheimer's disease. Neurobiology of aging *28*, 977-986.
Ziylan, Y., Lefauconnier, J., Bernard, G., and Bourre, J. (1990). Blood-brain barrier permeability: regional alterations after acute and chronic administration of ethinyl estradiol. Neuroscience letters *118*, 181-184.
Zlokovic, B.V. (2005). Neurovascular mechanisms of Alzheimer's neurodegeneration. Trends in neurosciences *28*, 202-208.
Zlokovic, B.V. (2008). The Blood-Brain Barrier in Health and Chronic Neurodegenerative Disorders. Neuron *57*, 178-201.
Zonneveld, H.I., Goos, J.D., Wattjes, M.P., Prins, N.D., Scheltens, P., van der Flier, W.M., Kuijer, J.P., Muller, M., and Barkhof, F. (2014). Prevalence of cortical superficial siderosis in a memory clinic population. Neurology *82*, 698-704.